**Predicting Maternal-Fetal Disposition of Drugs Using *In Vitro* and *In Silico* Tools**

Zufei Zhang

A dissertation

submitted in partial fulfillment of the

requirements for the degree of

Doctor of Philosophy

University of Washington

2017

Reading Committee:

Jashvant D. Unadkat

Nina Isoherranen

Edward J. Kelly

Program Authorized to Offer Degree:

Pharmaceutics

University of Washington

**Abstract**

Predicting Maternal-Fetal Disposition of Drugs Using In Vitro and In Silico Tools

Zufei Zhang

Chair of the Supervisory Committee:

Professor Jashvant D. Unadkat

Department of Pharmaceutics

During pregnancy, physiological and ADMET changes in the maternal-fetal dyad can significantly alter drug pharmacokinetics (PK) in the mother and may necessitate dosing regimen adjustments. One clinically important example is CYP3A. Its activity increases by ~2-fold during the third trimester (T3) as shown by 1'-hydroxymidaozlam *in vivo* clearance, resulting in sub-therapeutic plasma concentrations of CYP3A substrates (Unadkat et al., 2007; Hebert et al., 2008). However, it is logistically challenging and/or ethically not feasible to conduct such PK studies in the pregnant mother, especially during first and second trimesters (T1 and T2, respectively). Therefore, the magnitude of hepatic CYP3A induction *in vivo* across different trimesters was predicted using two model systems, namely, the HepaRG cells and human hepatocytes. After incubation with individual or combinations of pregnancy-related hormones at their clinically observed plasma concentrations in different trimesters, the change in the activity of hepatic CYP3A was measured. Both *in vitro* systems predicted ~2-fold induction in CYP3A activity throughout pregnancy based on the above T3 induction data. This predicted 2-

fold increase in CYP3A activity during T1 and T2 is in accordance with T2 pharmacokinetic (PK) data of several CYP3A substrates (e.g. buprenorphine(Bastian et al., 2016), nifedipine,(Marin et al., 2007), and indinavir (Cressey et al., 2013)). Assessing fetal exposure to drugs during pregnancy remains a major challenge as fetal exposure to drugs is not only driven by maternal PK but also may be further influenced by placental passage and fetoplacental metabolism/transport. Additionally, due to safety and ethical concenrns, fetal blood sampling is not possible until the time of birth. Thus mechanistic, non-invasive *in silico* prediction methods, such as physiologically-based pharmacokinetic (PBPK) models, offer an alternative to predicting the *in vivo* disposition of drugs in the maternal-fetal pair during pregnancy. However, at present, the fetus is commonly treated as a single compartment in existing maternal-fetal PBPK models developed for pharmaceutical agents (Gaohua et al., 2012), often lumped with the placenta and the amniotic cavity. As such, model verification using term umbilical venous data, the **only** fetal exposure data available, is not possible. To bridge this gap in knowledge, we constructed a novel MATLAB® maternal-fetal (m-f) PBPK model in collaboration with Simcyp®, by expanding our previously verified pregnancy PBPK model. The expansion was accomplished by incorporating a fetal PBPK consisting of 7 body compartments into the pregnancy PBPK model, as well as the placenta and the amniotic fluid compartment. Using a series of simulation exercise using this m-f-PBPK model, we delineated the key factors determining fetal plasma drug exposure and clarified the commonly held misconceptions surrounding UV:MP ratio data. We also predicted that fetal development may play an important role in modulating fetal plasma AUC. Finally, to verify, we verified the performance of this m-f-PBPK model with

drugs that cross the placenta predominantly via passive diffusion by simultaneously predicting maternal and fetal disposition of two model drugs. The model performed reasonably well predicting the observed maternal-fetal plasma drug concentration-time (C-T) profiles of both drugs at the time of delivery. The aims of this thesis were to test whether mechanistic physiologically-based pharmacokinetic (PBPK) models integrating *in vivo* observations and *in vitro* experimental results could be utilized to predict maternal and fetal drug exposure to several probe drugs during pregnancy. The results obtained demonstrate that: 1) the magnitude of *in vivo* hepatic CYP3A induction during T1 and T2 can be predicted from relevant *in vitro* systems such as HepaRG cells and hepatocytes; 2) PBPK modeling and simulation can be used as theoretical tools to discern key factors determining fetal exposure to drugs; and 3) the presented m-f-PBPK model can be used to predict maternal and fetal plasma drug C-T profiles of passive diffusion drugs. The predicted 2-fold increase in CYP3A activity will be used to inform dose adjustments of CYP3A substrates during T1 and T2, when pregnant women are normally precluded from PK studies for safety concerns. The presented m-f-PBPK model provides one step further towards a more physiologically faithful platform for quantitative prediction of drug PK in the coupled maternal-fetal pair **throughout pregnancy**, and allows generalization beyond the probe drugs studied when fetoplacental expression data become available.

Dedication

To my beloved parents, Chengliang Zhang and Lili Guo:

If it was not for you, I would not have started this.

To my husband, Jieyang Hu and little sister Feili Wu:

If it was not for you, I would not have finished this.

Acknowledgements

I am forever indebted to my doctoral advisor Professor Jashvant D. Unadkat for his tireless encouragement and life changing guidance. I have learned much from him, and it has been a privilege to work with him. He has shown me the perseverance and dedication it takes to be a good scientist and mentor, helping me push past my own limits. I could not have asked for a better mentor.

To my thesis reading and doctoral supervisory committee members, Drs. Isoherannen, , Kelly and Anderson, I wish to express my sincere gratitude for their encouragement, support, and guidance. In particular, their enthusiasm and scientific curiosity helped me find joy in this project, which is what gave me the strength to see this through until the end.

To the faculty of the Pharmaceutics and Medicinal Chemistry departments, I wish to thank you for fostering a collegial environment and providing your students an endless set of opportunities to learn and prosper. I am truly grateful to have had the chance to learn from this group of excellent scientists and teachers.

To the staff of the Pharmaceutics and Medicinal Chemistry departments, I wish to thank you for your help and encouragement.

I would like to express my sincere gratitude to our collaborators at Simcyp: especially Drs. Amin Rostami, Janak Wedagedera, and Lu Gaohua. The modeling part of this thesis would not have possible without their guidance and support.

I would also like to thank all the past and present members of Unadkat Lab. They have been a constant source of friendship and moral support in both my professional and personal life. To my friends in the Pharmaceutics and Medicinal Chemistry departments, although there is not enough room to list all your names, you know who you are, and I thank you for the help and camaraderie throughout my time here.

Finally, I would like to acknowledge all my friends and family who have come with me on this journey. First, I owe a debt of deep gratitude to my parents. The past six years has not been an easy journey. They have provided unconditional love, motivation, and support in everything I do. I also want to express my heart-felt thanks to my in-laws, Dr. Dingming Hu and Wanyi Liang for their love, understanding, and support. My acknowledgement also goes out to Feili Wu, who became my roommate during graduate school and later became my little sister. Her tremendous growth has continued to inspire me during the years of my doctoral pursuit. To my husband, Jieyang Hu, I am blessed to have you in my life. Your faith in me has given me the strength and determination to pull through all my hard times. One last acknowledgement goes out to my dog Ginger who has been my stalwart companion, helping me get through long nights by being adorable.

Contents

# Chapter 1 Introduction

## 1.1 Pregnancy and altered pharmacokinetics: an overview

Despite the common concerns about the safety of medication use during pregnancy, epidemiological studies have documented that women take a variety of medications during pregnancy (Mitchell et al., 2011). Many women enter pregnancy with pre-existing conditions. Those conditions include asthma, epilepsy, depression, diabetes. To ensure the well-being of the mother and therefore a healthy pregnancy, the mother needs to continue taking her medications during pregnancy. In addition, a sizable portion of pregnant women develop acute illness or pregnancy-related complications (e.g. gestational hypertension, gestational diabetes) that require pharmacotherapy. For instance, according to a recent report from the Centers for Disease Control and Prevention, the prevalence of gestational diabetes was found to be as high as 9.2% in the surveyed pregnant population (DeSisto et al., 2014).

While the use of medication during pregnancy is common, very little is known about the effect of pregnancy on drug disposition in the pregnant mothers as they are usually excluded from clinical studies. During pregnancy, profound physiological changes occur in the mother that can potentially modulate the absorption, distribution, metabolism, excretion, and transport (ADMET) processes of drugs dosed to pregnant women. Indeed, published studies conducted in pregnant women have revealed that the ADMET processes of many drugs are altered by pregnancy to various extents. However, for the vast majority of approved drugs, there are is no available clinical data as studies have not been or cannot be carried out in the pregnant population. For those drugs, evidence-based decisions on dose adjustments during pregnancy cannot be made and thus

mechanistic bottom-up model-based predictions may serve as an alternative. In order to quantitatively predict drug disposition during pregnancy across drugs, a systematic review of the magnitude of changes in these processes is needed. The observed pharmacokinetic (PK) changes in pregnant women may be broadly grouped into five descriptive categories: absorption, distribution, metabolism, renal excretion, and drug transport. A high level summary of current knowledge of these changes, along with some supporting clinical examples, is organized and presented below based on the above categories.

### 1.1.1 Absorption

Since many drugs are given orally during pregnancy, we focus here on the effect of pregnancy on oral absorption of drugs (i.e. the rate at and the extent to which an oral dose gets into systemic circulation). In particular, how pregnancy alters the rate and the extent of oral absorption.

In theory, changes in gastric physiology caused by pregnancy could alter both the rate and the extent of drug absorption. Pregnancy is generally thought to prolong gastric emptying and transit times as well as reduce gastrointestinal motility, which in turn will result in slowing of oral absorption. On the other hand, increased gastric pH caused by enhanced gastric mucus secretion (Murray et al., 1957) enhances ionization of weak acid and thus may slow down the dissolution of weakly acidic drugs and decrease their membrane permeability compared with weak bases. These physiological changes in gastrointestinal (GI) tract may partially explain the significantly lower $C_{max}$ and much greater $t_{max}$ of orally administered acetaminophen (a weak acid) observed in T3 pregnant women (Simpson et al., 1988). However, conflicting data exist regarding changes in

maternal gastric physiology during pregnancy. For example, Macfie et al. failed to detect any significant delay of acetaminophen absorption ($t_{max}$) in all three trimesters (Macfie et al., 1991). Furthermore, Sandhar et al. found that the gastric emptying times measured by applied potential tomography technique observed did not differ between T3 pregnant women and nonpregnant controls (Sandhar et al., 1992). The current inconsistency in literature is partly due to the limited techniques of measurement imposed by pregnancy. Nonetheless, it should be noted that oftentimes, it is the alterations in AUC, rather than $C_{max}$ and $t_{max}$ , that affect the efficacy/toxicity of many drugs.

How pregnancy affects the extent of absorption (i.e. bioavailability F; calculated as the product of $F_a$, $F_g$, and $F_h$) remains unclear for most drugs. This is because PK studies conducted in pregnant women involving intravenous administration face significant challenges imposed by pregnancy. F cannot be estimated from oral data alone. However, to date, only a few drugs have been dosed to pregnant women both intravenously and orally. O'Hare and coworkers gave six pregnant women sotalol, a BCS class I β-adrenoceptor antagonist (Benet, 2010), intravenously and orally during the third trimester (T3; GWs 32-36) and 6 weeks postpartum. Bioavailability was ~90% and did not differ between T3 and postpartum (O'Hare et al., 1983). Another example is phenytoin, a BCS class II banticonvulsant used by epileptic pregnant women (NICHD). Lander et al. evaluated phenytoin PK in five first trimester (T1) pregnant women and found that the average oral biovailability to be ~90% (Lander et al., 1984), which is close to that reported in non-pregnant population [~85% (Richens, 1979)]. Phillipson and coworkers evaluated PK of three β-lactams in pregnant women with urinary traction infections. Study participants received both IV and oral doses of ampicillin

(n=6),(Philipson, 1977) cephradine (n=12) (Philipson et al., 1987) , and cefazolin (n=6) (Philipson et al., 1987) during the second trimester (T2) or the third trimester (T3) and ≥ 6 weeks postpartum. For all three β-lactams oral bioavailabity did not differ between T2/T3 and postpartum. Of note, ampicillin is a substrate of intestinal PEPT1 and PEPT2 substrate, whereas cefazolin is gut MRP4 substrate (Shugarts and Benet, 2009). The effect of pregnancy on the activity of these transporters has not been studied.

In conclusion, our understanding of gastric physiology during pregnancy needs to be improved. Likewise, more clinical data during pregnancy are needed to elucidate the effect of pregnancy on the rate and the extent of oral drug absorption. Ideally, the PK of drugs demonstrating varying extents of absorption caused by differing solubility, ionization, permeability, gut transport mechanisms should be systematically studied to shed light on the effect of pregnancy on drug absorption,

### 1.1.2 Distribution

Volume of distribution is a proportionality factor relating the amount of drug in the body to the measured plasma drug concentration. A few volume of distribution terms have been introduced to account for the dynamic processes of drug distribution in the human body (e.g. $V_c$, $V_\beta$, and $V_{ss}$). Although the terminal volume of distribution, $V_\beta$ , is frequently reported in the literature, one should bear in mind that $V_\beta$ can significantly exceeds the steady-state volume of distribution $V_{ss}$. This divergence stems from the differences in the definition of these two parameters. $V_\beta$ equals the ratio of the intravenous bolus dose to the product of AUC and β ($V_\beta = \frac{D}{AUC \cdot \beta}$). β is the smaller exponential coefficient of the two-compartment model. As a composite parameter, β is

corrupted by distribution processes during the terminal phase. In contrast, by definition, $V_{ss}$ takes into account both distribution and elimination ($V_{ss} = \frac{D \cdot AUMC}{AUC^2}$). Therefore, cautions must be exercised when interpreting the effect of pregnancy on drug volume of distribution.

In theory, changes in body water volume, plasma drug binding, and tissue drug binding will result in an altered volume of distribution. Pregnancy is accompanied by hemodilution and changes in body composition. Total body water increases gradually with gestational age, whereas most of the total body fat is deposited during the second trimester with very little gained during the first or the third trimester (Abduljalil et al., 2012). Maternal plasma volume, for instance, increases by 7%, 42%, and 50% during T1, T2, and T3, respectively. The distribution of both hydrophilic and lipophilic drugs can be affected by pregnancy. For the former, the increase in total body water, both intravascular (plasma volume) and extravascular (breasts, uterus, peripheral systems) may lead to a larger space that hydrophilic drugs can distribute into. Muller et al. found that the $V_\beta$ of intravenously administered amoxicillin was higher during pregnancy than postpartum (Muller et al., 2008). Romero et al. evaluated the $V_\beta$ of theophylline in six term pregnant non-smoking women and found slightly higher $V_\beta$ compared to that reported in healthy, non-smoking adults (Romero et al., 1983). Likewise, for lipophilic drugs, the increase in the free fraction in plasma as a result of diluted plasma drug binding proteins and in total body fat can result in a higher volume of distribution. Indeed, the reported volume of distribution for several drugs differs significantly between the pregnant and the non-pregnant populations. For example, both the $V_\beta$ and $V_{ss}$ of thiopental, a highly lipophilic anesthetics, increased considerably compared with non-

pregnant subjects (564 L vs 233L for $V_\beta$ , and 288 L vs 97.5 L for $V_{ss}$) (Morgan et al., 1981). As stated earlier, these reported changes in $V_\beta$ can potentially be confounded by changes in drug elimination and therefore should not be interpreted out of context.

### 1.1.3 Metabolism

Drug metabolism mediated by drug metabolizing enzymes (DMEs) in the body can be loosely categorized into hepatic metabolism and extrahepatic metabolism. Extrahepatic metabolism may occur in the gut, kidneys, lungs and other extrahepatic organs. While the liver often serves as a major site of drug metabolism, extrahepatic metabolism of drugs cannot be readily discounted as the latter may play an important role in modulating the systemic or local drug exposure and thus drug efficacy/toxicity.

Obviously, it is not possible to evaluate the effect of pregnancy on the disposition of every drug that has been prescribed to pregnant women. A logical approach would be to conduct phenotyping studies using probe drugs. Then, the effect of pregnancy on *in vivo* activity of a given DME can be assessed by comparing the dose-normalized plasma drug clearance with that of postpartum controls or in non-pregnant population. With the aid of modeling and simulation, this approach will allow us to extrapolate across dosing regimens and beyond the drugs tested (see **Chapters 3 and 4**). However, there are some caveats of this phenotyping approach that one should be aware of. First, as stated previously, logistical and ethical reasons limit prospective PK studies to T3 pregnant women. As a result, early gestation data (i.e. T1 and T2) for many CYP isoforms, non-CYP phase I and phase II enzymes, and transporters are not available or not definitive. These knowledge gaps include some key enzymes involved in the disposition of drugs routinely given to pregnant women. For instance, the *in vivo* activity of CYP3A has not

been assessed by valid probes during T1 and T2. To bridge this gap in knowledge, we conducted studies presented in **Chapter 2.** Secondly, unless drugs are intravenously dosed, the observed change in clearance (CL/F) will be confounded by changes in F (see above).

A review of existing literature indicates that the effect of pregnancy on the activity of DMEs is enzyme-specific (Anderson and Carr, 2009; Jeong, 2010; Isoherranen and Thummel, 2013). Studies conducted in pregnant women show that the activity of CYP1A2 and CYP2C19 is suppressed, whereas the activity of CYP3A and CYP2D6 is increased. Furthermore, the extent of this pregnancy effect may vary with gestational age. For instance, the degree of CYP1A2 activity suppression, as measured by caffeine clearance in pregnant volunteers, was 30%, 50%, and 65% , during T1, T2, and T3, respectively (Tracy et al., 2005). For a complete list of enzymes whose activity *in vivo* has been found to change during pregnancy and the known longitudinal patterns of these changes, see **Table 1.1**. The reader is also referred to many excellent reviews on this topic in the literature (Anderson, 2005; Isoherranen and Thummel, 2013; Tasnif et al., 2016).

### 1.1.4 Renal Excretion

Renal excretion of drugs consists of glomerular filtration clearance (GFR), active tubular secretion, and reabsorption of drugs. The first component, glomerular filtration, is commonly measured by creatinine or inulin clearance. Recent studies revealed that creatinine is both freely filtered and secreted by kidney proximal tubules via OCT2 (Ciarimboli et al., 2012), thereby overestimating GFR. Hence, inulin clearance is deemed a more accurate measurement of GFR. Overall, inulin clearance demonstrates a

progressive increase over the course of pregnancy. It starts to increase in the first trimester, plateaus during T2 with an average increase of 37% (Abduljalil et al., 2012) and falls off in the last few weeks of pregnancy in some individuals (Sturgiss et al., 1996). The latter two components, the tubular secretion and the reabsorption of drugs, are mediated by membrane drug transporters expressed in the kidneys. Renal drug transporters are primarily located in the kidney proximal tubules. Important examples include P-gp, MRP, OATs, and OCTs.

In contrast to GFR, very little is known as to the effect of pregnancy on the activity of renal drug transporter mediated tubular secretion/reabsorption. This can be attributed to, at least in part, the challenge in distinguishing active secretion from tubular reabsorption from urine and plasma data. As a result, in existing literature, only the apparent renal transporter activity (i.e. the remainder of renal clearance after subtraction of renal filtration clearance) has been measured during pregnancy. Nonetheless, lines of evidence (summarized below) show that pregnancy seems to alter the activity of three renal transporters: P-gp, OAT1, and OCT2.

Hebert et al. investigated P-gp activity during pregnancy using digoxin (Hebert et al., 2008). The net secretion clearance of digoxin was found to significantly increase during pregnancy, indicating enhanced vectorial transport from blood to kidney lumen that is thought to be mediated by renal P-gp and OATP4C1 in tandem (He et al., 2014). Therefore, the observed increase in digoxin renal secretion may be attributed to enhanced activity of renal P-gp or renal OATP4C1 or both. Of note, in the same study, intestinal P-gp activity, as evaluated indirectly by $AUC_{0\text{-}4h}$, did not differ from that obtained postpartum.

Andrew et al. evaluated amoxicillin PK in 16 women during T2 (18-22 weeks gestation) and T3 (30-34 weeks gestation) as well as ≥ 3 months postpartum (Andrew et al., 2007). They found that renal OAT1-mediated net renal secretory clearance of amoxicillin markedly increased by 64% and 36% at T2 and T3, respectively, as compared with postpartum [net renal secretory CL of 4.1 ±1.7 mL/min/kg (T2) and 3.4 ±0.7 mL/min/kg (T3) vs. 2.5 ±0. 8 mL/min/kg (postpartum)].

Eyal et al. evaluated metformin PK during T1, T2, T3, and ≥ 3 months postpartum (Eyal et al., 2010). Metformin renal clearance increased significantly in T2 (49%) and T3 (29%) compared with postpartum ($p<0.01$). After accounting for the increase in GFR, the net renal secretion clearance of metformin was found to increase by 45% in T2 and 38% in T3 compared to postpartum values ($p<0.01$). This observed increase in metformin renal clearance suggests enhanced activity of renal OCT2. This piece of data is consistent with *in vitro* and animal studies in which Oct2 expression and activity in the kidneys can be regulated by steroidal hormones (Urakami et al., 2000; Shu et al., 2001).

### 1.1.5 Drug Transport

In addition to the ADME processes discussed above, drug transport is increasingly recognized as an important determinant of drug disposition, efficacy, and toxicity. Drug transporters are cell membrane proteins expressed throughout the human body that mediate the uptake or efflux of drug molecules into and out of the cells. When present in the small intestine, liver, or kidneys, they participate in the systemic disposition of many drugs, whereas those expressed in blood-tissue barriers have been shown to play important roles in drug distribution (Schinkel, 1999).

During pregnancy, the circulating concentrations of many steroid hormones increases significantly with advancing gestation (Jeong, 2010). Therefore, the activity of drug transporters that are regulated by these hormones, such as BCRP and OCT2, is expected to alter in a gestational-age dependent manner. The *in vivo* effects of pregnancy on renal transport of drugs have been inferred by measurement of renal net secretory clearance in pregnant women receiving transporter probe substrates (**Table 1.1**). These results, when significantly different from those obtained postpartum or from non-pregnant controls, indicate that the activity of renal drug transporter(s) is altered by pregnancy. However, one cannot readily disregard the possibility that the observed change in net renal secretory clearance may be confounded by changes in tubular reabsorption. Therefore, additional *in vitro* studies would help confirm *in vivo* findings and provide insights into renal drug disposition during pregnancy.

In contrast, the effects of pregnancy on the activity of drug transporters in other organs, such as liver and gut, remain unclear for the following reasons:

- It is challenging to conduct prospective PK studies in pregnant women using probe substrates and specific inhibitors that are selective for a single transporter. However, to date, such probes/inhibitors that can be administered to pregnant women are not available.
- Common co-expression of DMEs and transporters complicates the identification of transporter activity when a drug is subject to both metabolism and transport. For example, despite the presence of hepatic sinusoidal uptake and/or efflux clearance(s), when a drug has high permeability across the hepatic sinusoidal membrane, the loss of drug from systemic circulation will be solely driven by hepatic metabolic clearance

(Patilea-Vrana and Unadkat, 2016). Therefore, the effect of pregnancy on the activity of hepatic drug transporter(s) cannot be identified.

## 1.2 Predicting the effect of pregnancy on hepatic CYP3A activity during T1 and T2

### 1.2.1 Pregnancy and the altered CYP3A activity

Indisputably, the cytochrome P450 (CYP) isozyme CYP3A is the most important drug-metabolizing enzyme. It has the broadest substrate specificity compared to other CYP isoforms and is involved in the disposition of more than 50% of marketed drugs (Wilkinson, 2005). Regarding the pregnant women, CYP3A also plays an important role as it determines the clearance of many drugs prescribed to pregnant women. Those drugs include antihypertensive (nifedipine), anti-epileptics (carbamazepine), HIV antiretrovirals (saquinavir, indinavir, ritonavir, lopinavir, etc.).

The activity of CYP3A is induced by approximately 99% during T3 as measured by 1'-hydroxymidazolam formation clearance (Hebert et al., 2008). This induction can result in suboptimal or even subtherapeutic plasma concentrations of drugs cleared by CYP3A. A compelling example is the HIV protease inhibitor indinavir, a CYP3A substrate. In a clinical study conducted in HIV-infected T3 pregnant women, we found that the oral clearance of indinavir was 3 times higher during T3 compared to postpartum (or in non-pregnant women and men), rendering the standard dosing regimen ineffective in these pregnant women (Unadkat et al., 2007). Another important example is nifedipine, a CYP3A probe drug used in the management of hypertension or as a tocolytic during pregnancy. As a result of the above mentioned ~2-fold induction in CYP3A activity, nifedipine oral clearance is increased and therefore its half-life and maximal plasma

concentration are decreased during T3, suggesting an increase in starting dose (Prevost et al., 1992).

As demonstrated by indinavir, dose adjustments in T3 pregnant women are needed for narrow therapeutic window drugs to compensate for the 99% increase in CYP3A activity. However, to date, definitive PK studies using specific CYP3A probe drugs have only been conducted in pregnant women during T3. The effect of pregnancy on CYP3A activity during early gestation, specifically, T1 and T2, remains unclear. Considering that many CYP3A-cleared drugs are routinely prescribed to pregnant women, it is of concern whether CYP3A activity is induced during T1 and T2. More importantly, would the magnitude of CYP3A induction be clinically significant for CYP3A cleared drugs? Another open and important question concerns the exact culprit of this induction. Although hormonal regulation of CYP3A has long been a subject of interest among pharmacologists, the exact mechanism(s) of the observed 2-fold change in CYP3A activity among T3 pregnant women remains to be fully elucidated. To address the above questions, we conducted a series of investigations as presented in **Chapter 2**. In addition, to provide the reader with context, a brief overview of existing knowledge on CYP3A regulation by endogenous compounds is provided in the following section.

### 1.2.2 CYP3A regulation by pregnancy-associated hormones

Pregnancy is accompanied with significant changes in the circulating concentrations of various hormones due to the altered endocrine system (**Figure 1.1**). For instance, the hypothalamic-pituitary-adrenal (HPA) axis is activated during pregnancy. The plasma levels of circulating maternal corticotropin-releasing hormone (CRH) increase exponentially from T1 due to the CRH production in the placenta, decidua, and fetal

membranes (Mastorakos and Ilias, 2003). As a result, the average total plasma cortisol in young non-pregnant women based on several publications (181.5nM) is significantly lower than T1 (418nM) . The average reported plasma concentration of cortisol further increases to ~800nM during T2 and remains at such high concentrations during T3 (Zhang et al., 2015). Plasma concentrations of progesterone and estrogen increase substantially after 6 weeks of pregnancy, with the site of synthesis shifting from the ovary to the placenta {Hytten, 1971 #5293}. During pregnancy, the placenta also secretes a 22 KD polypeptide structural variant of the pituitary growth hormone (GH), which differs from GH by 13 amino acids (Lacroix et al., 2002). The plasma concentration of this placental GH isoform is detectable in maternal serum as early as the $5^{th}$ week of gestation and continues to rise until it peaks at 30-40 weeks (Wu et al., 2003). From the beginning of T2, the pituitary form is gradually replaced by the placenta GH and becomes undetectable in maternal serum by T3 (Caufriez et al., 1993).

Many naturally occurring or synthetic glucocorticoids have been shown to induce CYP3A at physiologically relevant concentrations. 10nM Dexamethasone markedly enhanced CYP3A4 mRNA and protein expression in primary human hepatocyte culture, such that by day 6 CYP3A activity measured by testosterone 6β-hydroxylation approached that in freshly isolated human hepatocytes (Liddle et al., 1998). Our lab also observed in human hepatocytes, upon exposure to various cortisol concentrations observed in T3, significant induction in CYP3A4 mRNA and activity (Papageorgiou et al., 2013). The effect of glucocorticoids on CYP3A has been investigated in the non-pregnant population. Therapeutic use of glucocorticoids (oral dexamethasone and

intravenous cortisol) to patients led to an average of ~55% increase of $^{14}CO_2$ production in erythromycin breath test (Watkins et al., 1989).

Although estrogens have been shown to interact with CYPs in mammals, the effect of estrogens on human DMEs appears to be isoform-specific and donor dependent. T3 concentrations of estradiol ($E_2$) consistently increased $ER_\alpha$ mRNA expression but did not induce CYP3A activity in hepatocytes from female donors (Papageorgiou et al., 2013). Direct incubation using 10X T3 plasma concentrations of $E_2$ with frequent media renewal only resulted in moderate induction in sandwich cultured human hepatocytes (SCHH) from some donors, suggesting this induction is donor-dependent (Choi et al., 2013). The responsiveness of CYP3A activity to *in vivo* estrogen levels, however, is questionable. Hepatic CYP3A activity measured by intravenous midazolam did not differ among phases of menstrual cycles (Kharasch et al., 1999). Hormone replacement therapy with estrogen and progesterone showed no effect on hepatic CYP3A activity as determined by the clearance of midazolam (Gorski et al., 2000). Collectively, these data suggest that estrogens and progesterone might have a modest effect on *in vitro* induction of CYP3A in a subset of population. However, whether this can translate into clinically significant induction in CYP3A needs further investigation.

Like the above hormones, pituitary GH also demonstrated the potential to induce CYP3A activity. Liddle et al found that CYP3A mRNA level increased markedly in cultured human hepatocytes treated with GH.(Liddle et al., 1998) GH replacement in GH-deficient individuals restored CYP3A4 activity (as measured by erythromycin breath test) to levels comparable to those observed in healthy individuals.(Jaffe et al., 2002)

### 1.2.3 Predicting the magnitude of change in hepatic CYP3A activity during T1 and T2 using *in vitro* systems

Prior to conducting the work presented in **Chapter 2**, our laboratory had shown that the clinically observed 2-fold induction of CYP3A activity is most likely hepatic through the pregnant CYP3A4-promoter-luciferase transgenic mouse model and PBPK modeling and simulation (Zhang et al., 2008; Ke et al., 2012). Moreover, the phenomenon of increased CYP3A activity (as measured by 1'-hydroxymidazolam formation clearance) could be reproduced in HepaRG cell line and in human hepatocytes (Papageorgiou et al., 2013). Among the pregnancy related hormones (PRHs) tested, cortisol, a glucocorticoid hormone, was the major inducer of CYP3A activity during T3 in sandwich cultured human hepatocytes (SCHH) from premenopausal donors. The magnitude of CYP3A induction by a cocktail of all five PRHs (cortisol, progesterone, estradiol, growth hormone and its placental form) at their T3 plasma concentrations is close to that observed *in vivo* (~4 vs. 2 fold). The induction pattern of SCHH by PRHs is replicated by HepaRG cells. However, in this study, the rapid depletion of hormones in the incubation media was not accounted for. In addition, only the plasma concentrations observed in T3 pregnant women were tested.

To recapitulate the observed *in vivo* CYP3A induction, *in vitro* systems must contain molecular entities that are involved in the hormone regulation of CYP3A. HepaRG cell line originates from a French female donor who suffered hepatocarcinoma. As a well-characterized hepatic progenitor cell line, these cells express all the nuclear receptors that have been indicated in CYP3A induction (Kanebratt and Andersson, 2008). Another choice was the gold standard, human hepatocytes from female donor of reproductive age.

We hypothesized that the magnitude of *in vivo* hepatic CYP3A induction during T1 and T2 can be quantitatively predicted from studies using SCHH and HepaRG cells exposed to pregnancy-related hormones at plasma concentrations observed during T1 and T2. We tested the above hypothesis with the following specific aims:

**Aim1a**. Use midazolam as a CYP3A probe to confirm that cortisol is the major pregnancy-related inducer at T1 and T2 hormone plasma concentrations (taking hormone depletion into consideration in SCHH and HepaRG cells).

**Aim1b**. (i) Determine the magnitude of induction in hepatic CYP3A activity *in vitro* using SCHH or HepaRG cells incubated with T1, T2, or T3 hormone plasma concentrations and (ii) Predict the magnitude of *in vivo* CYP3A induction during T1 and T2 using the scaling factor that relates the observed *in vitro* induction (99% during T3) to *in vivo* hepatic CYP3A induction

The studies conducted to address each of the above specific aims are detailed in **Chapter 2** that follows. This chapter is formatted as a manuscript submitted with slight modification.

## 1.3 Development of a Maternal-Fetal PBPK Model

### 1.3.1 Review of existing animal models and *ex vivo human placenta perfusion model* to study fetal exposure to drugs

Although drug use during pregnancy has become prevalent, our knowledge of fetal exposure to drugs is far less than sufficient. At present time, *in vivo* human studies are not possible due to the technical and ethical challenges associated with pregnancy. Furthermore, fetal blood sampling is limited to the time of birth when umbilical blood

samples can be safely obtained. To estimate fetal exposure to drugs, animal studies and the human placenta perfusions have been conducted as summarized below.

Several animal models have been proposed to study drug transfer across the placenta. Numerous studies using small rodents, such as mice, rats, and guinea pigs, have been conducted to evaluate the trans-placental passage and fetal tissue distribution of drugs. In such studies, the drug of interest is injected into the pregnant female. Then, after sacrificing the animals at various time points post injection, the placentae and whole fetuses are harvested to assess drug exposure profiles in fetoplacental tissues and in fetal plasma/blood. In addition, several investigators have used genetically mutated mice to evaluate the role of specific drug transporters in fetal exposure to probe drugs. For example, Zhang et al. demonstrated that the presence of murine Bcrp significantly limited fetal distribution of nitrofurantoin in pregnant mouse while exerting only a minor effect on the systemic clearance of the drug (Zhang et al., 2007). Although frequently used by researchers, the limitations of studies using pregnant rodent models must be appreciated. First, in these studies, single time point fetal/maternal plasma concentration ratios are frequently reported as a measure of fetal drug distribution, rather than fetal/maternal plasma AUCs (Jonker et al., 2002; Enokizono et al., 2007). Secondly, due to the small size of pups, blood from all or one than one pup belonging to each pregnant mother is usually pooled to generate the fetal plasma drug concentration-time (C-T) profiles (Samtani and Jusko, 2007; Zhang et al., 2007). Furthermore, in many cases, only the drug concentration in the homogenates from whole fetuses (individual or pooled) was reported (Samtani and Jusko, 2007; Shuster et al., 2014a)

Besides rodents, larger mammals, such as sheep and primates, have also been used to study the maternal-fetal transfer of drugs. In these animals, intravascular catheters can be placed both in the mother and in the fetus to obtain matched fetal and maternal plasma drug C-T profiles after administering drugs to the pregnant mother. Many studies of similar type were done in chronically catheterized fetal and maternal sheep/primates in which drugs were infused either to the fetus or the mother to steady-state. Such study design allows the determination of the clearances in either direction across the placenta (Mihaly et al., 1982; Pereira et al., 1994). In addition, pregnant primates have proven to be a valuable tool to study fetal exposure to HIV drugs because (1) similar pharmacokinetics to those in humans may be achieved and (2) primates are susceptible to the human immunodeficiency virus, allowing for the study of maternal-fetal transfer of HIV drugs. Finally, it should be pointed out that despite the above advantages of animal models, significant species differences in placenta morphology may prevent meaningful extrapolation to humans. For example, the sheep placenta is syndesmochorial consisting of five layers. Compared with the three-layered hemochorial placenta in humans or non-human primates , it presents a greater diffusion barrier (Rudolph, 1985).

Alternatively, *ex vivo* dual perfusion using human placentae may provide more reliable predictions of fetal drug exposure as it most closely resembles the *in vivo* situation. Usually, after the collection of term placentae, fetal and maternal vessels (both arteries and veins) are identified and carefully cannulated. Then, perfusion from either fetal or maternal side is performed. At various time points, sampling can take place in maternal and fetal compartments as well as placental tissue (Panigel et al., 1967; Schneider et al., 1972). A recent literature review found that after accounting for protein binding and

blood pH, steady-state placenta perfusion results were able to accurately predict *in vivo* transfer of drugs as measured by cord: maternal plasma drug concentration ratios ($R^2$ =0.85, P < 0.0001) (Hutson et al., 2011). Compared to the above animal models, *ex vivo* placental perfusion model is a much more physiologically relevant system and can be useful for predicting fetal exposure to drugs. However, a limitation of the perfusion model is that the availability of human placentae is usually limited to term or near term. Predictions based on term placentae perfusion data cannot be necessarily extrapolated to earlier gestational ages.

### 1.3.2 Towards a physiologically realistic fetal PBPK model

Fetal exposure to drugs ingested by the pregnant mother (i.e. fetal plasma AUC) cannot be feasibly or ethically studied in fetuses. Instead, single time point fetal cord blood sampling is the most common approach to study fetal drug exposure as it can be easily completed in third trimester opportunistic PK studies. While such "real life" data are more meaningful than those obtained from *ex vivo* placental perfusions or *in vitro* cell line experiments, they also leave many clinical questions unaddressed. First of all, these single time point umbilical venous: maternal plasma (UV:MP) drug concentration ratio data have been frequently reported and widely associated with fetal drug exposure. Often, this ratio, if it is greater than unity, is interpreted as accumulation of drug in the fetal compartment (Else et al., 2011). In contrast, a UV:MP ratio of less than unity is interpreted as low fetal exposure and has been attributed to low maternal drug concentrations(Chappuy et al., 2004a; Chappuy et al., 2004b), fetal metabolism (Chappuy et al., 2004c) and placental efflux(Marzolini and Kim, 2005). Few efforts have been made to contemplate whether this UV:MP ratio truly indicates the fetal: maternal

plasma AUC ratio (Tuntland et al., 1999; Unadkat et al., 2004). Additionally, if the UV:MP ratio deviates from the fetal: maternal AUC ratio, what factors will contribute to such deviation? More importantly, what factors determine the fetal exposure? Furthermore, because the vast majority of fetal exposure data are obtained at the time of term or near-term delivery, fetal drug exposure at early gestation is unknown.

Clearly, alternative approaches are needed to close these gaps in knowledge. One of the means to overcome these ethical and logistical constraints is to use physiologically-based pharmacokinetic (PBPK) modelling and simulation (M&S) approaches to predict drug disposition in the fetoplacental unit. PBPK models are mathematical models that depict individual or grouped organs as compartments interconnected by the systemic circulation. Physiological parameters (such as blood flows, tissue volumes), drug-specific parameters (ADME properties, plasma protein binding) as well as the associated population variability are incorporated to predict the disposition of drugs in the populations of interest.

In the past, many fetal PBPK models have been published. For example, Yoon et al. constructed a maternal-fetal PBPK model for manganese during human gestation and lactation. Manganese drug-specific parameters were either obtained from human data or extrapolated from rat data. The predicted fetal blood concentration at the end of pregnancy was close to the cord blood concentrations observed from several clinical studies (Yoon et al., 2011). Loccisano et al. developed a maternal-fetal PBPK model for perfluorooctanoic acid (PFOA) and perfluorooctane sulfonate (PFOS). The fetal portion of this model contains the placenta, fetal plasma, amniotic fluid, and the rest of the fetal body. Transfer of both PFOA and PFOS across the placenta was assumed to be a simple

diffusion process and the associated rate constants were the same as those estimated in rats from their previous work. For both compounds, the model-predicted concentrations in maternal plasma and fetal cord blood and the fetal: maternal plasma concentration ratios were all within a factor of 2 of the reported ranges.(Loccisano et al., 2013) While these published fetal PBPK models proved some success in predicting prenatal exposure to various environmental toxins and teratogenic substances, upon close examination, none of them are suitable for predicting the disposition of pharmaceutical agents. Their limitations include, but are not restricted to:

- Incomplete inclusion of pregnancy-caused changes in maternal and fetal physiology: These models do not incorporate several aspects of fetoplacental anatomy that differ significantly from those of adults (e.g. drug transporters on the placenta, unique fetal liver-bypassing circulation, fetal swallowing). One example is the distinct physiological milieu of the fetal liver. Fetal hepatic circulation differs substantially from that of the adult. The umbilical vein serves as the major supplier of fetal hepatic blood, rather than the portal vein. It drains the oxygenated blood from the placenta to perfuse fetal liver, with ~30-70% of the umbilical venous blood flow shunted to the fetal systemic circulation via the ductus venosus. This anatomical difference may result in differing first pass effect in the fetus and is important to account for. However, published fetal PBPK models have ignored this distinct feature of fetal hepatic circulation.
- Lack of known inter-individual variability in maternal drug disposition: The observed differences in maternal plasma drug C-T profile across individuals originated from the differing ADMET processes across individuals. Typically, to

account for these inter-individual variabilities, *a priori* variation of physiological parameters and drug-specific parameters is performed. Then, the expected PK in a population of virtual individuals, rather than in an average subject, can be simulated using a PBPK model. For example, the Simcyp® population simulator uses a correlated Monte Carlo approach to account for variabilities in demographic, anatomical, and physiological parameter(Jamei et al., 2009). To date, none of the published fetal PBPK models has taken this population approach. In contrast, in our m-f-PBPK model, interindividual variability in maternal physiology and ADME characteristics were systematically imported from the Simcyp® population simulator (see **Chapter 5**).

- Exclusion of fetal body compartments important for disposition of therapeutic drugs: According to the principle of parsimony, the development of any model, including PBPK models, should value both descriptive accuracy and simplicity. This explains why some published fetal PBPK models only contain a minimum number of body compartments that are important to the distribution and disposition of the chemicals of interest. While in the above mentioned cases, such structure is sufficient to serve the intended purpose of predicting fetal exposure to environmental toxins, the exclusion of certain body compartments (e.g. placenta, fetal liver) will most likely lead to inaccurate prediction of fetal disposition of therapeutic drugs as many of them are subject to placental drug transport and/or fetal metabolism.

Recently, our lab has successfully refined and verified a mechanistic maternal Physiologically Based Pharmacokinetic (m-PBPK) Model during pregnancy that can predict the disposition of drugs cleared by one or more CYP enzymes(Ke et al., 2012; Ke

et al., 2013a). However, because it only contains a lumped tissue compartment representing the placenta and fetus, this model cannot be used to predict fetal exposure to drugs. Therefore, the goals of the investigation presented in **Chapter 4** were to: (1) develop a m-f-PBPK model by incorporating a physiologically relevant fetal-PBPK into our previously verified m-PBPK; (2) illustrate that the UV:MP ratio does not necessarily represent the extent of fetal drug exposure; (3) identify key factors that can modify fetal drug exposure; and (4) predict the impact of gestational age on fetal drug exposure. The necessity of individual goals is further explained in in the introduction of **Chapter 4**. This chapter is formatted as manuscript per submitted with slight modifications. Due to the word limit, information on the general background on fetal physiology and ontogeny could not be included and thus is provided in the sections that follow.

### 1.3.3 Fetal physiology

Over the course of pregnancy, a myriad of physiological changes take place in the coupled maternal-fetal pair. These changes include the rapid expansion of fetal organ sizes and blood flows, the placental vasculature and surface area, and the development of enzymes and membrane proteins in the fetoplacetnal unit. Particularly, the human placenta serves as the sole link between the fetus and the mother that mediates the exchange of oxygen, nutrients, and necessary regulatory compounds. Throughout pregnancy, the development of the placenta is tightly synchronized with that of the fetus, rendering it an inseparable part of the fetoplacental unit. It is important to bear in mind that fetal exposure to drugs used by the mother depends not only on the maternal plasma drug C-T profile, but also on the rate and extent at which the xenobiotic molecules cross the placenta barrier and the subsequent fetal disposition (e.g. fetal metabolism).

Therefore, the above mentioned physiological changes in both the mother and in the fetoplacental unit need to be incorporated into our m-f-PBPK model.

The longitudinal patterns in maternal physiological parameters during pregnancy have been summarized in a recent literature meta-analyses (Abduljalil et al., 2012). These reported gestational-age dependent changes in maternal physiology have been incorporated into our verified maternal pregnancy PBPK (Ke et al., 2012; Ke et al., 2013a; Ke et al., 2013b) and thus are not further elaborated here. In contrast, to our knowledge, a systematic literature review on the gestational age-dependent changes in fetoplacental physiological parameters necessary to populate a fetal PBPK model was lacking and needed to be conducted (see **Chapter 4**). To provide context regarding developmental processes occurring in the fetoplacental unit, major developmental timelines and the current knowledge regarding the ontogeny of DMEs and drug transporters in the fetoplacental unit is reviewed in the following subsections.

#### 1.1.3.1 Major developmental timelines of the human fetus

Human prenantal development is a continuous process that averages ~38 weeks beginning from fertilization. In clinical settings, the start of gestation is usually counted from the first day of the last menstrual cycle, resulting in a gestation of ~40 weeks. For clarification, it is the gestational age (2 weeks plus post-conceptional age), rather than the post-conceptional age that refers to the length of pregnancy, that is used clinically and therefore throughout this thesis. By convention, human prenatal development is divided into two distinct periods: the embryonic period extends from gestational weeks (GWs) 2 to 10, and the remainder of pregnancy (beyond the end of GW 10) called “the fetal period” (Polin et al., 2004).

The formation of most internal organs and external body structures begins during the embryonic stage. It is worth mentioning that; morphogenesis of most organs is complete by the end of embryonic period with a few exceptions, such as the brain and the spinal cord. Major time lines of fetal organ development are summarized in **Table 1.2**. An important point one must be bear in mind is that the attainment of the gross form of an organ does not necessarily warrant the fully functioning of the organ. For example, the fetal kidneys closely resemble that of the newborn as early as GW5, but the formation of glomeruli (blood filtering capillaries) in the kidneys is not completed until GW 32. The maturation of glomerular filtration and the development of renal proximal tubule active transport systems continue through birth and well beyond.

The final and longest stage of prenatal development is the fetal period. At the end of GW10, the precursors for most organs have already formed. Organ growth and differentiation continues during the fetal period. The fetal period is characterized by the rapid expansion in organ sizes typically in a nonlinear fashion. In addition to organ growth, cell differentiation and the development of complex enzyme and membrane protein systems (see below) also take place in various organs. Although the fetus is thought to be less sensitive to teratogens compared to the embryo, exposure to environmental toxins or drugs can still cause abnormalities or minor congenital malformations. For instance, the critical period for brain growth and development begins from GW3 and lasts until GW16. However, since the functional differentiation of brain continues until the end of gestation, exposure to teratogens during the fetal period can produce mental retardation (Chung, 2004)

### 1.1.3.2 Fetoplacental ontogeny of DMEs and drug transporters

Through modeling and simulation we have illustrated that fetoplacental metabolism or placental drug transport will affect fetal plasma drug concentrations when these clearance pathways become large relative to the transplacental passive diffusion clearance of the drug. Therefore, quantifying these various clearance pathways and incorporating such information into our m-f-PBPK model is necessary to predict fetal disposition of drugs. A drug must first cross the placenta to gain access to fetal circulation. Therefore, for drugs undergoing metabolism and/or transport processes in the placenta, the placenta functionally resembles the "fetal gut". Once the drug enters the fetal blood, its ultimate fate is largely determined by metabolism and transport mediated by fetal DMEs and drug transporters. The current literature shows that the placenta is richly endowed with various drug transporters and that as in adults, the fetal liver is the main site expressing xenobiotic-metabolizing CYP isoforms with the greatest amounts compared with other fetal organs(Hakkola et al., 1996a; Hakkola et al., 1996b; Hakkola et al., 1998; Unadkat et al., 2004). Development of fetoplacental DMEs and drug transporters begins at the early stages of pregnancy and continue until birth. Importantly, their developmental patterns seem to vary for each isoform and each organ, thus posing two clinically relevant questions: To which extent does the expression and activity of these DMEs and drug transporters change as gestation proceeds? In addition, how will these changes translate into the plasma and tissue C-T profiles of drugs and subsequently efficacy/toxicities? The first question has been pursued by many toxicologists and pharmacologists in this field. Over the years, there have been great advances in understanding the ontogeny of fetoplacental DMEs and drug transporters (i.e. their gestational age-dependent changes in expression and activity). In particular, in our case, these data will aid in the modeling of

fetoplacental disposition of drugs that have significant metabolic and/or transport component, which will in turn help resolve the second question raised above. However, resources to understand the functioning of the placenta and fetal liver are limited, resulting in data scarcity in terms of the expression temporal patterns. The majority of studies have focused on transcript or protein expression, rather than activity. To summarize available information in the literature, a broad overview of literature whereby attention was placed upon what we know and what remains to be studied was conducted. The results are tabulated in **Tables 1.3** and **1.4**.

### 1.3.3 Model verification for drugs that passively diffuse across the placenta

The latest statistics show a steep rise in the use of medication during pregnancy. Between 2006 and 2008, about 82% of pregnant women took medication sometime during pregnancy and about 50% took medication during T1.(Mitchell et al., 2011) Naturally, fetal exposure to drugs becomes a concern as the fetus is exposed to drugs whenever the mother takes drugs, especially during the organogenesis period (gestational week 3-8). Thus it is important that fetal drug exposure be estimated throughout entire pregnancy, particularly during early gestation.

Although there has been significant progress in our knowledge of pregnancy and fetal development, there is a lack of adequate data on the safety and efficacy of commonly used approved medications for pregnant women and fetal exposure to these pharmacotherapeuctics due to, at least in part, the absence of fetal exposure data. The single time point fetal exposure data obtained at the time of delivery do not reflect fetal exposure unless at steady-state after intravenous infusion (see **Chapter 3** for details). In many cases, it is the fetal plasma C-T profile over time that is needed to assess drug

efficacy and/or toxicity. Furthermore, these term or near-term data cannot be readily extrapolated back into early gestation. As a result, there is a pressing need to quantitatively assess fetal exposure to drugs, not only at term but also during early gestation.

As indicated above, we have refined and verified a maternal pregnancy PBPK (m-PBPK) model that incorporates known changes in maternal physiology and activity of drug metabolizing enzymes. This m-PBPK model successfully predicted the plasma C-T profiles of drugs cleared by a single or multiple CYP enzymes in pregnant women.[4, 5] We further expanded the lumped fetoplacental tissue compartment into a full fetal PBPK (f-PBPK) model. Fetal organs important for drug disposition and the temporal patterns of fetal physiological changes (when available) were included in our maternal-fetal PBPK (m-f-PBPK) model. It has the capacity of including placental transport and fetoplacental metabolism of drugs when quantitative data on transporters and metabolic enzymes become available. Currently, in the absence of such information, verification of this model was limited to drugs that traverse the placenta predominantly via passive diffusion. Therefore, the primary goal of the study detailed in **Chapter 4** was to verify this m-f-PBPK model's performance for drugs that passively diffuse across the placenta. The secondary goal was to test the hypothesis that the *in vivo* passive diffusion clearance (CLPD) can be estimated using *in vitro* data. To accomplish these goals, midazolam was used as an *in vivo* calibrator and two other passive diffusion drugs, namely theophylline and zidovudine, were chosen as our verification drugs.

## 1.4 Introduction Summary

As described previously, the effect of pregnancy on disposition of drugs can result in clinical consequences and is in much need of further investigation. Our proposed studies in **Chapters 2** focus on identifying the key hormone(s) that results in the increased CYP3A activity during T3 and predicting the magnitude of induction in CYP3A activity during early gestation using an established *in vitro* model (HepaRG cells) and the gold standard (human hepatocytes). The results of these studies will provide an improved understanding that is essential in explaining the regulation of CYP3A during pregnancy. In addition, the predicted magnitude of CYP3A induction during T1 and T2 will also be of great value for future dose adjustments of CYP3A drugs during early gestation.

In addition, as elaborated in **sections 1.2** and **1.3**, the fetus is exposed to drugs ingested by the mother. Fetal exposure to drugs could have both beneficial and adverse clinical consequences but cannot be assessed until at the time of delivery. The presented novel m-f-PBPK model enables us to evaluate open questions that have long been asked, but unanswered. Using modeling and simulation, **Chapter 3** evaluates 1) whether the frequently reported UV:MP ratio can be utilized as a surrogate for fetal exposure relative to the mother ; 2) which drug-specific factors determine fetal exposure to drugs; and 3) how fetal exposure to the same dosing regimen varies with gestational age. **Chapter 4** verified the usefulness of this m-f-PBPK model with drugs that passively diffuse across the placenta. Using a proposed *in vitro*-to-*in vivo* extrapolation approach, this model predicted the maternal and fetal disposition of two validation drugs reasonably well. Taken together, the presented studies in **Chapters 3** and **4** are pivotal in a priori predicting fetal drug exposure during pregnancy and lay the groundwork for rational dosing regimen adjustments in the underrepresented pregnant population that have unmet medical needs.

**Table 1.1. Changes in the activity of DMEs and drug transporters during pregnancy**

| | Probe drug(s) | Effect of pregnancy on activity (compared to postpartum) | | | PK parameter | References |
|---|---|---|---|---|---|---|
| | | early | middle | late | | |
| DMEs | | | | | | |
| CYP1A2 | caffeine | ↓~30% | ↓~50% | ↓~65% | oral CL | (Tracy et al., 2005) |
| CYP2B6 | bupropion | N.D | ↔ | ↔ | hydroxyl-bupropion/ bupropion metabolic ratio* | (Fokina et al., 2016) |
| | efavirenz | N.D | N.D. | ↔ | oral CL | (Cressey et al., 2012) |
| CYP2C9 | phenytoin | ↑50% | ↑50% | ↑50% | Mean unbound apparent oral clearance CL | (Yerby et al., 1990; Kulo et al., 2013) |
| CYP2C19 | proguanil | N.D | N.D | ↓50% | proguanil/ cycloguanil metabolic ratio | (McGready et al., 2003) |
| CYP2D6 | metoprolol | | ↑80% | ↑200% | oral CL | (Ryu et al., 2016) |
| CYP2E1 | acetaminophen | N.D | N.D | ↑80% | paracetamol oxidative metabolic CL | (Kulo et al., 2013) |

| | | | | | | |
|---|---|---|---|---|---|---|
| CYP3A | midazolam | N.D | N.D | ↑99% | 1'-hydroxymidazolam formation CL | (Hebert et al., 2008) |
| UGT1A4 | lamotrigine | ↑197% | ↑236% | ↑248% | oral CL | (Fotopoulou et al., 2009) |
| | | | ↑>65% | ↑>65% | oral CL | (Tran et al., 2002) |
| Transporters | | | | | | |
| P-gp | digoxin | N.D | N.D | ↑107% | renal net secretory CL | (Hebert et al., 2008) |
| OAT1 | amoxicilin | N.D | ↑64% | ↑36% | renal net secretory CL | (Andrew et al., 2007) |
| OCT2 | metformin | N.D | ↑45% | ↑38% | renal net secretory CL | (Eyal et al., 2010) |

N.D. not determined; CL: clearance

* The authors detected that the fraction of bupropion eliminated as hydroxyl-bupropion glucuronide was higher in late pregnancy compared with postpartum.

**Table 1.2. Summary of the major timelines of fetal organogenesis**

| Gestational Week | Cardiovascular | Neural | Skin | Respiratory | GastroIntestinal | Liver | Kidney |
|---|---|---|---|---|---|---|---|
| 2 | Heart begins formation from mesoderm | | A single transparent layer of cells | | | | |
| 3 | Circulatory system function begins | Primary neurulation occurs and lead to development of the brain and spinal cord. | | | The anterior intestinal portal of the primitive gut grows into fetal foregut and (the primitive gut) | The fetal liver bud originating from the fetal foregut) start forming the hepatic diverticulum | |
| 4 | | | | | | | |
| 5 | | Neural groove and folds are first seen; major divisions of brain can be distinguished. | | | | Liver begins forming blood and producing lymphocytes | Kidneys appear |
| 6 | Heart begins to beat | | | laryngotracheal groove forms on the floor of foregut | | | |
| 7 | | | Epidermis becomes 2 layers | left and right lung buds resembles tubulo-acinous gland | | | Formation of urethra and production of urine |

| | | | | | | | |
|---|---|---|---|---|---|---|---|
| 8 | Separation of aortic arch and pulmonary aorta | | | | | | |
| 9 | | | Epidermis and then further differentiates into 3 layers | Completion of subsegmental bronchi structure | | Bile ducts became reorganized | Rupture of cloacture membrane |
| 10 | | cerebellum cell layer forms | | | Perforation of anal membrane | | |
| 12 | | | | | Intestines appear in abdomen | | |
| 13 | The first sulcus appears | | | | | | |
| 14 | | | | lungs appear glandular and begin to secrete surfactant | | | |
| 15-19 | | | All epithelial layers are reaching final arrangement | | | | |
| 20 | | | Skin is covered by vernix caseosa | | | | |
| 21 | | | Aeriderm disappears and stratum corneum | | | | |

| | | | | | | | |
|---|---|---|---|---|---|---|---|
| | | | develops as a result of skin keratinization | | | | |

References: (Polin et al., 2004; Hill, 2016)

**Table 1.3. Developmental expression of Phase I and Phase II enzymes in the fetal liver and placenta**

| Enzyme | Fetal liver | | | References | Placenta | | | References |
|---|---|---|---|---|---|---|---|---|
| | T1 | T2 | T3 | | T1 | T2 | Term | |
| CYP1A1 | R,P,A | R | N.D. | (Vyhlidal et al., 2013) | R,P,A | N.R. | R,P,A | (Hakkola et al., 1996a; Sitras et al., 2012) |
| CYP1A2 | N.D. | N.D. | N.D. | (Hakkola et al., 1998) | R | N.R. | N.D. | (Hakkola et al., 1996a; Hakkola et al., 1996b) |
| CYP2C 8/9/19 | P,A* | P,A* | P,A* | (Koukouritaki et al., 2004; Johansson et al., 2014) | R | N.R. | N.D. | (Hakkola et al., 1996a; Hakkola et al., 1996b) |
| CYP2D6 | N.R. | R,P,A | R,P, A | (Stevens et al., 2008) | R | N.R. | N.D. | (Hakkola et al., 1996a; Hakkola et al., 1996b) |
| CYP2E1 | N.D. | R,P,A | P | (Jones et al., 1992) | R[?],P,A[?] | N.R. | R,P[?],A[?] | (Hakkola et al., 1996a) |
| CYP3A4 | R** | P | P | (Hakkola et al., 2001; Fanni et al., 2014) | R,P | N.R. | R,P,A | (Hakkola et al., 1996a; Maezawa et al., 2010) |
| CYP3A5*** | R,P,A | R,P,A | R,P, A | (Shuster et al., 2014b; Vyhlidal et al., 2015) | R,P | N.R. | R,P ,A[?] | (Hakkola et al., 1996a) |

| | | | | | | | | |
|---|---|---|---|---|---|---|---|---|
| CYP3A7 | R,P,A | R,P,A | R,P, A | (Stevens et al., 2003; Leeder et al., 2005; Shuster et al., 2014b) | R,P | N.R. | $R^{?}$ ,P ,$A^{?}$ | (Hakkola et al., 1996a; Maezawa et al., 2010) |
| CYP19 | P,A | P,A | | (Doody and Carr, 1989; Toda et al., 1994) | N.R. | N.R. | R,P,A | (Toda et al., 1994; Deshmukh et al., 2003) |
| SULT1A1 | N.R. | P,A | P,A | (Richard et al., 2001) | N.R. | P,A | P,A | (Stanley et al., 2001) |
| SULT1A3 | N.R. | P,A | P,A | (Richard et al., 2001) | N.R. | P,A | P,A | (Stanley et al., 2001) |
| SULT1E1 | N.R. | N.R. | R,P, A | | N.R. | P,A | P,A | (Stanley et al., 2001) |
| SULT2A1 | N.R. | N.R. | P,A | | N.R. | P,A | P,A | (Stanley et al., 2001) |
| UGT1A | N.R. | A | A | (Leakey et al., 1987; Burchell et al., 1989) | R,P | N.R. | $R,P^{+}$ | (Collier et al., 2002; Collier et al., 2004; Reimers et al., 2011) |
| UGT2B | R | A | R,A | (Pacifici et al., 1982; Leakey et al., 1987; Court et al., 2012; Ekstrom et al., 2013) | R,P | N.R. | R,P,A | (Collier et al., 2002; Collier et al., 2004) |
| GSTA1/2 | P | R | N.R. | (Pacifici et al., 1988; Shao et al., 2007) | N.R. | N.R. | N.R. | |

| | | | | | | | | |
|---|---|---|---|---|---|---|---|---|
| GSTM3/4/5 | N.R. | R | N.R. | (Shao et al., 2007) | N.R. | N.R. | N.R. | |
| GSTP1 | P | P,R | N.R. | (Shao et al., 2007) | N.R. | N.R. | N.R. | |
| GSTT1 | N.D. | N.D./R | N.R. | (Shao et al., 2007) | N.R. | N.R. | N.R. | |

R: mRNA; P: protein, A: activity; N.D.: not detected; N.R.: not reported

* CYP2C9 and CYP2C19 isoforms were detected.

**CYP3A4 mRNA was only detected in a subset of fetal liver samples.(Hakkola et al., 2001)

***CYP3A5 mRNA and protein expression was found to substantially vary among a panel of fetal liver samples and may be attributed to genetic variations and other factors such as environmental exposures and epigenetic alterations. (Vyhlidal et al., 2015)

+ While Collier et al. failed to detect UGT1A isoforms in human term placentae, Reimer et al. demonstrated UGT1A4 protein in term placenta and possibly another UGT1A isoform.

**Table 1.4. Developmental expression of Phase I and Phase II enzymes in the placenta**

| Transporter | T1 | T2 | T3 | Localization in placental syncytiotroph-oblast | Longitudinal Trend | References |
|---|---|---|---|---|---|---|
| P-gp | R,P | N.R. | R,P,A | Apical | ↓ | (Mathias et al., 2005) |
| BCRP | R,P | R,P | R,P,A | Apical | ↔ /↑ | (Mathias et al., 2005; Yeboah et al., 2006; Mao, 2008) |
| MRP1 | R | N.R. | R,P,A | Basal | ↑ | (St-Pierre et al., 2000; Nagashige et al., 2003; Pascolo et al., 2003; Vaidya et al., 2009) |
| MRP2 | N.R. | N.R. | R,P,A | Apical | ↑* | (Meyer zu Schwabedissen et al., 2005a; May et al., 2008) |
| MRP3 | R | N.R. | R | Apical | ↑ | (Patel et al., 2003) |
| MPR5 | N.R. | R,P | R,P | Basal | ↓ | (Meyer zu Schwabedissen et al., 2005b) |
| MRP5 | N.R. | R,P | R,P | Basal | ↓ | (Meyer zu Schwabedissen et al., 2005b) |

| | | | | | | |
|---|---|---|---|---|---|---|
| SERT | N.R. | N.R. | R,P | Apical | N.R. | (Ramamoorthy et al., 1993; Viau et al., 2009) |
| NET | N.R. | N.R. | R | Apical | N.R. | (Bottalico et al., 2004) |
| ENT1 | N.R. | N.R. | P | Apical | N.R. | (Barros et al., 1995; Griffiths et al., 1997a) |
| ENT2 | N.R. | N.R. | P | Basal | N.R. | (Griffiths et al., 1997b) |
| CNT1 | N.R. | N.R. | P,A | Both apical and basal | N.R. | (Errasti-Murugarren et al., 2011) |
| OCT1 | N.R. | N.R. | R,P | N.R. | N.R. | (Lee et al., 2013) |
| OCT2 | N.R. | N.R. | R,P | N.R. | N.R. | (Lee et al., 2013) |
| OCT3 | R,P | R | R,P,A | Basal | ↔ | (Sata et al., 2005) (Lee et al., 2013) |
| OATP1A2 | R | N.R. | R | Apical | ↓ | (Patel et al., 2003) |

R: mRNA; P: protein, A: activity; N.R. Not reported;

* full term vs pregerm (32-37 GW)

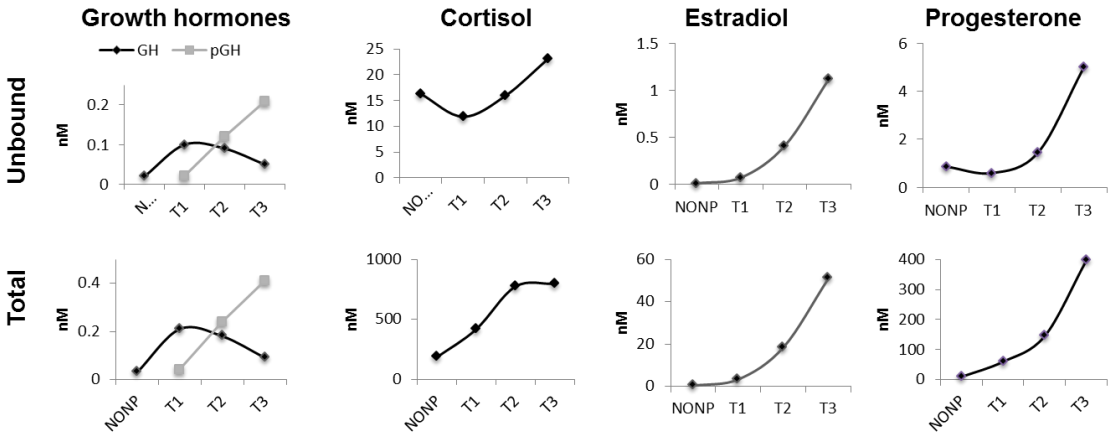


**Figure 1.1. Longitudinal changes in the circulating plasma unbound or total concentrations of pregnancy related hormones reported in pregnant women.**

NONP: nonpregnant.

# Chapter 2 Prediction of Gestational Age-Dependent Induction of In Vivo Hepatic CYP3A Activity Based on HepaRG Cells and Human Hepatocytes

The work presented in this chapter was previously published
in
Drug Metabolism and Disposition 43:836-842(2015)

## 2.1 Abstract

In pregnant women, CYP3A activity increases by 100% during the third trimester (T3). Due to logistical and ethical constraints, little is known about the magnitude of CYP3A induction during the first (T1) and second (T2) trimesters. Our laboratory has shown that sandwich-cultured human hepatocytes (SCHH) and HepaRG cells have the potential to predict the magnitude of *in vivo* induction of CYP3A activity likely to be observed in T1 and T2. Therefore, we incubated SCHH and HepaRG cells with plasma concentrations of various pregnancy-related hormones (PRHs, individually or in combination) observed during T1, T2, or T3 in pregnant women. Then, CYP3A activity was measured by 1'-OH-midazolam formation. In all three trimesters, only cortisol (C) consistently and significantly induced CYP3A activity, while other individual hormones (progesterone, estradiol or growth hormones) failed to induce CYP3A activity. At physiologically relevant 1X plasma concentrations, the magnitude of CYP3A induction by C or the combination of all PRHs did not change significantly with gestational age. The pattern of induction of CYP3A activity in SCHH by the hormones was similar to that in HepaRG cells. Based on these data, we conclude that C remains the major inducer of CYP3A activity earlier in gestation. Moreover, we predict that the magnitude of CYP3A induction during T1 and T2 will be similar to that observed during T3 (~100% increase vs. postpartum). This prediction is consistent with the observation of similar increase in T2 and T3 oral clearance of indinavir (a CYP3A cleared drug) vs. postpartum.

## 2.2 Introduction

Despite the general apprehension surrounding the use of drugs during pregnancy, a pregnant woman is frequently prescribed medication to treat a variety of preexisting chronic conditions (e.g. HIV infection, epilepsy, hypertension, solid organ transplantation), acute conditions (e.g. influenza), or pregnancy-related conditions (e.g. nausea, gestational diabetes or hypertension). If left untreated, these conditions could have deleterious consequences to the mother and/or her fetus. Therefore, it is not surprising that between 2006-2008, about 82% of pregnant women took medication sometime during pregnancy and about 50% took medication during the first trimester (Mitchell et al., 2011).

Pregnancy is associated with a myriad of physiological changes including hepatic metabolism (Abduljalil et al., 2012). Amongst these is approximately a 2-fold induction of CYP3A activity during the third trimester (T3), as measured by 1'-OH-midazolam formation clearance (Hebert et al., 2008). Based on genotyping data and modeling and simulation, we have shown that this induction of CYP3A activity is primarily due to induction of hepatic CYP3A4 activity (Hebert et al., 2008; Ke et al., 2012). Many drugs routinely prescribed to pregnant women are cleared by CYP3A enzymes, such as protease inhibitors (e.g. ritonavir), antihypertensive drugs (e.g. nifedipine), and hypoglycemics (e.g. glyburide). The magnitude of induction in CYP3A activity observed during T3 can result in subtherapeutic plasma concentrations of drugs such as the HIV drug, indinavir (Unadkat et al., 2007). Logistical and ethical constraints make it difficult to conduct prospective mechanistic studies in pregnant women using validated CYP3A substrates, especially in 1$^{st}$ (T1) or 2$^{nd}$ trimester (T2). As a result, the magnitude of

induction of CYP3A activity during T1 orT2 is not known. This lack of information makes it difficult for clinicians to design dosing regimens of CYP3A cleared drugs during T1 or T2.

The plasma concentrations of several pregnancy-related hormones (PRHs) rise substantially as gestation proceeds (Table 2.1). Our laboratory has previously demonstrated that a cocktail of PRHs, (the hormone combination containing cortisol (C), progesterone (P), 17β-estradiol ($E_2$), and placental growth hormone (PGH)/growth hormone (GH); hereafter referred to as the PRH cocktail), at their T3 plasma concentrations observed in pregnant women, induced CYP3A activity in sandwich cultured human hepatocytes (SCHH) to an extent comparable to that observed *in vivo* during T3. Of all these hormones, cortisol was the most potent inducer of CYP3A activity in SCHH. Additionally, the induction pattern observed in SCHH was replicated in HepaRG cells (Papageorgiou et al., 2013). Both these *in vitro* models demonstrated their potential to predict the magnitude of CYP3A induction in early pregnancy. Therefore, we hypothesized that the magnitude of *in vivo* hepatic CYP3A induction during T1 and T2 can be quantitatively predicted from studies in SCHH or HepaRG cells exposed to PRHs at plasma concentrations observed in pregnant women (for brevity, referred to as "concentrations" hereafter) during T1 and T2. The studies presented here were conducted in HepaRG and SCHH to examine the temporal relationships between concentrations of PRHs and induction of CYP3A activity over the course of pregnancy, and, based on these data, to predict the magnitude of induction in CYP3A activity during T1 and T2.

## 2.3 Materials and Methods

### 2.3.1 Chemicals and Reagents

Growth hormone, 17β-estradiol, cortisol, progesterone, diazepam were purchased from Sigma-Aldrich (St. Louis, MO); placenta growth hormone was obtained from GenWay Biotech, Inc. (San Diego, CA). Midazolam, 1-OH-midazolam, 1-OH-midazolam-$d_4$, 17β-estradiol-$d_5$ were purchased from Cerilliant Corporation (Round Rock, TX). Acetic acid (ACS grade), acetonitrile (MS grade) were obtained from Fisher Scientific (Pittsburgh, PA). William Medium E (WME), Dulbecco's Phosphate-Buffered Saline (DPBS), GlutaMax-I, Penicillin-Streptomycin (10 000U/mL), and Insulin-Transferrin-Selenium (ITS) were purchased from Life Technologies (Carlsbad, CA). Matrigel® (growth factor reduced, phenol red free) was obtained from BD Biosciences (San Jose, CA).

### 2.3.2 Hormone Depletion in HepaRG cells or SCHH

In-house differentiated HepaRG cells or SCHH in 96 well plates were incubated (in triplicate or duplicate, respectively) with varying concentrations of PRHs (Table 3). Media was sampled at various time points up to 12 hours. To quantify cortisol or progesterone, media samples (15 µL) were protein precipitated with 85 µL acetonitrile containing diazepam (internal standard, 10ng/mL) and centrifuged at 3000g for 15 min prior to LC/MS-MS analysis. To quantify estradiol, media samples (15 µL) were spiked with 15 µL estradiol-$d_5$ (internal standard, 100ng/mL in 10% acetonitrile), extracted with 800 µL methyl tertiary butyl ether, and then centrifuged at 3000g for 15 min. The organic phase was evaporated under nitrogen. The dried residue was reconstituted and

derivatized using dansyl chloride to enhance electrospray ionization following the procedure described previously (Kushnir et al., 2008).

The above samples were analyzed by LS-MS/MS using an Agilent 1290 Infinity UPLC system coupled to an Agilent 6400Triple Quad mass spectrometer. An Acquity UPLC BEH $C_{18}$ Column (1.7 µm, 2.1 mm X 50 mm; Waters Corporation, Milford, MA) was used with the mobile phase consisting of 0.1% acetic acid (v/v) in water (A) or 0.1% acetic acid (v/v) in acetonitrile (B)( total flow rate0.25 $mL/min^{-1}$). For cortisol and progesterone assay, the following linear gradient was used: 80% mobile phase A, 0-0.3min; 80-20%, 0.3-1.5min; 20%, 1.5-2.5min; 20%-80%, 2.5-2.6min; 20%, 2.6- 4min. Multiple Reaction Monitoring (MRM) pairs selected for cortisol, progesterone, and diazepam were 363.2/121.1, 315.2/97.1, and 285/193 respectively. For estradiol assay, the following gradient was chosen: 50% mobile phase A, 0-0.1min; 50-5%, 0.1-0.7min; 95%, 0.7-2.5min; 95%-50%, 2.5-2.6min; 50%, 2.6- 4min. MRM pairs selected for dansyl-estradiol and dansyl-estradiol-$d_5$ were 506.1/171.1 and 511/171.1, respectively.

### 2.3.3 Hormonal Treatment of HepaRG Cells or SCHH

Proliferative state HepaRG cells were kindly provided by Biopredic International (Overland Park, KS). The cells were in-house expanded and differentiated according to the provider's protocols. Differentiated HepaRG cells were cultured in 96 well plates at a density of ~ 0.8 million cells/mL. Since the commercially available HepaRG maintenance and induction medium supplements contain hydrocortisone succinate, a CYP3A inducer, we conducted induction studies in the absence of hydrocortisone succinate to avoid confounding interpretation of our data (Papageorgiou et al., 2013). In brief, the differentiated HepaRG cells were maintained for 72 h in WME supplemented

with GlutaMAX-I, ITS, and Pennicillin-Streptomycin. At the end of maintenance period, the medium was removed and cells were treated with control (a cocktail of C, GH, $E_2$ and P at their unbound concentrations observed in non-pregnant women; hereafter referred to as "CTRL") or various PRHs individually or in combination at unbound, 1X, or 10X T1, T2, or T3 concentrations (Table 2.1). Because some of the hormones were depleted, the actual incubation concentrations were adjusted, based on their half-life of depletion (Table 2.3), such that the AUC/$\tau$ of the hormone media concentration approximated the values listed in Table 2.1. In addition, to compensate for this depletion, during the 72h induction period with the PRHs, induction media were renewed every 12 h (see Results). When comparing CYP3A activity by T1, T2 or T3 concentrations, these experiments were conducted on the same day with the same batch of HepaRG cells or SCHH. In all the experiments, a positive control (10 µM rifampin, RIF) and a vehicle control were included. All incubations contained 0.1% pH 9 DI $H_2O$ and 0.9% methanol. CYP3A activity in these HepaRG cells was determined as described below. Except for CTRL (n=6), experiments were performed in triplicate.

Cryopreserved human hepatocytes from three premenopausal donors (Table 2.2) were either commercially procured (Hu1587 and Hu1595; Life Technologies, Carlsbad, CA) or provided *gratis* (Hu4059; TRL, Research triangle, NC). Hepatocytes were plated in collagen-coated 96 well plates at a density of ~ 0.7 million viable cells/mL and overlaid with Matrigel® according to the manufacturer's instructions. Since the hepatocyte medium supplements normally contain dexamethasone (DEX), a well-documented glucocorticoid CYP3A inducer, we omitted the addition of DEX to the maintenance and induction media. At the end of 72 h maintenance period, the SCHH were treated

(including change of media) as described above for HepaRG cells. CYP3A activity in these SCHH was determined as described below. All experiments were performed in triplicate.

### 2.3.4 Cortisol Concentration-CYP3A activity induction Relationship in SCHH

SCHH (batch Hu1587) in collagen-coated 96 well plates were maintained in DEX free medium for 72 h and then treated with CTRL treatment or various concentrations of cortisol, ranging from T1 unbound concentration to 50X T3 concentrations as described above (concentrations were adjusted, where appropriate, to compensate for depletion). CYP3A activity in these SCHH was determined as described below. CYP3A activity in these SCHH was determined as described below. All treatments were performed in duplicate except for the unbound cortisol concentrations and CTRL treatments (n=3).

### 2.3.5 CYP3A Activity Assay

At the end of the induction period, induction media were aspirated, HepaRG cells or SCHH were rinsed twice with pre-warmed DPBS (~150 µL) and incubated for 60 min (HepaRG cells) or 20 min (SCHH) with 2 µM midazolam dissolved in serum-free WME. Then, an equal volume of ice-cold acetonitrile containing 10 nM 1'-OH-midazolam-d4 (internal standard) was immediately added to the supernatant and assayed by LC-MS/MS as described previously (Shirasaka et al., 2013).

### 2.3.6 Statistical and Data Analysis

Data are expressed as mean ± SD values unless otherwise stated. One-way analysis of variance (ANOVA) followed by post hoc tests (Dunnett's test when the PRH treatment groups were compared to the CTRL treatment or Tukey's test when PRH treatment

groups were compared with each other) were performed. The $E_{max}$ and $EC_{50}$ of induction of CYP3A activity by cortisol was estimated by fitting the simple $E_{max}$ or the sigmoid $E_{max}$ model to the concentration-response data using nonlinear regression (Graphpad Prism 5.0, La Jolla, CA). The baseline value of induction ($E_0$) was fixed to 1. The model with the smaller AIC value was selected (Ludden et al., 1994).

## 2.4 Results

### 2.4.1 Hormone depletion when incubated with HepaRG or SCHH

In HepaRG cells, cortisol at the unbound concentration observed in non-pregnant women was depleted with a half-life of ~13 h, while at T3 1X and 10X concentrations, cortisol was not depleted (Table 2.3). In contrast, estradiol and progesterone were more rapidly depleted. To compensate for this depletion, the induction media in all future experiments (including SCHH) were renewed every 12h and the concentrations of the hormones in the media were adjusted so that the average concentration ($AUC/\tau$) approximated the corresponding average concentrations during pregnancy. GHs depletion was not measured as an assay to measure the depletion of PGH is currently not available.

### 2.4.2 Induction of CYP3A Activity in HepaRG cells by Cortisol or Cortisol plus other PRHs

A pilot study using T3 unbound, 1X, or 10X concentrations of individual PRHs was conducted. Except for cortisol, none of the PRHs induced CYP3A activity to a significant extent (Figure 2.1). Therefore, only cortisol and cortisol containing PRH combinations were included in all subsequent experiments described below (including SCHH).

As observed above, cortisol or cortisol plus other hormones consistently, significantly, but variably induced CYP3A activity at 1X or 10X (but not at the unbound) concentrations, compared with CTRL treatment (Figure 2.2). At 10X concentrations, treatments containing C+$E_2$ or C+ P induced CYP3A activity greater than C alone (Figure 2.2B, D, E). But, this greater induction was not consistently present in treatments containing GHs. Our positive control, 10 μM RIF, significantly induced CYP3A activity (range: 5~19-fold), whereas CYP3A activity in the presence of the vehicle control was not significantly different from CTRL (data now shown).

### 2.4.3 Gestational-Age Dependent Induction of CYP3A Activity in HepaRG Cells by Cortisol or PRH Cocktail

The magnitude of induction of CYP3A activity was not significantly different across the three trimesters at 1X concentrations of the hormones. At 10X concentrations, significant differences emerged (Figure 2.3D). PRH cocktail resulted in varying temporal patterns in different batches at 10X concentrations. No consistent cortisol or PRH cocktail concentration-dependent induction in CYP3A activity was observed.

### 2.4.4. Induction of CYP3A Activity in SCHH by Cortisol or Cortisol plus other PRHs

Similar to HepaRG cells, cortisol and PRH cocktail consistently, variably and significantly induced CYP3A activity in SCHH at 1X and 10X concentrations (and in 1 out of 3 donors at the unbound concentration, data not shown). In batch Hu1587 alone, treatments containing C+GHs or C+$E_2$ induced CYP3A activity greater than C alone (Figure 2.4, A-E). In all three batches, 10 μM RIF significantly induced CYP3A activity

(range: 9~16-fold). CYP3A activity in vehicle control was not significantly different from that observed in CTRL.

### 2.4.5 Gestational-Age Dependent Induction of CYP3A Activity in SCHH by Cortisol or PRH Cocktail

As in HepaRG cells, at 1X concentrations, induction of CYP3A in SCHH was independent of gestational age. At 10X concentrations, CYP3A induction was similar throughout all three trimesters except, in one batch (Hu1587), CYP3A activity was modestly increased (~30%) by PRH cocktail in T3 vs. earlier trimesters.

### 2.4.6 Concentration-Dependent Induction of CYP3A activity in SCHH by Cortisol

Cortisol induced CYP3A activity in SCHH (batch Hu1587) in a concentration-dependent manner. The simple $E_{max}$ model rather than the sigmoid $E_{max}$ model was considered to be the best model for the data based on the AIC value (AIC values: -43.624 and -35.716, respectively). At cortisol plasma concentrations spanning from T1 to T3, the induction of CYP3A activity reached a plateau and remained constant.

## 2.5 Discussion

Previously, we have shown that of all the PRHs studied, cortisol was the major inducer of CYP3A activity in HepaRG cells and SCHH at T3 concentrations (Papageorgiou et al., 2013). Consistent with these findings, cortisol remained the major inducer in HepaRG cells at T1 or T2 concentrations (Figures 2.2, 2.3). Therefore, all subsequent studies examined the induction of CYP3A activity by cortisol alone or in combination with other PRHs. We chose to use the combination of GH and PGH in our incubations as both are present during pregnancy. The plasma concentration of GH decreases while that of PGH

increases as pregnancy proceeds (Fuglsang and Ovesen, 2006). In addition, these two hormones interact with the same receptor with similar affinity (Baumann et al., 1991) and trigger the same intracellular signaling pathways (Silva et al., 2002). Since some of the hormones were rapidly depleted when incubated with HepaRG cells or SCHH, we adjusted the incubation concentrations of the hormones and frequency of change of media to account for this depletion.

Induction of CYP3A activity by cortisol or PRHs in HepaRG cells or SCHH was quite variable from batch to batch. The source of this variability is not clear but may be due to varying percent of hepatocyte-like cells vs. biliary cells between the different batches and passages in our in-house differentiated HepaRG cells (Schulze et al., 2012).

Interestingly, in general, the batch of cells demonstrating the highest CYP3A induction by RIF also exhibited the highest CYP3A induction by cortisol alone or in combination. But, this variability in induction of CYP3A activity by cortisol (or PRHs) cannot be quantitatively explained by induction in CYP3A activity by RIF. For example, in SCHH, at T3 1X concentration, cortisol induced CYP3A activity in batch Hu4059 ~4-fold greater than in batch Hu1595. In contrast, RIF induced CYP3A activity in batch Hu4059 only ~50% greater than that in batch Hu1595.

Incubation of HepaRG cells or SCHH with the unbound concentrations of PRHs observed during T1, T2 or T3 did not result in induction of CYP3A activity. Therefore, only the 1X and 10X concentration data are shown in Figures 2.2-2.5. Although there was some batch to batch variability; in general, the induction of CYP3A activity in HepaRG cells at 1X concentrations of cortisol alone was comparable to that when cortisol was combined with other PRH(s) (Figure 2.2A, C, E). Of note, at 10X

concentrations, induction of CYP3A activity with C+$E_2$ or C+P was greater than C alone. However, this was not always the case when induction in CYP3A activity by the triple combinations of hormones (e.g. C+GHs+P) or the PRH cocktail was compared with C alone.

Based on these observations and due to our previous data in SCHH on C+GHs demonstrating greater induction of CYP3A activity than C alone (Papageorgiou et al., 2013), the number of hormonal combination treatments examined in SCHH was reduced. Similar to HepaRG cells, despite interbatch variability, the magnitude of induction of CYP3A activity by dual hormone treatments or PRH cocktail was in general comparable to that by C alone at both 1X and 10X concentrations. One batch of SCHH (Hu1587) exhibited a modestly greater induction of CYP3A activity by the dual hormone treatments (C+$E_2$ or C+GHs) compared with C alone at 1X and 10X concentrations. At T1, T2 or T3 10X concentrations, the PRH cocktail induced CYP3A activity greater than C alone.

The pattern of induction observed above is consistent with our previous observations where cortisol alone was the major inducer of CYP3A activity in HepaRG cells or SCHH (Papageorgiou *et al.*, 2013). This work, together with our previous report, provides strong evidence that cortisol is a major inducer of CYP3A activity throughout pregnancy. Indeed, unequivocal data exist that glucocorticoids induce CYP3A activity in human hepatocytes and *in vivo* (Watkins et al., 1989; Lu and Li, 2001). However, the mechanism(s) by which this induction occurs is not clear. Evidence suggests that at low plasma concentrations of glucocorticoids, these hormones induce CYP3A activity via the glucocorticoid receptor (GR), while at supraphysiological concentrations, PXR is

involved (Lehmann et al., 1998; Pascussi et al., 2000). Aside from glucocorticoid receptor and PXR, multiple lines of evidence suggest that a PXR-independent mechanism(s) may be involved in induction of CYP3A activity {Schuetz, 2000 #2762;Zimmermann, 2009 #2763;Xie, 2000 #3482}. Others have also reported enhanced induction of CYP3A activity by cortisol in the presence of GH (Thangavel et al., 2011). They attributed this to greater activation and nuclear translocation of transcriptional factors (i.e. HNF-4α and PXR) and enhanced binding of these factors to CYP3A4 regulatory region (Thangavel et al., 2011). Previous studies have demonstrated that at supraphysiological concentrations estradiol or progesterone activates PXR (Handschin and Meyer, 2003; Mnif et al., 2007). However, this does not signify that estradiol, progesterone, or both, induces CYP3A activity at plasma concentrations observed in pregnant women. Indeed, consistent with our data, at these lower plasma concentrations of estradiol or progesterone, these hormones failed to consistently induce CYP3A activity in human hepatocytes (Choi et al., 2013).

Based upon the above data, we examined the induction of CYP3A activity by cortisol alone or by PRH cocktail at T1, T2, or T3 1X or 10X concentrations in both HepaRG cells and SCHH. Although the absolute magnitude of CYP3A induction varied between these two *in vitro* models, the induction of CYP3A activity by1X concentrations of cortisol or PRH cocktail was independent of gestational age (Figures 2.3 and 2.5). In contrast, at 10X concentrations, some significant differences manifested, but these differences were modest.

The plasma concentration of cortisol rises considerably as pregnancy proceeds. Cortisol plasma concentration increases from T1 to T2 by ~2-fold and then remain constant

during T3. But this increase did not translate into a significant difference in induction of CYP3A activity (Figure 2.3A, 2.3B; Figure 2.5A, 2.5B). To gain insight into this observation, we determined the relationship between cortisol concentration and induction of CYP3A activity in one batch of SCHH (Figure 2.6). The results show that at the total cortisol plasma concentration (181.5nM) observed in non-pregnant women (Lindholm and Schultz-Moller, 1973; Maroulis et al., 1976; Kalleinen et al., 2008; Matsuzaka et al., 2013) or in pregnant women during T1, T2, or T3, the CYP3A activity would be predicted to be induced by 45%, 120%, 170%, and 170% respectively. While the predicted induction in CYP3A activity during T1 appears numerically lower than that during T2 or T3, our experimental data show that this difference is not statistically significant (Figures 2.3 and 2.5). This is because at 1X cortisol concentrations spanning T1-T3, the induction of CYP3A activity appears to be approaching a plateau. Based on these data, we predict that the magnitude of CYP3A induction during T1 or T2 will be similar to that during T3 (~2-fold). Evidence in the literature supports our predictions. Although not an optimum CYP3A probe, urinary dextromethorphan/3-OH-morphinan ratio remains constant throughout pregnancy (Tracy et al., 2005). Also, the clearance of CYP3A substrates, indinavir and nifedipine, during T2, is comparable to that observed during T3 (Marin et al., 2007; Cressey et al., 2013).

In summary, this work, together with our previous report, provides strong evidence that cortisol is the major inducer of CYP3A activity throughout pregnancy in HepaRG cells and SCHH. Moreover, we predict that the magnitude of induction in CYP3A activity during earlier trimesters will be about 2-fold, similar to that in the third trimester. Although these predictions should ideally be validated with CYP3A probe studies, our

predictions are consistent with the limited clinical data on the disposition of CYP3A cleared drugs (dextromethorphan, nifedipine and indinavir) during T2 and T3. The mechanism(s) by which cortisol induces CYP3A activity remains unclear. Given the consistency between HepaRG cells and SCHH in the pattern of induction of CYP3A activity by PRHs, we propose that HepaRG cells can serve as a model to elucidate the molecular mechanism(s) by which cortisol induces CYP3A activity during pregnancy.

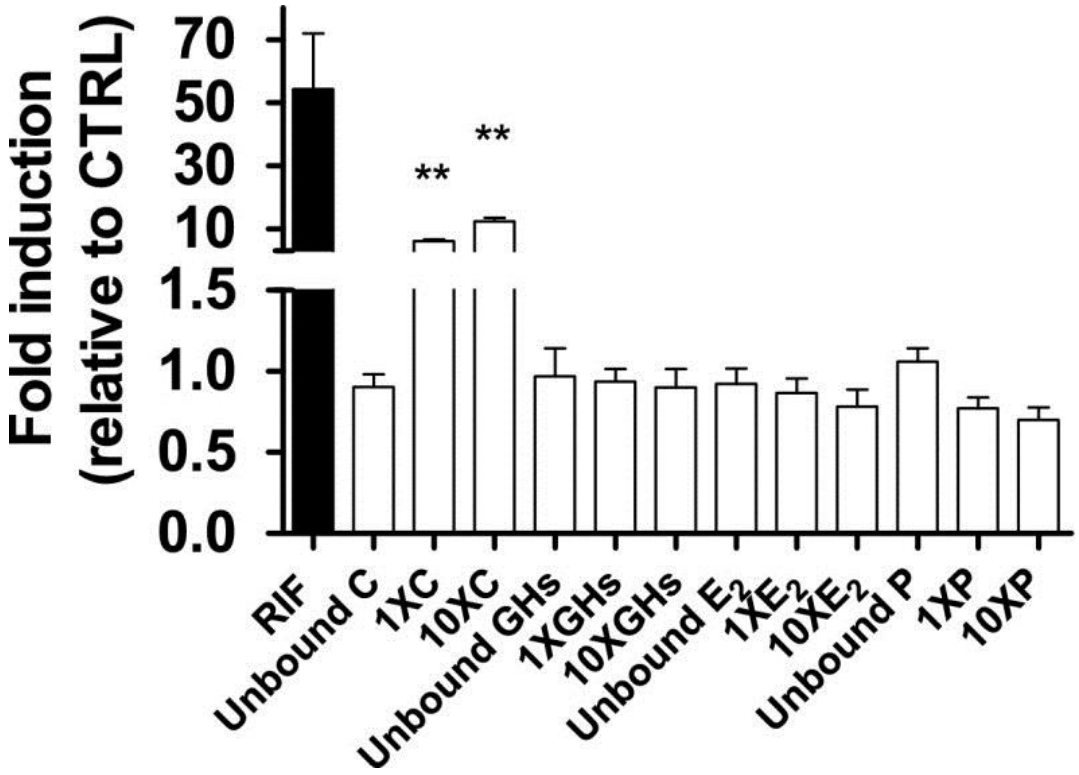


**Figure 2.1. CYP3A activity in HepaRG cells incubated with T3 plasma concentrations of individual PRHs observed in pregnant women or 10 μM RIF**.

Fold induction (mean ± S.D.; n = 3) is expressed relative to control treatment (CTRL, n = 6; unbound plasma concentrations of C + GH + E2 + P observed in nonpregnant women). Data were analyzed by one-way analysis of variance followed by Dunnett's test. *, $P < 0.05$; **, $P < 0.01$; ***, $P < 0.001$ compared with CTRL.

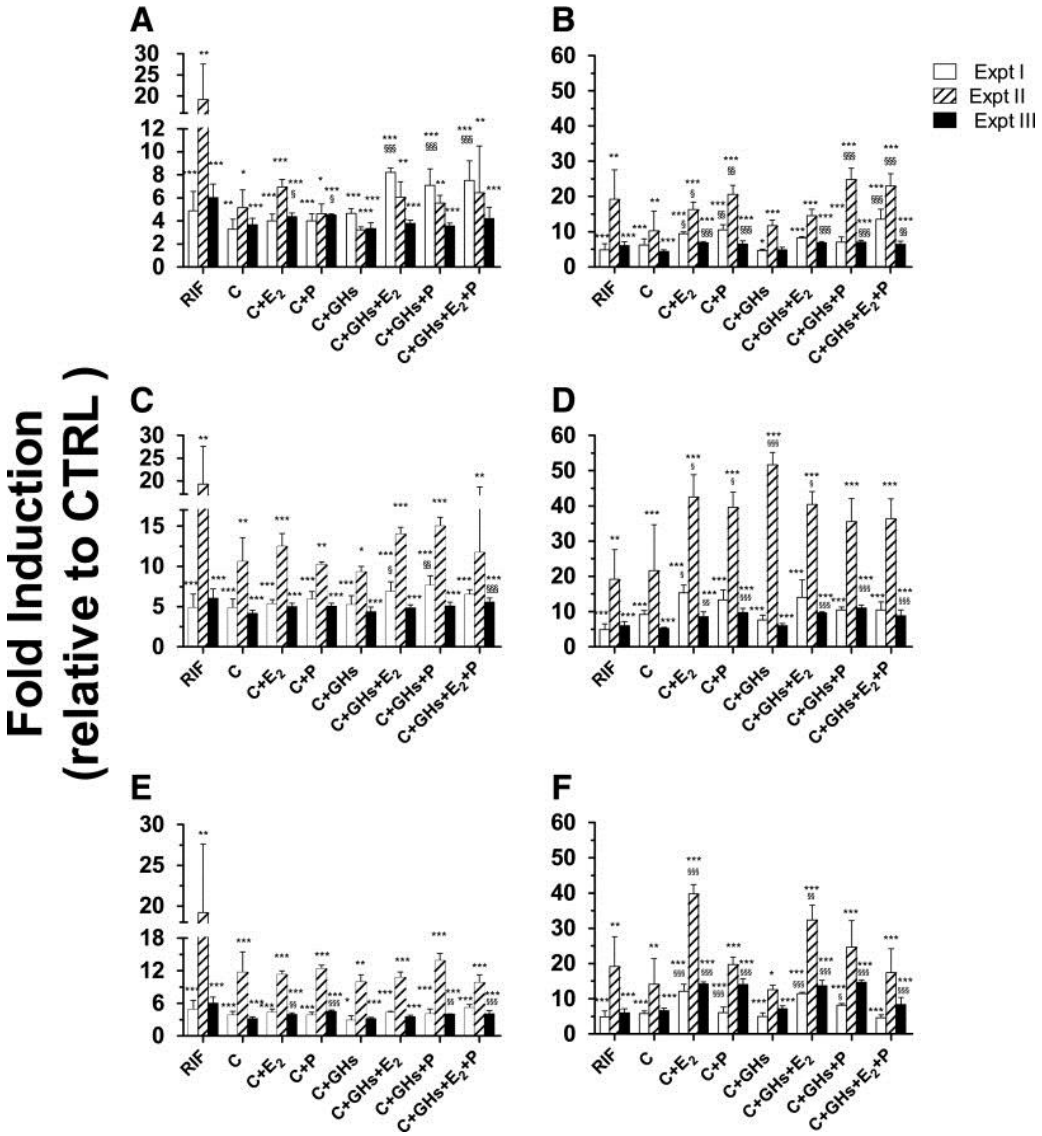


**Figure 2.2. CYP3A activity in HepaRG cells incubated with T1 (A, B), T2 (C, D), or T3 (E, F) at 1X (A, C, E) or 10X (B, D, F) plasma concentrations of PRHs observed in pregnant women or 10 µM Rifampicin (RIF)**. Fold induction (mean ± SD; n=3) is expressed relative to control treatment (CTRL, n=6; unbound plasma concentrations of C+GH+E2+P observed in non-pregnant women). Data were analyzed by one-way ANOVA followed by Dunnett's test. *, $p<0.05$; **, $p<0.01$; ***, $p<0.001$ compared with CTRL. §, $p<0.05$; §§, $p<0.01$; §§§, $p<0.001$ compared with cells exposed to C alone.

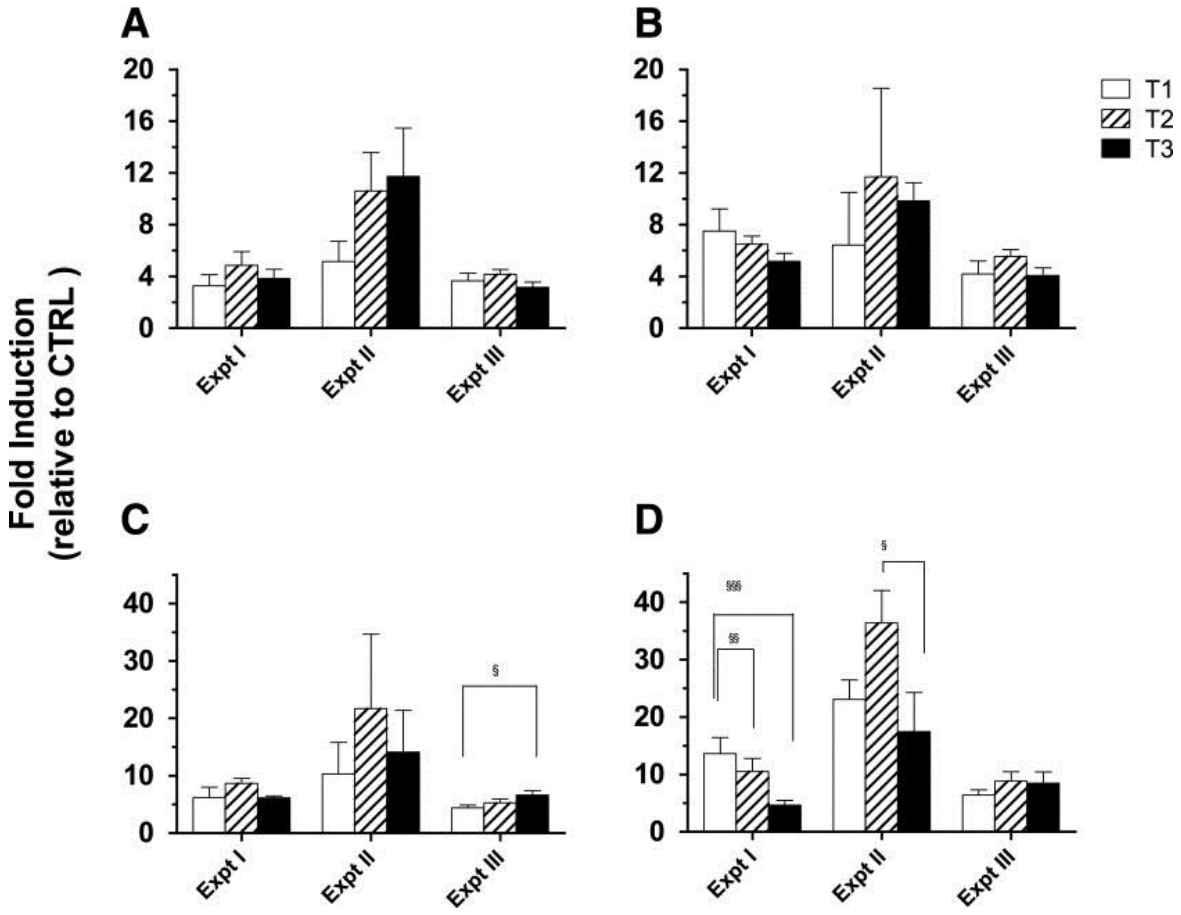


**Figure 2.3. CYP3A activity in HepaRG cells incubated with 1X or 10X plasma concentrations of cortisol (A and C respectively) or PRH cocktail (B and D respectively) observed in pregnant women**. Fold induction (mean ± S.D.; n = 3) is expressed relative to control treatment (CTRL, n = 6; unbound plasma concentrations of C + GH + E2 + P observed in nonpregnant women). Data were analyzed by one-way analysis of variance followed by Tukey's multiple comparison to detect any difference in the magnitude of CYP3A induction among T1, T2, and T3. §, $P < 0.05$; §§, $P < 0.01$; §§§, $P < 0.001$ compared with the indicated trimester.

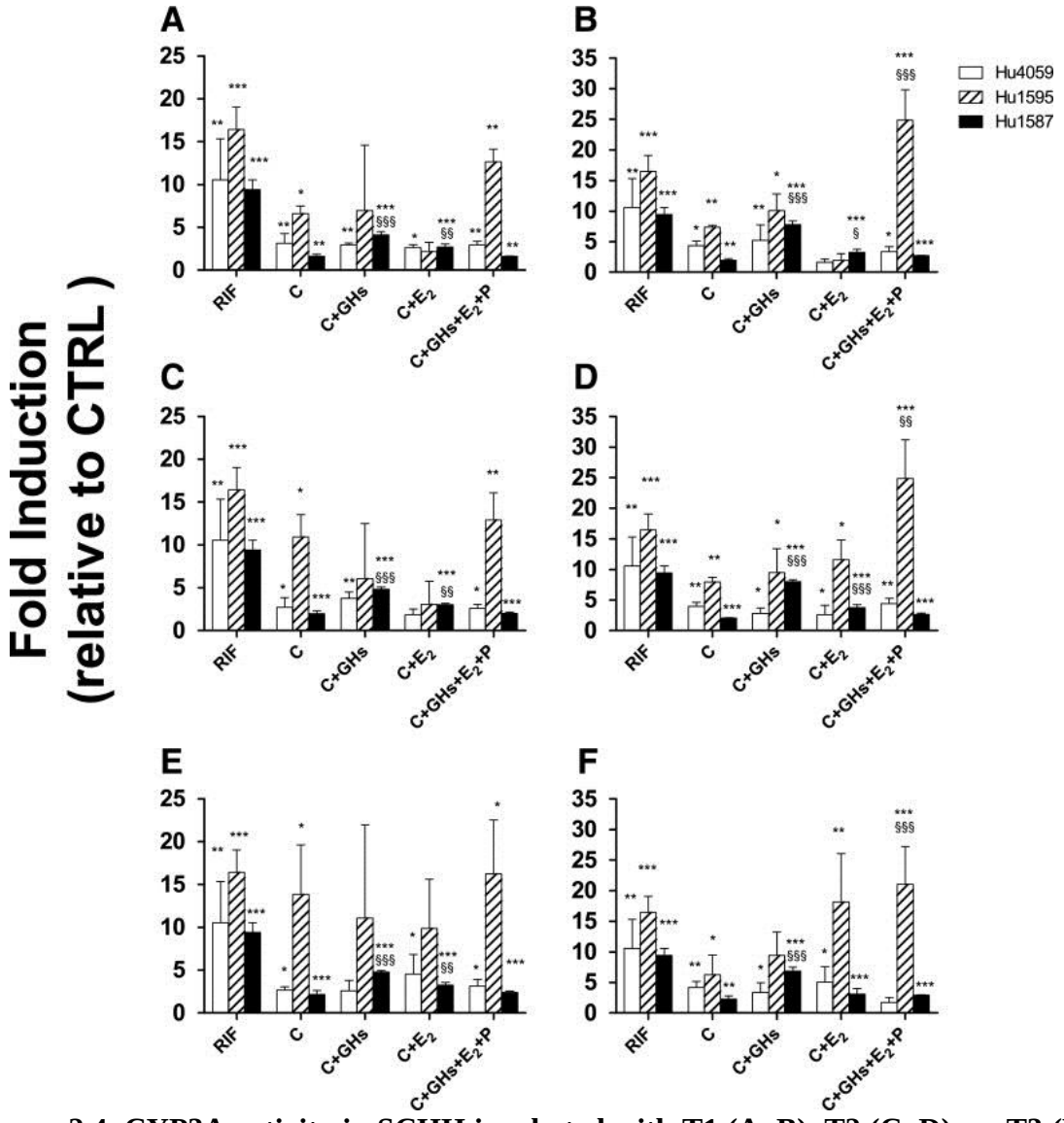


**Figure 2.4. CYP3A activity in SCHH incubated with T1 (A, B), T2 (C, D), or T3 (E, F) at 1X (A, C, E) or 10X (B, D, F) plasma concentrations of PRHs observed in pregnant women or 10 µM Rifampicin (RIF).** Fold induction (mean ± SD; n=3) is expressed relative to control treatment (CTRL; unbound plasma concentrations of C+GH+E2+P observed in non-pregnant women). Data were analyzed by one-way ANOVA followed by Dunnett's test. *, $p<0.05$; **, $p<0.01$; ***, $p<0.001$ compared with CTRL. §, $p<0.05$; §§, $p<0.01$; §§§, $p<0.001$ compared with SCHH exposed to C alone.

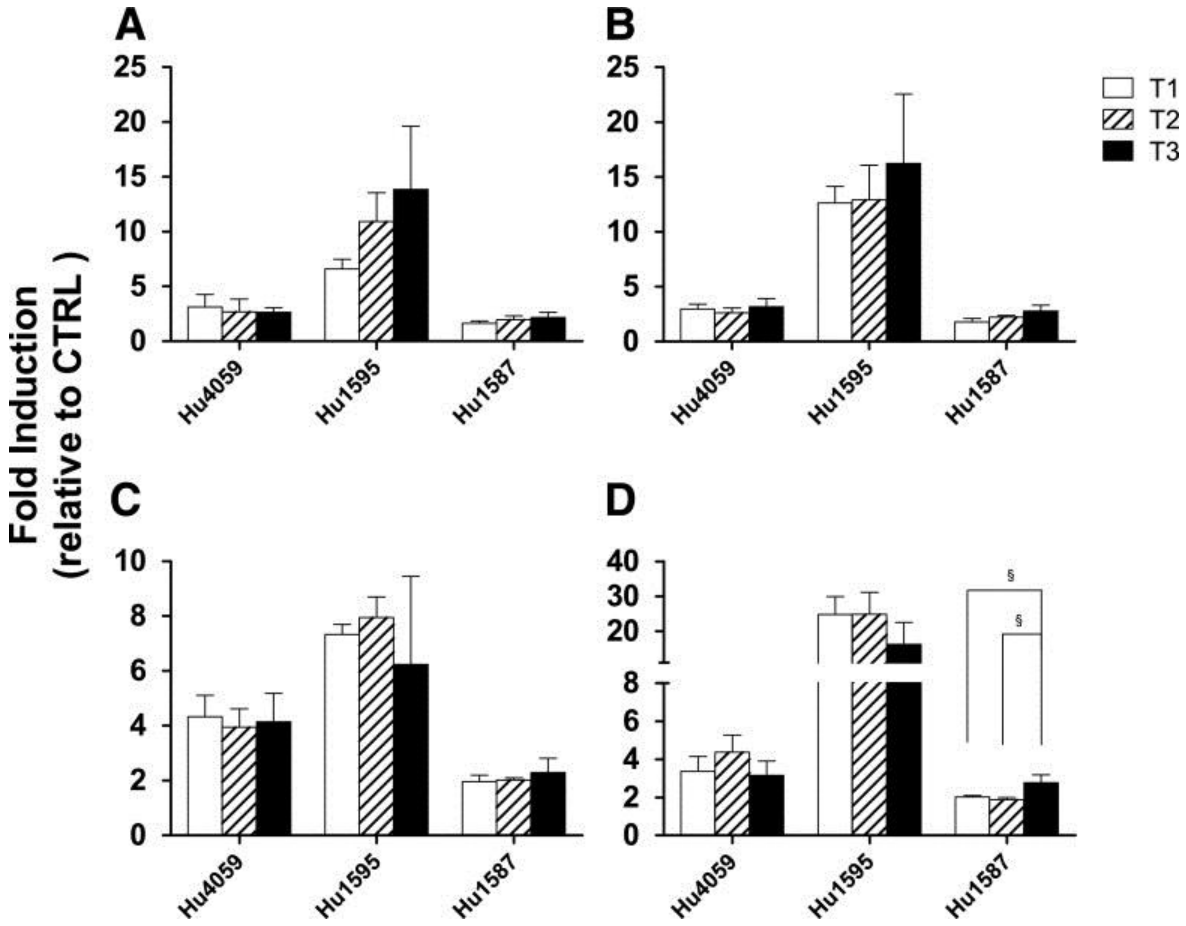


**Figure 2.5. CYP3A activity in SCHH incubated with 1X or 10X plasma concentrations of cortisol (A and C respectively) or PRH cocktail (B and D respectively) observed in pregnant women**. Fold induction (mean ± SD; n=3) is expressed relative to control treatment (CTRL, n=3; unbound plasma concentrations of C+GH+E2+P observed in non-pregnant women). Data were analyzed by one-way ANOVA followed by Tukey's multiple comparison to detect any difference in the magnitude of CYP3A induction amongst T1, T2, and T3. §, $p<0.05$; §§, $p<0.01$; §§§, $p<0.001$ compared with the indicated trimester.

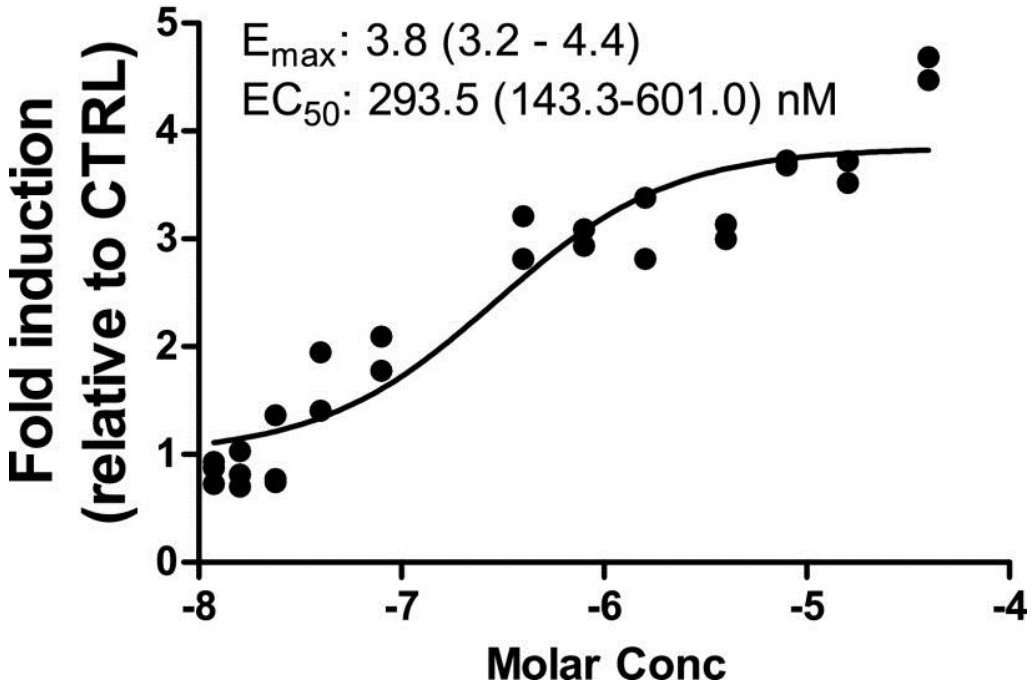


**Figure 2.6. CYP3A activity in SCHH (Hu1587) incubated with various plasma concentrations of cortisol**. Fold induction is expressed relative to control treatment (CTRL, n=3; unbound plasma concentrations of C+GH+E2+P observed in non-pregnant women). Data are expressed as individual data points. Emax and EC50 (estimate and 95% confidence interval) were estimated by fitting the simple Emax model to the data.

**Table 2.1. Plasma Concentrations of Pregnancy-related Hormones Observed in Pregnant Women during 1st (T1), 2nd (T2) or 3rd (T3) Trimester and Targeted to Use in This Study after Correcting for Depletion**

| Hormone | Non-pregna | T1 | | T2 | | T3 | |
|---|---|---|---|---|---|---|---|
| | Unbound | Total | 10X Total | Total | 10X Total | Total | 10X Total |
| | nM | nM | nM | nM | nM | nM | nM |
| Cortisol (C) [1-5] | 16.3 | 418 | 4178 | 774 | 7744 | 798 | 7980 |
| Estradiol ($E_2$) [5] | 0.01 | 3.4 | 33.8 | 18.5 | 185 | 51 | 510 |
| GH[6] | 0.02 | 0.21 | 2.1 | 0.18 | 1.8 | 0.1 | 1.0 |
| PGH[7, 8] | N/A | 0.04 | 0.4 | 0.24 | 2.4 | 0.4 | 4.0 |
| Progesterone | 0.87 | 60 | 600 | 145 | 1450 | 395 | 3950 |

1. Huang et al., 2007; 2. Carr et al., 1981; 3. Demey-Ponsart et al., 1982;

4. Jung et al., 2011; 5. Soldin et al., 2005; 6. Caufriez et al. ,1998; 7. Wu et al., 2003;

8. Baumann et al, 1988; 9. Meulenberg et al., 1989

Data represent weighted arithmetic means from the above cited studies.

**Table 2.2. Demographic Information of the Hepatocyte Donors**

| Batch Number | Age (yrs) | Ethnicity | Sex | Medication | Cause of Death |
|---|---|---|---|---|---|
| Hu4059 | 17 | Caucasian | F | N/A | N/A |
| Hu1587 | 43 | Caucasian | F | Vitamin D, multivitamin, caltrate plus | N/A |
| Hu1595 | 31 | Caucasian | F | Diazepam, fluticasone furoate, hydrocodone-acetaminophen, methocarbamol | N/A |

N/A – not available

**Table 2.3. Depletion Half-lives of Steroid Hormones when incubated with HepaRG cells or SCHH**

| Hormone | | HepaRG Cells | | SCHH | |
|---|---|---|---|---|---|
| | | Conc (nM) | Half life (h) | Conc (nM) | Half life (h) |
| Estradiol | 1X | 51 | NQ | 319 | 2.0 ±0.5* |
| | 10X | 510 | 3.3 ± 0.7 | 3187 | 1.6 ±0.4* |
| Progesterone | 1X | 395 | 7.5 ±1.0 | 705 | 1.4 ±0.4* |
| | 10X | 3950 | 9.2 ±0.7 | 19100 | 1.6 ±1.0* |
| Cortisol | Unbound | 16.3 | 13.0 ±2.4* | 48.8 | NQ |
| | 1X | 798 | ND | 798 | ND |
| | 10X | 7980 | ND | 7980 | ND |

Data expressed as mean ± SD; ND, no depletion; NQ, not quantified; *, n= 3

# Chapter 3 Development of a Maternal-Fetal Physiologically Based Pharmacokinetic Model I: Factors that Determine Fetal Drug Exposure

The work presented in this chapter is under preparation for submission to Drug Metabolism and Disposition

### 3.1 Structured Summary

AIM

Determining fetal drug exposure is not possible for both logistical and ethical reasons. Therefore, we developed a maternal-fetal physiologically based pharmacokinetic (m-f-PBPK) model to predict fetal exposure to drugs. We used this m-f-PBPK to: (1) quantitatively demonstrate the impact of fetoplacental metabolism and placental transport on fetal drug exposure; (2) predict the impact of gestational age on fetal drug exposure; and (3) show that umbilical venous: maternal plasma (UV:MP) ratios do not necessarily reflect fetal drug exposure;

METHODS

We expanded our previously published maternal MATLAB® PBPK by incorporating a fetal-PBPK. The resulting m-f-PBPK was populated with gestational age-dependent changes in maternal drug disposition and maternal-fetal physiology. Then, we verified the implementation of this m-f-PBPK model by comparing the predicted UV:MP ratios at steady-state with those obtained at steady-state by 3-compartment maternal-fetal model. Next, the impact on fetal drug exposure by fetoplacental metabolic clearance(s) and placental transport or gestational age was evaluated via sensitivity analyses or simulations.

RESULTS

UV:MP ratios do not measure the extent of fetal drug exposure unless obtained at steady-state after intravenous infusion to the mother. Our simulations yielded novel insights on the quantitative contribution of fetoplacental metabolism and placental transport towards

fetal drug exposure and suggest that fetal drug exposure will likely change with gestational age.

CONCLUSIONS

Using our m-f-PBPK model integrating gestational age-related changes in maternal-fetal physiology and in maternal drug disposition, the impact of fetoplacental metabolic clearance(s) and placental transport was quantitatively evaluated. Further, the misconceptions surrounding the UV:MP ratio were clarified.

### 3.2 Introduction

Fetal exposure to drugs has becoming increasingly common. This can be attributed to, at least in part, the rising use of therapeutic drugs among pregnant women (Mitchell et al., 2011) as pre-existing maternal conditions (e.g. epilepsy, asthma) or conditions developed during pregnancy (e.g. gestational diabetes and hypertension) must be treated to ensure the health and welfare of the mother and therefore her fetus. Sometimes, it is the unborn child that is the target of the treatment (e.g. to prevent maternal-fetal HIV transmission (McGowan and Shah, 2000)). Consequently, the ability to quantitatively evaluate fetal exposure to drugs and risk of toxicity, not only at term, but also earlier during pregnancy when the fetus is most vulnerable to teratogens is desired.

Unlike in the general population, fetal exposure to drugs ingested by the pregnant mother cannot be feasibly or ethically studied in fetuses prior to birth. Even at the time of birth, assessment of fetal exposure to drugs is usually limited to a single cord plasma concentration measurement and reported as the umbilical vein: maternal plasma drug concentration ratio (UV:MP ratio). This UV:MP ratio, however, does not reflect the extent of fetal drug exposure relative to that in the mother in most clinical scenarios (see

**Results** and **Discussion**). Nor does it provide information on fetal drug exposure over time [i.e. fetal plasma AUC ($AUC_f$)] or maximum fetal plasma drug concentration ($C_{max,f}$) that drives drug efficacy and/or toxicity in the fetus. Further, since cord blood sampling is limited to term fetal drug exposure during early gestation remains unknown. Clearly, to overcome these gaps in knowledge, mechanistic understanding of the determinants of fetal drug exposure and alternative, non-invasive approaches to predict fetal exposure across gestational ages, such as **P**hysiologically-**b**ased **P**harmacokinetic (PBPK) modeling and simulation, are urgently needed.

While a number of attempts to develop fetal PBPK models for environmental toxins and teratogens have been made {Loccisano, 2013 #3859;Yoon, 2011 #2686;Clewell, 2007 #3571}, upon closer examination, none of these models are suitable for predicting fetal exposure to therapeutic agents prescribed to pregnant women. Their limitations include: (1) incomplete inclusion of pregnancy-caused changes in maternal and fetal physiology; (2) not accounting for the alterations in maternal drug disposition; (3) lack of known inter-individual variability in maternal drug disposition, and (4) exclusion of fetal body compartments important for disposition of therapeutic drugs. Recently, our lab has successfully refined and verified a mechanistic maternal PBPK model (m-PBPK) that can predict the maternal disposition of drugs cleared by one or more CYP enzymes during pregnancy {Ke, 2012 #2841;Ke, 2013 #2858;Ke, 2013 #2858;Ke, 2014 #3959}. However, this model only contains a lumped tissue compartment representing the placenta and fetus. Therefore, the goals of the current investigation were to: (1) develop a maternal-fetal PBPK (m-f-PBPK) model by incorporating a physiologically relevant fetal-PBPK into our previously verified m-PBPK; (2) verify the m-f-PBPK model at

steady-state (after maternal infusion) by comparing the predicted UV:MP ratios with those obtained by a steady-state 3-compartment maternal-placental-fetal model; (3) show that the UV:MP ratio (even at distributional equilibrium) does not represent the extent of fetal drug exposure; (4) **quantitatively** demonstrate the impact of fetoplacental metabolism and placental transport on fetal drug exposure; and (5) **quantitatively** predict the impact of gestational age on fetal drug exposure.

## 3.3 Materials and Methods

### 3.3.1 Model structure and general assumptions

Briefly, a m-f-PBPK model was built using MATLAB® (R2014b, Mathworks, Natick, MA) by adding the placenta, the amniotic fluid compartment and fetal organs important in drug disposition (e.g. liver and kidney) and distribution (e.g. brain) (**Figure 3.1**) to our verified m-PBPK model (Ke et al., 2012; Ke et al., 2013a; Ke et al., 2013b). The remaining fetal organs were lumped into a single peripheral compartment. Our model also accounted for the marked differences in fetal circulation compared to that in the mother (Polin et al., 2004). For instance, it is the venous blood that carries oxygenated blood (via the umbilical vein) from the placenta to the fetus. The majority of this flow by-passes the fetal liver through the ductus venosus before perfusing fetal tissues (**Table 1**).

General model assumptions include:

- The bidirectional unbound maternal-placental and fetal-placental transplacental passive diffusion clearances ($CL_{PD,u}$ ) across the placenta are equal and always present.

- For a given drug, the magnitude of $CL_{PD,u}$ is directly proportional to the placenta villous surface area which increases with gestational age.
- The UV plasma drug concentration represents the systemic fetal plasma venous drug concentration.
- Fetal renal clearance is negligible during the first 20 weeks of gestation (Polin et al., 2004). After week 20, it consists of only glomerular filtration clearance which can be estimated from fetal plasma protein binding and inulin clearance estimated in preterm (week 23 - 40) and term neonates (within first 14 days of life).
- Compared with fetal swallowing, the movement of amniotic fluid between the amniotic sac and maternal circulation is negligible (Gilbert and Brace, 1993). Therefore, fluid transfer between these two compartments was considered to be zero.

### 3.3.2 Collection and analyses of fetal physiological parameters

To populate the m-f-PBPK model with fetal physiological parameters, a systematic literature search was carried out using PUBMED to obtain these parameters (**Table 3.1)**. The search strategy was aimed to identify cohort studies whereby the parameter(s) of interest was longitudinally examined during gestation. Data from the control arm of case-control studies and healthy subjects of cross-sectional studies were considered for inclusion. Other inclusion criteria included: (1) human; (2) uncomplicated singleton pregnancies; (3) otherwise uneventful pregnancies with condition(s) thought not to affect the parameter of interest (e.g. preterm birth data were used to estimate fetal renal function). If the data were not tabulated and only graphs were present, individual data points were digitized using Digitizer (a free MATLAB® tool available on http://www.mathworks.com/matlabcentral/). When multiple qualified studies were

available for a physiological parameter of interest, data were pooled, stratified by gestational age (measured in weeks from the first day of the last menstrual cycle) and summarized using the approach previously published (Abduljalil et al., 2012). Once the physiological values were extracted from the literature, polynomial, exponential, or power function models were fitted to the data using nonlinear regression using the approach described by Abduljalil et al. (Abduljalil et al., 2012).

### 3.3.3 Sensitivity analyses to identify key determinants of fetal drug exposure

To identify the quantitative impact of key factors (e.g. fetal metabolic clearance) that influence maternal-placenta/fetal plasma concentration-time (C-T) profiles of a drug at term , we conducted a series of simulations of a hypothetical drug X using our newly developed m-f-PBPK model (at week 40). Drug X was designed to mimic relatively hydrophilic drugs administered to pregnant women such as the nucleoside HIV drugs (**Supplementary Table S1**). Drug X was administered as a single oral dose or to steady-state through continuous intravenous (IV) infusion (steady-state$_{inf}$).

Additional assumptions made for the hypothetical drug X:

- Drug X is neutral, follows linear kinetics, and has negligible binding in the maternal and fetal plasma and in the placenta. Therefore, all concentrations and clearances should be read as their corresponding unbound values.
- Maternal absorption of drug X is first order and does not change during pregnancy [i.e. absorption rate constant ($k_a$), fraction absorbed ($F_a$), and fraction escaping gut metabolism ($F_g$)].
- Maternal and fetal tissue-to-plasma partition coefficients ($K_p$'s) are identical for drug X and remain constant throughout pregnancy.

- Except where indicated, fetal renal clearance of drug X is negligible.
- Drug X swallowed by the fetus (i.e. the amniotic fluid) is instantly and completely absorbed from the fetal intestine and is not metabolized there.

While some of the above assumptions were made to simplify simulations and need not be made (e.g. maternal plasma protein binding of drug X), others were made (e.g. fetal renal secretion of drugs) because these values cannot be determined.

Except where indicated, the simulations were conducted using our m-f-PBPK model where only one parameter was changed at a time (**Table 2**) at week 40. Then, we simulated the impact of gestational age on exposure of the maternal-fetal unit to drug X under various scenarios (**Table 3**). Week 20 and week 40, respectively, represent the gestational age when fetal skin keratinization begins and when cord blood sampling is possible. For simplicity, maternal drug X metabolic clearance (i.e $CL_{m0}$) was held constant. Fetal metabolic clearance was assumed to be directly proportional to fetal body volume as the metabolism of HIV nucleoside drugs (i.e. phosphorylation) occurs throughout the body. Where invoked, placental efflux clearance ($CL_{PM}$) was assumed to be mediated by P-gp, and the magnitude of this clearance was assumed to be proportional to the expression of P-gp in the placenta. At term, P-gp mediated $CL_{PM}$ was arbitrarily set at 20% of $CL_{PD}$. From week 20 to week 40, placental P-gp expression decreases by 5-fold based on our data on placental P-gp expression (Mathias et al., 2005). This change in expression was then scaled up to the whole placenta based on change in the gestational age-dependent placental volume.

### 3.3.4 Model verification at steady-state after maternal infusion of the drug

At steady-state attained by IV infusion of the drug to the mother (steady-state$_{inf}$ ), maternal-fetal plasma concentration of drugs can be described by a model consisting of maternal (M), placental (P), and fetal (F) compartments (steady-state$_{inf}$ model; **Figure 3.2**) even for a drug that demonstrates multi-compartmental behavior. Moreover, at steady-state$_{inf}$, the fetal:maternal (F:M) plasma drug concentration ratio (i.e. the $C_{f,ss,\inf} / C_{m,ss,\inf}$ ratio below) predicted by this steady-state$_{inf}$ model should be equal to the F:M plasma AUC ratio predicted by the m-f-PBPK model after a single dose of the drug or within a dosing interval at steady-state (assuming linear pharmacokinetics). Therefore, these $C_{f,ss,\inf} / C_{m,ss,\inf}$ ratios predicted by this steady-state$_{inf}$ model were compared against F:M plasma AUC predictions made by our m-f-PBPK model as a means to ensure the correct implementation of our m-f-PBPK model.

For simplicity, besides the assumption that the bidirectional maternal-placental and placental-fetal passive diffusion clearances ($CL_{PD.u}$) are equal and always present, this steady-state$_{inf}$ model also assumes for the drug: (1) negligible binding of the drug and therefore all concentrations and clearances should be read as their corresponding unbound values; (2) $CL_{PD}$ does not exceed placental blood flow; (3) uptake and efflux transporters are located on the apical (maternal-facing) side of the placenta; (4) fetal renal excretion is negligible.

Using this steady-state$_{inf}$ model, the F:M plasma and placenta:maternal plasma (P:M) drug concentration ratios at steady-state$_{inf}$ can be described by the following equations (see **Supplementary THEORY I** for derivation).

$$\frac{C_{f,ss,\inf}}{C_{m,ss,\inf}} = \frac{CL_{PD} + CL_{MP}}{CL_{PD} + 2CL_{f0} + CL_{p0} + CL_{PM} + (\frac{CL_{p0} + CL_{PM}}{CL_{PD}}) \cdot CL_{f0}} \text{ (Eq. 1)}$$

$$\frac{C_{p,ss,\inf}}{C_{m,ss,\inf}} = \frac{(CL_{PD} + CL_{MP}) \cdot (1 + \frac{CL_{f0}}{CL_{PD}})}{CL_{PD} + 2CL_{f0} + CL_{p0} + CL_{PM} + (\frac{CL_{p0} + CL_{PM}}{CL_{PD}}) \cdot CL_{f0}} \text{ (Eq. 2)}$$

where $C_{f,ss,inf}$, $C_{p,ss,inf}$ and $C_{m,ss,inf}$ are steady-state$_{inf}$ drug concentrations in the fetal plasma, placenta, and maternal plasma, respectively; $CL_{PD}$ is the bidirectional passive diffusion clearance; $CL_{f0}$ and $CL_{m0}$ are the irreversible fetal and maternal metabolic clearances, respectively; $CL_{PM}$ and $CL_{MP}$ are the efflux and uptake transporter mediated clearances, respectively.

It is immediately evident that the $C_{f,ss,\inf} / C_{m,ss,\inf}$ ratio is independent of maternal clearance. When fetoplacental metabolism and placental transport are absent, this ratio reduces to unity. The differing impact of these individual clearance pathways on the $C_{f,ss,\inf} / C_{m,ss,\inf}$ ratio (and therefore, as indicated above, F:M plasma AUC ratio) is further discussed in **Supplementary information**. This analysis, as detailed below, yielded novel and surprising quantitative information on the impact of fetoplacental metabolism and placental transport on fetal exposure to drugs.

### 3.4 Results

#### 3.4.1 Fetal physiological parameters

The time-variant fetal physiological parameters used to populate the m-f-PBPK model show that the gestational age-dependent changes in fetal physiological parameters are pronounced (**Table 1**). For example, umbilical venous blood flow (i.e. fetal placental

blood flow) increases by approximately 6.2-fold (from 3.3 L/h to 20.2 L/h) from week 20 to week 40. Some fetal physiological values change with gestational age in an opposite direction to the corresponding values in the mother, as demonstrated by changes in the concentration of plasma drug binding proteins. For example, the fetal and maternal plasma albumin concentrations increase and decrease, respectively, with gestational age.

### 3.4.2 Impact of maternal metabolism and placental passive drug permeability on fetal exposure to Drug X in the absence of placental/fetal metabolism or placental transport

As expected, at steady-state after IV infusion of drug X, both steady-state$_{inf}$ maternal and fetal venous plasma (fetal plasma) drug X concentrations and the time to reach steady-state$_{inf}$ were inversely dependent on the maternal drug clearance ($CL_{m0}$) when $V_{ss}$ was held constant (**Figure 3.3a**). In contrast, drug X maternal plasma C-T profile, but not the fetal plasma C-T profile, was independent of the transplacental passive diffusion clearance of the drug ($CL_{PD}$). Moreover, the maternal and fetal steady-state$_{inf}$ concentrations were independent of $CL_{PD}$ (**Figure 3.3b**). Similarly, the steady-state$_{inf}$ UV:MP ratio (i.e. the $C_{f,ss,\inf} / C_{m,ss,\inf}$ ratio above) remained unity irrespective of changes in $CL_{m0}$ or $CL_{PD,}$ but the time to reach steady-state$_{inf}$ was prolonged with lower $CL_{m0}$ or $CL_{PD}$ (**Figure 3.3c, d**). Of note, the predicted $C_{f,ss,\inf} / C_{m,ss,\inf}$ ratio, using the steady-state$_{inf}$ model, is expected to remain unity in the absence of placental transport and fetoplacental metabolism.

Following a single 400mg oral dose of drug X, fetal drug exposure (plasma $AUC_f$) was inversely proportional to $CL_{m0}$ (**Figure 3.3e**) but independent of $CL_{PD}$ (**Figure 3.3f**) though the fetal plasma $t_{max}$ ($t_{max,f}$) and $C_{max,f}$ were affected. As expected, the UV:MP

ratio varied over time until maternal-fetal distributional equilibrium was achieved. Interestingly, the distributional equilibrium UV:MP ratio was greater than the expected value of unity. Furthermore, this deviation from unity reduced with decrease in $CL_{m0}$ (38 to 1.5; **Figure 3.3g**) or increase in $CL_{PD}$ (1.7 to 38, **Figure 3.3h**). However, as predicted by the steady-state$_{inf}$ model, the F:M plasma AUC ratio predicted by the m-f-PBPK model remained unity (**Supplementary Table S2** ).

### 3.4.3 Impact of placental drug transport, fetal metabolism, and placental metabolism on fetal exposure to drug X

Overall, variations in these pathways (**Table 2**) produced significant changes in fetal plasma C-T profiles without affecting maternal pharmacokinetics (PK) (data not shown). As expected, following a single oral dose of 400 mg drug X , fetal plasma, $C_{max,f}$ and placental concentrations were inversely correlated with metabolism in the placenta (**Figure 4a**), fetus (**Figure 3.4b**) or both (**Figure 3.4c**). As the placental metabolism ($CL_{p0}$) became larger relative to $CL_{PD}$, the magnitude of reduction in $AUC_f$ and placental AUC ($AUC_p$) was identical (**Figure 3.4a2**). In contrast, an increase of the same magnitude in fetal metabolism ($CL_{f0}$) resulted in a greater reduction in $AUC_f$ compared to $AUC_p$ (**Figure 3.4b2**). For example, when $CL_{p0}$ equaled $CL_{PD}$, $AUC_p$ and $AUC_f$ were both reduced by 50%, whereas when $CL_{f0}$ equaled $CL_{PD,}$ a greater reduction in $AUC_f$ was seen compared with $AUC_p$ (67% vs. 33%) (**Figure 3.4a2, b2**). When both metabolic processes were present ($CL_{p0}$ and $CL_{f0}$) and equal to $CL_{PD}$, the reduction in the $C_{max,f}$, $AUC_p$ (60%), and $AUC_f$ (80%) was even greater (**Figure 3.4c**). The addition of uptake ($CL_{MP}$) or efflux ($CL_{PM}$) clearance on the apical side of the placenta altered fetoplacental exposure to drug X in opposite directions (**Figure 3.4d, e**). While increasing $CL_{MP}$

resulted in higher fetal plasma drug concentrations and $C_{max,f}$ (**Figure 3.4d1**) as well as increased F:M and P:M plasma AUC ratios (**Figure 3.4d2**), increasing $CL_{PM}$ lowered $C_{max,f}$ (**Figure 3.4e1**) and reduced F:M and P:M plasma AUC ratios (**Figure 3.4e2**). The simulated F:M and P:M plasma AUC ratios using the m-f-PBPK model matched the predicted F:M and P:M drug concentration ratios using the steady-state$_{inf}$ model. However, even under fetal-maternal distributional equilibrium the UV:MP ratio (**Figure 4a3-e3**) deviated from its respective steady-state$_{inf}$ F:M plasma drug concentration ratio (**Eq. 1**) and therefore did not represent F:M plasma AUC ratio (**Supplementary Table S2**).

### 3.4.4 Impact of gestational age on fetal disposition of drug X

Maternal and fetal plasma C-T profiles following a single 400mg oral dose of drug X at weeks 20 and 40 were simulated using the m-f-PBPK model under various scenarios outlined in **Table 2** and **Table 3**. Gestational age significantly altered fetal plasma C-T profile while minimally affecting maternal PK (**Figure 5**). Furthermore, the impact of gestational age on fetal exposure to drug X depended on the clearance mechanisms within the fetoplacental unit. In scenario 1 (**Figure 5a, b**) where drug X was assumed to passively diffuse across the placenta without placental drug transport or irreversible clearance in the fetoplacental unit (e.g. metabolism), despite a modest 16% decrease in $C_{max.f}$, the F:M plasma AUC ratio remained unity and did not change with advancing gestational age. In scenario 2 (**Figure 5c, d**), addition of fetal metabolism produced significant reduction in both the $C_{max,f}$ and $AUC_f$ resulting in F:M plasma AUC ratio of 0.48 and 0.50 at week 20 and week 40, respectively. In Scenario 3 (**Figure 5e, f**) where P-gp mediated placental efflux clearance ($CL_{PM}$) was assumed to be 20% of $CL_{PD}$ with no

fetal metabolism, advancing gestation age from week 20 to week 40 and the associated decrease in $CL_{PM}$ resulted in substantial changes in the shape of fetal C-T curve as well as plasma $AUC_f$; that is, $C_{max,f}$ increased by 118.5% in tandem with a pronounced 3.6-fold increase in fetal AUC. Finally, in Scenario 4 (**Figure 5g, h**), the combination of both fetal metabolism and placental efflux further reduced fetal exposure. When compared with previous scenarios, this scenario resulted in the lowest $C_{max,f}$ and $AUC_f$ at both gestational ages.

### 3.5 Discussion

Here we presented a maternal-fetal PBPK model to predict the fetal disposition of pharmaceutical drugs. The model is structured to be consistent with the unusual fetal vascular physiology and to allow future incorporation of placental transport and metabolism within the fetoplacental unit. In addition, a comprehensive literature reviewed was conducted to collect the available fetal physiological parameters and their gestational age-dependent changes (**Table 1**). Furthermore, using the m-f-PBPK model and simulations, for the first time, we have **quantitatively** shown, how several drug-related factors (i.e. fetal/placental metabolism and placental transport) affect the fetal exposure to drugs (**Figures 3** and **4**). We focused on the impact of varying the magnitude of these clearance pathways (hitherto not explored), rather than the impact of changes in plasma protein binding or pH, as the latter factors have been well described in the literature (the reader is referred to reviews on these topics such as by Hill et al. and by Macnamara et al.(Hill and Abramson, 1988; McNamara and Alcorn, 2002)). Owing to the inclusion of the gestational age-dependent changes in maternal-fetal physiology, we

also quantitatively predicted how fetal drug exposure will vary with gestational age under various scenarios.

The hypothetical Drug X was designed to be a neutral compound with intermediate permeability across the placenta and minimal plasma protein binding. Therefore, all the variables and parameters discussed here should be read as unbound values. A drug of these characteristics was chosen to quantitatively illustrate the impact of fetoplacental metabolism and placental transport on fetal exposure to drugs.

Contrary to the widely held belief, the UV:MP ratio, even at distributional equilibrium (after a single dose or at steady-state after multiple dosing), does not indicate fetal drug exposure relative to that in the mother ($AUC_f/AUC_m$) (**Figure 3, 4**). The only exception is when the drug is administered to steady-state via an infusion, a rare situation in clinical practice. The same UV:MP ratio is often deemed to infer the mechanisms by which the drug crosses the placenta. A greater than unity ratio is often interpreted as accumulation of the drug in the fetal compartment (Else et al., 2011). In contrast, a ratio of less than unity is interpreted as low fetal exposure and is attributed to low maternal drug concentrations (Chappuy et al., 2004a; Chappuy et al., 2004b), fetal metabolism (Ngan Kee et al., 2009), and/or placental efflux (Marzolini and Kim, 2005; Else et al., 2011). However, such interpretations can be false. While fetal/placental metabolism or placental transport processes cannot be discounted based on a single UV:MP ratio, such deviation from unity is more likely due to the time-dependent distributional kinetics of the drugs across the placenta as illustrated by our simulations. In the absence of fetal/placental metabolism or placental transport, the steady-state$_{inf}$ UV:MP ratio and therefore the F:M plasma AUC ratio after single or multiple doses (assuming linearity) should be unity (**Eq.**

**1**) . Indeed it is, as confirmed by our dynamic simulations using the m-f-PBPK model (**Figure 3a-d, 4a2-e2**). In all other cases, the degree of deviation of this ratio from unity not only varied with time but also depended on the magnitude of transplacental passive diffusion clearance ($CL_{PD}$, **Figure 3h**) and maternal clearance ($CL_{m0}$, **Figure 3g**). The extent of this deviation decreased when $CL_{PD}$ was increased (the drug rapidly diffused across the placenta) or when $CL_{m0}$ was decreased (longer $t_{1/2}$). Even in these cases where no active placental uptake was invoked, the UV:MP ratio at distributional equilibrium still exceeded unity (~1.7 and 1.5, respectively). While puzzling at first glance, these observations can be explained by the multi-compartmental PK of drug X. During the post-distributive phase, the peripheral:central compartment drug concentration ratio increases as the central compartment clearance is increased or as the inter-compartmental clearance is decreased (see **Supplementary Theory II for details** ). The above conclusions also hold true for multiple dosing regimens. For example, after last maternal dose, the UV:MP ratio of zidovudine ($t_{1/2}$ ~ 1.1 h)(Collins and Unadkat, 1989) range from 0.18 to 17.2 (Chappuy et al., 2004a), whereas that of theophylline ($t_{1/2}$ ~ 8h) is much less variable (from 0.98 to 1.59) (Ron et al., 1984). Similarly, another frequently reported ratio, the amniotic fluid:UV drug concentration ratio, varied with time and did not reflect fetal drug exposure.

Another common misconception about fetal drug exposure (i.e. AUCf) is that AUCf is mainly driven by maternal plasma drug concentrations and not by placental transport and/or fetoplacental metabolism. The reasoning behind it is that fetal/placental clearances are thought to be minor compared to maternal clearance of the drug, due to the small size of the placenta and the fetus (they constitute only about 0.8 % and 4.3% of

maternal body weight at term, respectively(Abduljalil et al., 2012)) and their limited metabolic capacities. The above reasoning is false because it fails to recognize an additional critical factor, CLPD. It is the ratio of these two clearances (i.e. the magnitude of fetoplacental clearance(s) relative to CLPD) that determines the fetal drug exposure relative to that in the mother. These determinants of fetal drug exposure, however, have been largely overlooked by others (Hill and Abramson, 1988; Marzolini and Kim, 2005; Myllynen et al., 2007; Bernick and Kane, 2012). The importance of these factors is illustrated by our steady-state infusion model (Figure 2), dynamic simulations using our m-f-PBPK model (Figures 3, 4), and "real life" examples from literature as discussed below.

For relative polar drugs with intermediate or low permeability (i.e. $CL_{PD}$) across the placenta, such as drug X, introduction of fetal/placental metabolism and/or placental transport can significantly alter fetal drug exposure if their magnitude is significant relative to $CL_{PD}$ (Figure 4a,b,c,e). Consistent with our simulations, due to fetal metabolism, two polar dideoxynucleoside HIV drugs, didanosine and zalcitabine, were shown to have steady-state$_{inf}$ F:M plasma drug concentration ratios of 0.48 and 0.63 in the chronically catheterized maternal-fetal macaques (Pereira et al., 1994; Tuntland et al., 1996). Furthermore, the site of drug clearance (placental, fetal, or both) had differential impact on $AUC_f$ and $AUC_p$ (Eq.1, Eq. 2, and Figure 4). . Because any drug taken by mother has to first traverse the placenta to reach fetal circulation, the placenta essentially behaves like the "fetal gut". If metabolism or drug efflux/influx occurs only in the placenta, then the change in placental and fetal drug exposure will be identical and will depend on the degree of pre-systemic "first pass"(Figure 4a, d, e, f). Instead, if

metabolism occurs in the fetus, this will result in a greater reduction in $AUC_f$ compared to $AUC_p$ because fetal metabolism affects only fetal and not placental drug exposure (Figure 4b, c). This "site effect" may have clinical implications as fetal toxicity can occur via toxicity to the placenta (e.g. formaldehyde) (Pidoux et al., 2015). In these cases, fetal toxicity cannot be readily ruled out even when fetal exposure to the toxin/drug is low.

Many lipophilic drugs will have high passive diffusion across the placenta. When $CL_{PD}$ of these drugs is much greater than fetal/placental metabolism or placental transport, the placenta becomes "transparent". In other words, fetal and maternal plasma concentrations rapidly equilibrate. In addition, $AUC_f$ will approach or equal $AUC_m$ after single dose or multiple dose administration of the drug (assuming linearity). However, in the presence of significant fetal/placental metabolism and/or placental transport, fetal drug exposure will be significantly altered. For example, in pregnant ewes, after IV infusion, the steady-state$_{inf}$ F:M plasma concentration ratio of remifentanil, a drug extensively hydrolyzed by non-specific esterases, was 0.1(Egan, 1995; Coonen et al., 2010). Other examples include several lipophilic HIV protease inhibitors that are P-gp substrates (e.g. indinavir, ritonavir, and saquinavir) (Unadkat et al., 2004). Their UV:MP ratios are considerably lower than unity(Marzolini and Kim, 2005). However, as pointed out earlier, these non-steady-state ratios should be interpreted with caution. Nevertheless, a role of placental P-gp efflux likely contributes to their low fetal exposure as these drugs are excellent substrates of P-gp as shown by transport studies in the perfused human placentae (McCormack and Best, 2014) and P-gp transfected cell lines (van der Sandt et al., 2001).

The expression of fetoplacental drug metabolizing enzymes (DMEs) and placental transporters are known to change with gestational age (Myllynen et al., 2009). For this reason, fetal drug exposure (with no change in maternal dosage regimen) is likely to change with gestational age (**Figure 5**). Our simulations confirmed this assertion. When drug X passively diffused across the placenta without being transported or metabolized in the fetoplacental unit (**Figure 5a, b**), progression of gestation did not affect $AUC_f$ because the latter was solely driven by $AUC_m$, which remained virtually the same from week 20 to week 40. In scenario 2, where only fetal metabolic clearance was present, $AUC_f$ was significantly reduced and appeared nearly equal between week 20 and week 40 (**Figure 5d**). This is because the $CL_{f0}$ /$CL_{PD}$ ratio remained similar from week 20 to week 40 (0.53 and 0.50, respectively) due to the fact that the fetal body volume (therefore fetal metabolic clearance) and the placental surface area (and therefore $CL_{PD}$) increased with gestational age in a nearly parallel fashion (**Table 3.1**). Placental P-gp expression is significantly higher during early gestation vs. term (Mathias et al., 2005). This gestational effect in P-gp expression resulted in lower fetal exposure to drug X at week 20, whereas at 40 weeks, due to lower placental P-gp efflux clearance, fetal exposure to drug X increased by 1.9-fold (**Figure 3.5e, f**). When both clearance pathways were present, the change in placental P-gp expression was a major determinant of the gestational-age effect on drug X $AUC_f$ (**Figure 3.5g, h**). It is worth mentioning that, for ease of data interpretation, drug X maternal metabolic clearance was assumed to be gestational age-independent. Also, as a relatively polar drug with minimal binding, there were minimal changes in drug X distribution (e.g. only a marginal 4.4% increase in $V_{ss}$; **Supplementary Table S1**) between week 20 and 40. Consequently the predicted

maternal disposition of drug X was virtually unchanged by the advancement of gestation. While this approach allowed us to highlight the changes in fetal C-T profile resulting from the gestational age-dependent alterations in fetoplacental clearance pathways and in fetoplacetnal physiology, this simplification approach might have underestimated the potential changes in $AUC_f$ caused by the advancement of pregnancy, as maternal systemic clearance of the drug may vary significantly across gestational ages. Parenthetically, we note that $AUC_m$ or $AUC_f$ should be independent of changes in maternal or fetal $V_{ss}$.

Like other fetal PBPK models, our m-f-PBPK model also has some limitations. Although the m-f-PBPK can predict fetal exospore to various drugs across gestational ages, the use of our model to predict fetal exposure to drugs prior to week 20 may be limited for the following reasons. First, data on fetal tissue blood flow rates prior to week 20 (**Table 3.1**) are not available. As a result, retrograde extrapolation to earlier gestational ages may not be reliable. Second, fetal skin is not completely keratinized and is highly permeable during the first half of gestation (Polin et al., 2004). Therefore, drugs that extensively partition into the skin/subcutaneous layer may readily cross into the amniotic fluid. Such movement of drugs could be incorporated into our model and we will do so in a future iteration of this model. In order for the model to be useful for drugs that are extensively metabolized by the fetus or transported/metabolized in the placenta, the model will need to be populated with gestational age dependent changes in the expression of these enzymes and transporters. Such studies, using quantitative targeted proteomics, are in progress in our laboratory.

In summary, through simulations we have shown that even when fetoplacental metabolic or placental transport clearance is small, it can significantly determine fetal drug exposure provided the magnitude of the clearance is comparable to the placental passive diffusion clearance of the drug. Our findings of quantitative contribution of fetoplacental metabolism and placental transport on fetal drug exposure are novel and have not been described before. In addition, we have shown that the single time point UV:MP ratio (except at steady-state after an IV infusion), routinely reported in the literature, cannot be used as an indicator of F:M plasma drug exposure ratio even at distributional equilibrium (after single or multiple dosing). Therefore, the only method to dynamically estimate fetal drug exposure in humans at term and earlier in gestation is through PBPK models. Here, for the first time, we present such a model. However, prior to using this model, it needs to be verified with fetal exposure data. Since our PBPK model is dynamic, such verification can be done at term where single UV concentrations are available for many drugs and is underway in our lab.

## 3.6 Supplementary Information

### 3.6.1 The three compartment mother-placenta-fetus model (Figure 3.2)

At steady-state after intravenous (IV) infusion of a drug into the maternal compartment,

$$CL_{PD} \cdot C_{p,ss,\text{inf}} = (CL_{PD} + CL_{f0}) \cdot C_{f,ss,\text{inf}} \quad \textbf{(Eq. 1)}$$

where $C_{f,ss,inf}$ and $C_{p,ss,inf}$ are drug concentrations in the fetal plasma and placenta at steady-state after infusion (steady-state$_{inf}$), respectively, $CL_{PD}$ is the bidirectional passive diffusion clearance, and $CL_{f0}$ is the irreversible fetal clearance. It is worth keeping in mind that passive diffusion of the drug across the placenta will be present for all drugs and will depend on the drug's lipophilicity.

Rearrangement of **Eq. 1** gives:

$$\frac{C_{f,ss,\inf}}{C_{p,ss,\inf}} = \frac{CL_{PD}}{CL_{PD} + CL_{f0}} \text{ (**Eq. 2**)}$$

Similarly, for the placenta,

$$CL_{PD}(C_{m,ss,\inf} - C_{p,ss,\inf}) + CL_{MP} \cdot C_{m,ss,\inf} = CL_{PD}(C_{p,ss,\inf} - C_{f,ss,\inf}) + (CL_{p0} + CL_{PM}) \cdot C_{p,ss,\inf}$$

(**Eq. 3**)

where $C_{m,ss,inf}$ is steady-state$_{inf}$ drug concentration in the maternal plasma; $CL_{PM}$ and $CL_{MP}$ are the non-saturated efflux and uptake placental transporter mediated clearances, respectively.

Rearranging and substituting **Eq. 2** into **Eq. 3** yields:

$$\frac{C_{f,ss,\inf}}{C_{m,ss,\inf}} = \frac{CL_{PD} + CL_{MP}}{CL_{PD} + 2CL_{f0} + CL_{p0} + CL_{PM} + (\frac{CL_{p0} + CL_{PM}}{CL_{PD}}) \cdot CL_{f0}} \text{ (**Eq. 4**)}$$

Substituting **Eq. 2** into **Eq. 4** and rearranging yields:

$$\frac{C_{p,ss,\inf}}{C_{m,ss,\inf}} = \frac{(CL_{PD} + CL_{MP}) \cdot (1 + \frac{CL_{f0}}{CL_{PD}})}{CL_{PD} + 2CL_{f0} + CL_{p0} + CL_{PM} + (\frac{CL_{p0} + CL_{PM}}{CL_{PD}}) \cdot CL_{f0}} \text{ (**Eq. 5**)}$$

The impact of fetal/placental metabolism and placental transport on the steady-state$_{inf}$ fetal:maternal plasma drug concentration ratio is apparent with the following examples:

(1) When, except for $CL_{PD}$, none of the above fetoplacental clearance pathways are present, **Eq. 4** simplifies to **Eq. 6**:

$$\frac{C_{f,ss,\inf}}{C_{m,ss,\inf}} = \frac{CL_{PD}}{CL_{PD}} = 1 \text{ (**Eq. 6**)}$$

In this case the placenta becomes "transparent", meaning that the $C_{f,ss,\inf} / C_{m,ss,\inf}$ ratio becomes unity.

(2) When only $CL_{p0}$ and $CL_{PD}$ are present, **Eq. 4** simplifies to **Eq. 7**:

$$\frac{C_{f,ss,\inf}}{C_{m,ss,\inf}} = \frac{CL_{PD}}{CL_{PD} + CL_{p0}} \quad \textbf{(Eq. 7)}$$

Now the $C_{f,ss,\inf} / C_{m,ss,\inf}$ ratio is determined by the magnitude of $CL_{PD}$ relative to $CL_{p0}$. For instance, when these two clearances are of the same magnitude, this ratio becomes 0.5.

(3) When only $CL_{f0\ and}$ $CL_{PD}$ are present, **Eq. 4** simplifies to **Eq. 8**:

$$\frac{C_{f,ss,\inf}}{C_{m,ss,\inf}} = \frac{CL_{PD}}{CL_{PD} + 2CL_{f0}} \quad \textbf{(Eq. 8)}$$

Now the $C_{f,ss,\inf} / C_{m,ss,\inf}$ ratio is determined by the magnitude of $CL_{PD}$ relative to $CL_{f0}$. Note that the $CL_{f0}$ term has a coefficient of 2. Therefore, the introduction of fetal clearance results in a further decrease in the $C_{f,ss,\inf} / C_{m,ss,\inf}$ ratio compared with the above case. For instance, when $CL_{PD}$ and $CL_{f0}$ are of the same magnitude, this ratio becomes 0.33.

(4) When both $CL_{p0}$ and $CL_{f0}$ as well as $CL_{PD}$ are present, **Eq. 4** simplifies to **Eq. 9**:

$$\frac{C_{f,ss,\inf}}{C_{m,ss,\inf}} = \frac{CL_{PD}}{CL_{PD} + 2CL_{f0} + CL_{p0} + \frac{CL_{p0} \cdot CL_{f0}}{CL_{PD}}} \quad \textbf{(Eq. 9)}$$

Now the $C_{f,ss,\inf} / C_{m,ss,\inf}$ ratio becomes a composite function that is determined by the magnitude of $CL_{f0}$ and $CL_{p0}$ relative to $CL_{PD}$. When $CL_{f0}$ and $CL_{p0}$ are of the same

magnitude as $CL_{PD}$, this ratio reduces to 0.2. Furthermore, when $CL_{p0} << CL_{PD}$, **Eq. 9** simplifies to **Eq. 8**, whereas when $CL_{f0} << CL_{PD}$ , **Eq. 9** simplifies to **Eq. 7**.

(5) When only $CL_{PM}$ and $CL_{PD}$ are present, **Eq. 4** simplifies to **Eq. 10**:

$$\frac{C_{f,ss,\inf}}{C_{m,ss,\inf}} = \frac{CL_{PD}}{CL_{PD} + CL_{PM}} \quad \textbf{(Eq. 10)}$$

Again, when placental efflux clearance is invoked the $C_{f,ss,\inf} / C_{m,ss,\inf}$ ratio is determined by the magnitude of $CL_{PD}$ relative to $CL_{PM}$. For example, when these two clearances are of the same magnitude, the $C_{f,ss,\inf} / C_{m,ss,\inf}$ ratio is 0.5.

(6) When only $CL_{MP}$ and $CL_{PD}$ are present, **Eq. 4** reduces to **Eq. 11**:

$$\frac{C_{f,ss,\inf}}{C_{m,ss,\inf}} = \frac{CL_{PD} + CL_{MP}}{CL_{PD}} \quad \textbf{(Eq. 11)}$$

Unlike the above cases, introduction of placental uptake clearance results in an increase in the $C_{f,ss,\inf} / C_{m,ss,\inf}$ ratio. Nonetheless, this ratio is dependent on the magnitude of $CL_{PD}$ relative to $CL_{MP}$. For example, when these two clearances are of the same magnitude, the $C_{f,ss,\inf} / C_{m,ss,\inf}$ ratio is 2.

**II.** Peripheral:central drug concentration ratio

For a drug that demonstrates two compartment pharmacokinetics, the differential equations for the rate of change in the amount of drug in the central and peripheral body compartments based on the model presented in **Figure S2** are

$$\frac{dX_c}{dt} = -(k_{10} + k_{12})X_c + k_{21}X_p \quad (1)$$

and

$$\frac{dX_p}{dt} = k_{12}X_c - k_{21}X_p \quad (2)$$

respectively.

where $X_c$ and $X_p$ are the amount of drug in the central compartment and the peripheral compartments, respectively, $k_{10}$ is the central compartment elimination rate constant, and $k_{12}$, and $k_{21}$ are the inter-compartmental distribution rate constants (**Figure S2**).

Take the Laplace transform of both sides of (1)

$$s \cdot \overline{X_c} - X_0 = -(k_{10} + k_{12}) \cdot \overline{X_c} + k_{21} \cdot \overline{X_p} \quad (3)$$

where $X_0$ is the dose available to the central compartment.

Similarly for (2)

$$s \cdot \overline{X_p} = k_{12} \cdot \overline{X_c} - k_{21} \cdot \overline{X_p} \quad (4)$$

Rearrange (3) and (4) to get:

$$\begin{cases} (s + k_{10} + k_{12})\overline{X_c} - k_{21}\overline{X_p} = X_0 \\ -k_{12}\overline{X_c} + (s + k_{21})\overline{X_p} = 0 \end{cases} \quad (5)$$

Solving Eq. 5 gives:

$$X_c = X_0 \cdot \left(\frac{\lambda_1 - k_{21}}{\lambda_1 - \lambda_2} e^{-\lambda_1 t} + \frac{k_{21} - \lambda_2}{\lambda_1 - \lambda_2} e^{-\lambda_2 t}\right)$$

$$X_p = X_0 \cdot \left(\frac{-k_{12}}{\lambda_1 - \lambda_2} e^{-\lambda_1 t} + \frac{k_{12}}{\lambda_1 - \lambda_2} e^{-\lambda_2 t}\right) \quad (6)$$

where $\lambda_1$ and $\lambda_2$ are microconstants.(Gibaldi and Perrier, 1982)

Hence, $$\frac{X_p}{X_c} = \frac{X_0 \cdot \left(\frac{-k_{12}}{\lambda_1 - \lambda_2} e^{-\lambda_1 t} + \frac{k_{12}}{\lambda_1 - \lambda_2} e^{-\lambda_2 t}\right)}{X_0 \cdot \left(\frac{\lambda_1 - k_{21}}{\lambda_1 - \lambda_2} e^{-\lambda_1 t} + \frac{k_{21} - \lambda_2}{\lambda_1 - \lambda_2} e^{-\lambda_2 t}\right)} \quad (7)$$

Rearranging Eq. 7 yields:

$$\frac{X_p}{X_c} = \frac{-k_{12}e^{-\lambda_1 t} + k_{12}e^{-\lambda_2 t}}{(\lambda_1 - k_{21})e^{-\lambda_1 t} + (k_{21} - \lambda_2)e^{-\lambda_2 t}} \quad (8)$$

In the post-distributive phase (i.e., as $e^{-\lambda_1 t}$ approaches zero)

Eq. 8 reduces to:

$$\frac{X_p}{X_c} = \frac{k_{12}}{k_{21} - \lambda_2} \quad (9)$$

Substituting $X_p$ and $X_c$ with $C_p V_p$ and $C_c V_c$ respectively and rearranging yields:

$$\frac{C_p}{C_c} = \frac{k_{12}}{k_{21} - \lambda_2} \cdot \frac{V_c}{V_p} \quad (10)$$

where $C_p$ and $C_c$ are drug concentrations in the peripheral and central compartment, respectively, and $V_p$ and $V_c$ are the volume of distribution for the central and peripheral compartments, respectively.

$\lambda_2$ is a hybrid parameter ( $\lambda_2 = \frac{1}{2}\left[ (k_{12} + k_{21} + k_{10}) - \sqrt{(k_{12} + k_{21} + k_{10})^2 - 4k_{21}k_{10}} \right]$ ) that reflects the drug elimination from the body. It increases as $k_{10}$ increases.(Gibaldi and Perrier, 1982) Therefore, increasing $k_{10}$ will result in higher $\frac{C_p}{C_c}$ and thereby elevating the peripheral (fetal):central (maternal) plasma drug concentration ratio.

On the other hand, for a passively diffused drug:

$$k_{12} = \frac{CL_{PD}}{V_c} \text{ and } k_{21} = \frac{CL_{PD}}{V_p}$$

where $CL_{PD}$ is the inter-compartmental passive diffusion clearance.

Substituting for $k_{12}$ and $k_{21}$ in Eq. 10 yields:

$$\frac{C_p}{C_c} = \frac{1}{1 - \frac{\lambda_2 V_p}{CL_{PD}}} \quad (11)$$

It is evident from **Eq. 11** that increasing $CL_{PD}$ will reduce the peripheral:central (fetal:maternal) drug plasma concentration ratio.

### 3.6.2 Impact of fetal renal clearance and amniotic fluid fetal swallowing rate on amniotic fluid exposure to drug X

Amniotic fluid drug concentration is often mistaken for an indicator of fetal drug exposure. For example, high amniotic fluid concentrations were associated with continuous fetal exposure to bupropion.(Fokina et al., 2016) But this is not the case. When a renally cleared drug enters the fetal circulation, it is excreted into amniotic fluid via fetal urination ($fCL_R$) and then reabsorbed through fetal swallowing of amniotic fluid ($fCL_{reabsorp}$; assuming instant and complete absorption) at late gestation.(Underwood et al., 2005) Therefore, high amniotic fluid drug concentrations do not necessarily result from high fetal exposure but rather is due to the much greater $fCL_R$ relative to $fCL_{reabsorp}$. This disconnect between the amniotic fluid and fetal plasma drug concentrations is illustrated in **Figure S1**. Amniotic fluid effectively acted as a "reservoir" for drug X because of its 9-fold higher $fCL_R$ (0.192 L/h) compared to $fCL_{reabsorp}$ (500mL/day). Drug X amniotic fluid drug concentrations, and therefore amniotic fluid drug AUC ($AUC_{af}$), increased proportionally with $fCL_R$ but was inversely related to $fCL_{reabosorp}$ (**Figure S1c-f**). In contrast, $AUC_f$ remained independent of the variations in $fCL_R$ or $fCL_{reabsorp}$ (**Figure S1e,f**). This is because the amniotic fluid acts as a distribution compartment not a compartment where drug elimination takes place. Indeed, the observed $AUC_{af}/AUC_m$ of tenofovir, a placental P-gp substrate, is as high as 2.76, although tenofovir $AUC_f/AUC_m$

of 0.45 was observed in the same study.(De Sousa Mendes et al., 2016) Again, like the UV:MP ratio, AF:UV ratio does not reflect fetal drug exposure (**Figure S1g-j**).

Amniotic fluid drug concentration is often mistaken for an indicator of fetal drug exposure. For example, high amniotic fluid concentrations were associated with continuous fetal exposure to bupropion.(Fokina et al., 2016) But this is not the case. When a renally cleared drug enters the fetal circulation, it is excreted into amniotic fluid via fetal urination ($fCL_R$) and then reabsorbed through fetal swallowing of amniotic fluid ($fCL_{reabsorp}$; assuming instant and complete absorption) at late gestation.(Underwood et al., 2005) Therefore, high amniotic fluid drug concentrations do not necessarily result from high fetal exposure but rather is due to the much greater $fCL_R$ relative to $fCL_{reabsorp}$. This disconnect between the amniotic fluid and fetal plasma drug concentrations is illustrated in **Figure S1**. Amniotic fluid effectively acted as a "reservoir" for drug X because of its 9-fold higher $fCL_R$ (0.192 L/h) compared to $fCL_{reabsorp}$ (500mL/day). Drug X amniotic fluid drug concentrations, and therefore amniotic fluid drug AUC ($AUC_{af}$), increased proportionally with $fCL_R$ but was inversely related to $fCL_{reabosorp}$ (**Figure S1c-f**). In contrast, $AUC_f$ remained independent of the variations in $fCL_R$ or $fCL_{reabsorp}$ (**Figure S1e,f**). This is because the amniotic fluid acts as a distribution compartment not a compartment where drug elimination takes place. Indeed, the observed $AUC_{af}/AUC_m$ of tenofovir, a placental P-gp substrate, is as high as 2.76, although tenofovir $AUC_f/AUC_m$ of 0.45 was observed in the same study.(De Sousa Mendes et al., 2016) Again, like the UV:MP ratio, AF:UV ratio does not reflect fetal drug exposure (**Figure S1g-j**).

### 3.6.3 Ordinary Differential Equations Defining the Mass Balance in the Fetal-PBPK

3.6.3.1 Symbols representing the variables and parameters used in the models

| | |
|---|---|
| V | volume (L) |
| C | concentration (μM) |
| (t) | gestational age-dependent |
| Q | blood flow rate (L/h) |
| $K_p$ | tissue: plasma partition coefficient |
| BP | blood: plasma partition ratio |
| CL | clearance (L/h) |

*Subscriptions:*

| | |
|---|---|
| subscription a | arterial |
| subscription F:M | from fetal to maternal |
| subscription M:F | from maternal to fetal |
| subscription A:M | from amniotic fluid to maternal |
| subscription M:A | from maternal to amniotic fluid |
| subscription af | amniotic fluid |
| subscription FP | from fetal placental blood to placenta |
| subscription PF | from placental to fetal placental blood |
| subscription p | plasma |
| subscription PD | passive diffusion |
| subscription pl | placenta |
| subscription PM | from placental to maternal placental blood |
| subscription MP | from maternal placental blood to placenta |
| subscription PD | passive diffusion |
| subscription af | amniotic fluid |

subscription gut gut

subscription kid kidneys

subscription liv liver

subscription per peripheral

subscription bra brain

subscription pl placenta

*Superscriptions*

superscription m maternal

superscription f fetal

superscription s placental

**3.6.3.2 Equations**

**Maternal placental blood**

The mass balance in the maternal placental blood compartment can be described using the following differential equation Eq. 1

$$\begin{aligned} V_{pl}^{m}(t)\frac{d\left[C_{pl}^{m}\right]}{dt} &= Q_{pl}^{m}(t)(C_{a}^{m}-C_{pl}^{m}) \\ &+ CL_{PM}\ fu_{pl}(t)C_{pl} - CL_{MP}\frac{fu^{m}(t)}{BP^{m}(t)}C_{pl}^{m} \\ &+ CL_{AM}\ fu_{af}^{f}(t)C_{af}^{f} - CL_{MA}\frac{fu^{m}(t)}{BP(t)}C_{pl}^{m} \\ &+ CL_{PDPM}\left( fu_{pl}^{s}(t)\frac{1}{\beta_{pl}^{s}}C_{pl}^{s} - \frac{fu^{m}(t)}{BP^{m}(t)}\frac{1}{\alpha^{m}}C_{pl}^{m}) \right) \end{aligned} \quad (1)$$

where $C_a^m$ is the artieral blood concentration in the mother.

**Placenta**

The mass balance in the placental membrane compartment can be described using the following differential equation Eq. 2

$$V_{pl}^{s}(t)\frac{d\left[C_{pl}^{s}\right]}{dt} = CL_{FP}\frac{fu^{f}(t)}{BP^{f}(t)}C_{pl}^{f} - CL_{PF}\,fu_{pl}^{s}(t)C_{pl}^{s}$$
$$+CL_{MP}\frac{fu^{m}(t)}{BP^{m}(t)}C_{pl}^{m} - CL_{SP}\,fu_{pl}^{s}(t)C_{pl}^{s}$$
$$+CL_{PDPF}\left(\frac{fu^{f}(t)}{BP^{f}(t)}\frac{1}{\alpha^{f}}C_{pl}^{f} - fu_{pl}^{s}(t)\frac{1}{\beta_{pl}^{s}}C_{pl}^{s}\right) \qquad (2)$$
$$+CL_{PDPM}\left(\frac{fu^{m}(t)}{BP^{m}(t)}\frac{1}{\alpha^{m}}C_{pl}^{m} - fu_{pl}^{s}(t)\frac{1}{\beta_{pl}^{s}}C_{pl}^{s}\right)$$
$$-CL_{p0}C_{pl}^{s}$$

where $CL_{p0}$ is the irreversible placental metabolism

The fetal unit comprises of the fetal placental blood, amniotic fluid, the fetal circulatory system, fetal liver, fetal gut, fetal kidneys, fetal brian, and a lumped peripheral compartment representing the rest of the fetus.

**Fetal Placental Blood**

The following equation is used to describe the concentration in the placenta/fetal compartment:

$$V_{pl}^{f}(t)\frac{d\left[C_{pl}^{f}\right]}{dt} = Q_{pl}^{f}(t)(C_{a}^{f} - C_{pl}^{f})$$
$$+CL_{PF}\,fu_{pl}^{s}(t)C_{pl}^{s} - CL_{FP}\frac{fu^{f}(t)}{BP^{f}(t)}C_{pl}^{f} \qquad (3)$$
$$+CL_{PDPF}\left(fu_{pl}^{s}(t)\frac{1}{\beta_{pl}^{s}}C_{pl}^{s} - \frac{fu^{f}(t)}{BP^{f}(t)}\frac{1}{\alpha^{f}}C_{pl}^{f}\right)$$

**Amniotic fluid**

$$V_{af}^{f}(t)\frac{d\left[C_{af}^{f}\right]}{dt} = CL_{MA}\frac{fu_{pl}^{m}(t)}{BP^{m}(t)}C_{pl}^{m} - CL_{AM}\,fu_{af}^{f}(t)C_{af}^{f} + \frac{CL_{renal}^{f}(t)}{BP^{f}(t)}C_{v}^{f} - CL_{reabs}^{f}C_{af}^{f} \quad (4)$$

where $CL_{renal}$ is the renal clearance based on the fetal venous plasma concentration (please see the following Eq.5 for fetal kidneys and Eq. 11for fetal central venous blood compartment).

**Fetal kidneys**

$$V_{kid}^{f}(t)\frac{d\left[C_{kid}^{f}\right]}{dt} = Q_{kid}^{f}(t)\left(C_{a}^{f} - \frac{C_{kid}^{f}}{Kp_{kid}^{f}(t)\big/BP^{f}(t)}\right) \quad (5)$$

Note the renal excretion has been considered in the previous equation (4), as well as in equation (11), and not directly from this kidney compartment.

**Fetal guts**

The following equation is used to describe the concentration in the gut:

$$V_{gut}^{f}(t)\frac{d\left[C_{gut}^{f}\right]}{dt} = Q_{gut}^{f}(t)\left(C_{a}^{f} - \frac{C_{gut}^{f}}{Kp_{gut}^{f}(t)\big/BP^{f}(t)}\right) + CL_{reabs}^{f}C_{af}^{f} \quad (6)$$

**Fetal liver**

The fetal liver is a well-stirred perfusion-limited organ, consisting of the tissue and its capillary blood. On the basis of well-stirred model, the emergent concentration is the driving concentration for hepatic metabolism.

Therefore the following equation is used to describe the concentration of liver compartment:

$$
\begin{aligned}
V_{liv}^{f}(t)\frac{d\left[C_{liv}^{f}\right]}{dt} &= Q_{port\_a}^{f}(t)C_{a}^{f} \\
&+ Q_{port\_v}^{f}(t)C_{pl}^{f} \\
&+ Q_{gut}^{f}(t)\frac{C_{gut}^{f}}{Kp_{gut}^{f}(t)\Big/BP^{f}(t)} \\
&- (Q_{hep\_ven}^{f}(t) + Q_{hep\_art}^{f}(t) + Q_{gut}^{f}(t))\frac{C_{liv}^{f}}{Kp_{liv}^{f}(t)\Big/BP^{f}(t)} \\
&- fu^{f}(t)\Big/BP^{f}(t)\cdot CL_{f0}\cdot\frac{C_{liv}^{f}}{Kp_{liv}^{f}(t)\Big/BP^{f}(t)}
\end{aligned}
\tag{7}
$$

where $CL_{f0}$ is the fetal hepatic metabolic clearance and subscription hep_ven and hep_art and gut refer to the hepatic blood supplied by umblical vein (minus ductus venosus blood flow) and by the hepatic artery, respectively. The former is from the fetal placental blood compartment (Figure 1).

**Fetal peripheral compartment**

$$
V_{per}^{f}(t)\frac{d\left[C_{per}^{f}\right]}{dt} = Q_{per}^{f}(t)\left(C_{a}^{f} - \frac{C_{per}^{f}}{Kp_{per}^{f}(t)\Big/BP^{f}(t)}\right) \tag{8}
$$

**Fetal brain**

$$
V_{bra}^{f}(t)\frac{d\left[C_{bra}^{f}\right]}{dt} = Q_{bra}^{f}(t)\left(C_{a}^{f} - \frac{C_{bra}^{f}}{Kp_{bra}^{f}(t)\Big/BP^{f}(t)}\right) \tag{9}
$$

where subscription bra means brain compartment.

Fetal central arterial blood compartment

$$V_a^f(t)\frac{d\left[C_a^f\right]}{dt} = (Q_{pl}^f(t) + Q_{kid}^f(t) + Q_{gut}^f(t) + Q_{port\_a}^f(t) + Q_{per}^f(t) + Q_{bra}^f(t))(C_v^f - C_a^f) \quad (10)$$

**Fetal central venous blood compartment**

$$\begin{aligned} V_v^f(t)\frac{d\left[C_v^f\right]}{dt} &= (Q_{pl}^f(t) - Q_{hep\_ven}^f(t))C_{pl}^f \\ &- (Q_{pl}^f(t) + Q_{kid}^f(t) + Q_{gut}^f(t) + Q_{hep\_art}^f(t) + Q_{per}^f(t) + Q_{bra}^f(t))C_v^f \\ &+ Q_{kid}^f(t)\frac{C_{kid}^f}{Kp_{kid}^f(t)\Big/BP^f(t)} \\ &+ Q_{per}^f(t)\frac{C_{per}^f}{Kp_{per}^f(t)\Big/BP^f(t)} \\ &+ Q_{bra}^f(t)\frac{C_{bra}^f}{Kp_{bra}^f(t)\Big/BP^f(t)} \\ &+ (Q_{gut}^f(t) + Q_{port\_a}^f(t) + Q_{port\_v}^f(t))\frac{C_{liv}^f}{Kp_{liv}^f(t)\Big/BP^f(t)} \\ &- \frac{CL_{renal}^f(t)}{BP^f(t)}C_v^f \end{aligned} \quad (11)$$

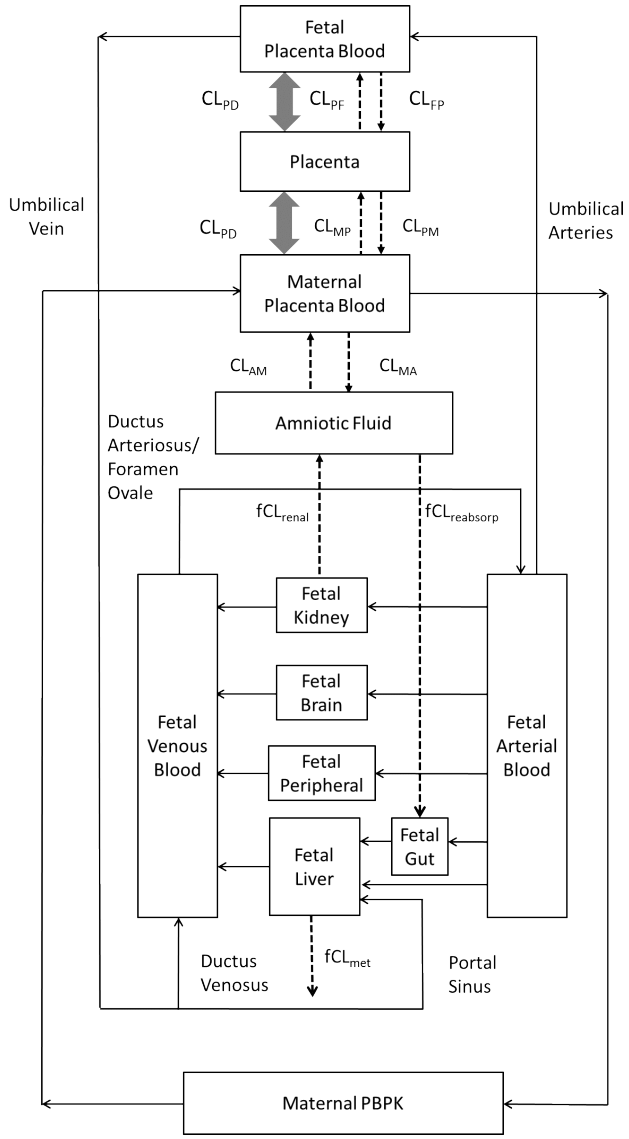


**Figure 3.1. Schematic diagram of the maternal-fetal full PBPK model**. Solid arrows indicate tissue blood flows and dashed arrows indicate clearances. CL: clearance; Prefixes: f-fetal; Subscripts: PD- passive diffusion, M- maternal, P- placenta, F- fetus, A- amniotic fluid, met- metabolism, renal-renal excretion, reabsorp- amniotic fluid swallowing. $CL_{FP/MP}$ and $CL_{PF/PM}$ represent unidirectional transporter-mediated clearances.

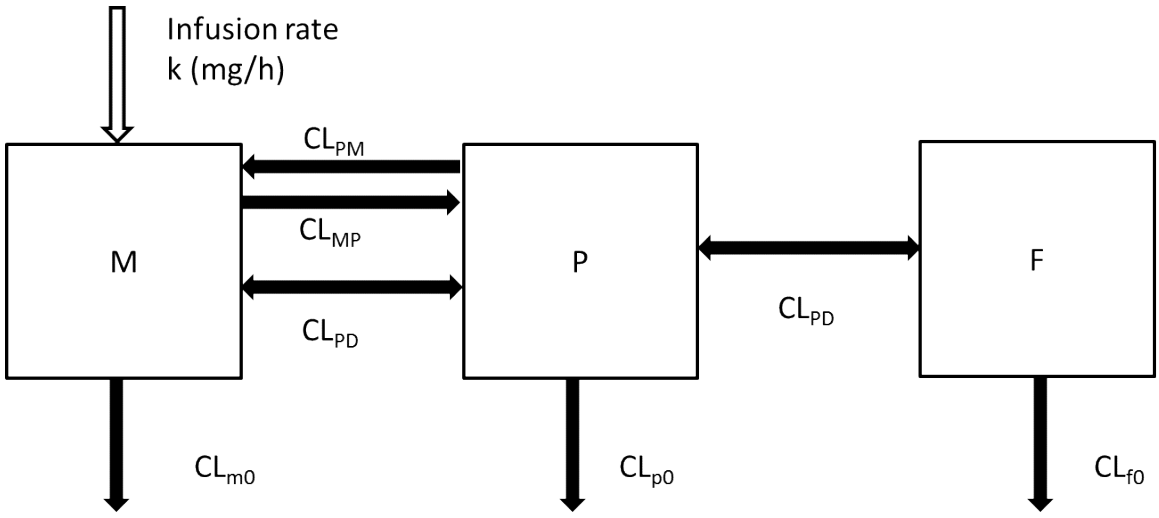


**Figure 3.2. A three compartment model representing the maternal (M), placental (P), and fetal (F) compartments**: 0- irreversible elimination. The remaining abbreviations are as in Figure 1. For simplicity, excretion of drugs from fetus into the amniotic fluid was assumed to be negligible.

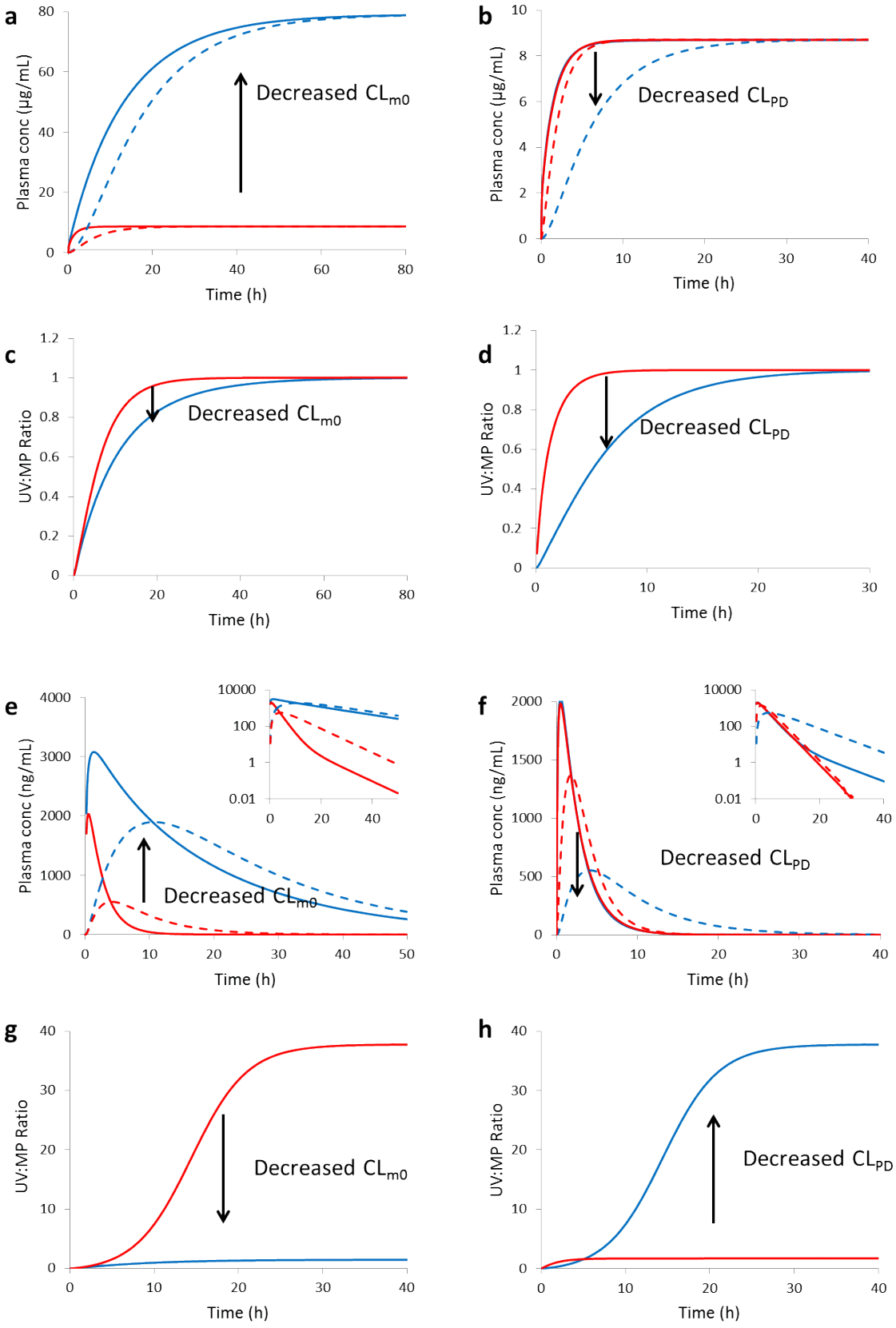
a
Plasma conc (µg/mL)
Time (h)
Decreased CLm0
b
Plasma conc (µg/mL)
Time (h)
Decreased CLPD
c
UV:MP Ratio
Time (h)
Decreased CLm0
d
UV:MP Ratio
Time (h)
Decreased CLPD
e
Plasma conc (ng/mL)
Time (h)
Decreased CLm0
f
Plasma conc (ng/mL)
Time (h)
Decreased CLPD
g
UV:MP Ratio
Time (h)
Decreased CLm0
h
UV:MP Ratio
Time (h)
Decreased CLPD

**Figure 3.3. Changes in maternal systemic clearance ($CL_{m0}$) or transplacental passive diffusion clearance ($CL_{PD}$) of drug X significantly influenced maternal-fetal drug X plasma concentration-time profiles at week 40**. Following IV infusion (400 mg/h) at week 40, decreasing $CL_{m0}$ from 45 L/h (red) to 4.5 L/h (blue) increased the steady-state maternal (solid lines) and fetal (dashed lines) plasma concentration of drug X as well as the time to reach steady-state (**a**). Decreasing $CL_{PD}$ from 18 L/h (red) to 1.8 L/h (blue) did not affect the maternal (the red and blue solid lines overlap) or fetal steady-state plasma concentration of the drug but did prolong the time to reach steady-state only in the fetal plasma (**b**). The corresponding UV:MP ratios indicate that, at steady-state, these ratios do not change with change in $CL_{m0}$ (45L/h, red; 4.5L/h, blue) (**c**) or $CL_{PD}$ (18L/h, red; 1.8L/h, blue) (**d**) but the time to reach the steady-state ratio was prolonged. Following a single oral dose (400 mg), increasing $CL_{m0}$ from 4.5L/h (blue) to 45 L/h (red) resulted in lower maternal plasma drug concentrations (solid lines) and subsequently lower fetal plasma drug X concentrations (dashed lines) (**e**). In contrast, increasing $CL_{PD}$ from 1.8L/h (blue) to 18L/h (red) significantly modified the shape of fetal plasma C-T curve (dashed lines) but not maternal plasma drug concentrations (solid lines; blue and red lines overlap) (**f**). Corresponding changes in UV:MP ratio indicate that higher $CL_{m0}$ (red) led to greater fluctuations in the UV:MP ratio as well as a lager UV:MP ratio at distributional equilibrium(**g**), whereas higher $CL_{PD}$ (red) not only shortened the time to reach distributional equilibrium but also reduced distributional equilibrium UV:MP ratio compared with lower $CL_{PD}$ (blue) (**h**). Insets show the curves on a semi-logarithmic scale. See **Table 3.2** for the clearance values used in these simulations.

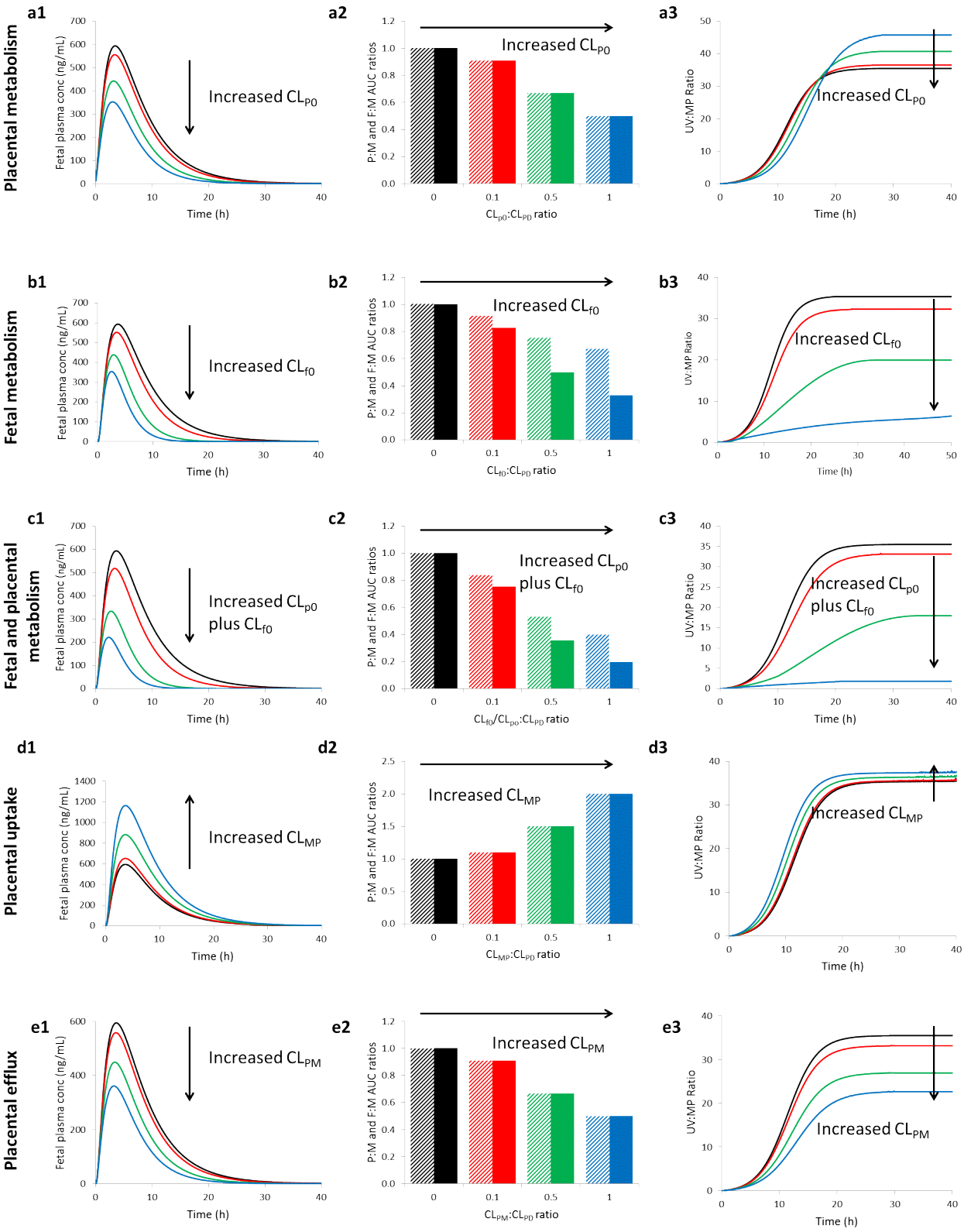
Placental metabolism
a1
Fetal plasma conc (ng/mL)
Time (h)
Increased $CL_{P0}$
a2
P:M and F:M AUC ratios
$CL_{p0}$:$CL_{PD}$ ratio
Increased $CL_{P0}$
a3
UV:MP Ratio
Time (h)
Increased $CL_{P0}$
Fetal metabolism
b1
Fetal plasma conc (ng/mL)
Time (h)
Increased $CL_{f0}$
b2
P:M and F:M AUC ratios
$CL_{f0}$:$CL_{PD}$ ratio
Increased $CL_{f0}$
b3
UV:MP Ratio
Time (h)
Increased $CL_{f0}$
Fetal and placental metabolism
c1
Fetal plasma conc (ng/mL)
Time (h)
Increased $CL_{p0}$ plus $CL_{f0}$
c2
P:M and F:M AUC ratios
$CL_{f0}/CL_{p0}$:$CL_{PD}$ ratio
Increased $CL_{p0}$ plus $CL_{f0}$
c3
UV:MP Ratio
Time (h)
Increased $CL_{p0}$ plus $CL_{f0}$
Placental uptake
d1
Fetal plasma conc (ng/mL)
Time (h)
Increased $CL_{MP}$
d2
P:M and F:M AUC ratios
$CL_{MP}$:$CL_{PD}$ ratio
Increased $CL_{MP}$
d3
UV:MP Ratio
Time (h)
Increased $CL_{MP}$
Placental efflux
e1
Fetal plasma conc (ng/mL)
Time (h)
Increased $CL_{PM}$
e2
P:M and F:M AUC ratios
$CL_{PM}$:$CL_{PD}$ ratio
Increased $CL_{PM}$
e3
UV:MP Ratio
Time (h)
Increased $CL_{PM}$

**Figure 3.4. Changes in fetoplacental clearance pathways differentially impacted fetal exposure to drug X, placental:maternal plasma (P:M) AUC ratio (hatched bar), fetal:maternal (F:M) plasma AUC ratio (solid bar), and the UV:MP ratio after a single 400 mg oral dose of drug X at week 40**. The placental passive diffusion clearance ($CL_{PD}$) of drug X was held at 1.8L/h. The clearance pathway varied is indicated in first panel of each row. The indicated clearance was set at 0 L/h, 0.18 L/h, 0.9 L/h, or 1.8 L/h, respectively (0%, 10%, 50%, or 100% of $CL_{PD}$; black, red, green, and blue lines, respectively). Other than $CL_{MP}$ (**d1**), increasing any of the indicated clearance pathways resulted in lower fetal plasma drug X concentrations (**a1-c1** and **e1**). When only $CL_{f0}$ was present, the F:M plasma AUC ratio was lower (**b2** and **c2**) than when only $CL_{P0}$ was present (**a2**). In all cases the predicted UV:MP ratio at distributional equilibrium was significantly greater than its steady-state$_{inf}$ value (the $C_{f,ss,\inf} / C_{m,ss,\inf}$ ratio; **Eq. 1**). The UV:MP ratio at distributional equilibrium decreased with increase in $CL_{f0}$, $CL_{f0}$ plus $CL_{p0}$, or $CL_{PM}$ and increased with an decrease in $CL_{p0}$ or increase in $CL_{MP}$ (**b3**, **c3**,**d3**,**a3**,and **e3**,respectively). See **Table 3.2** for the clearance values used in these simulations.

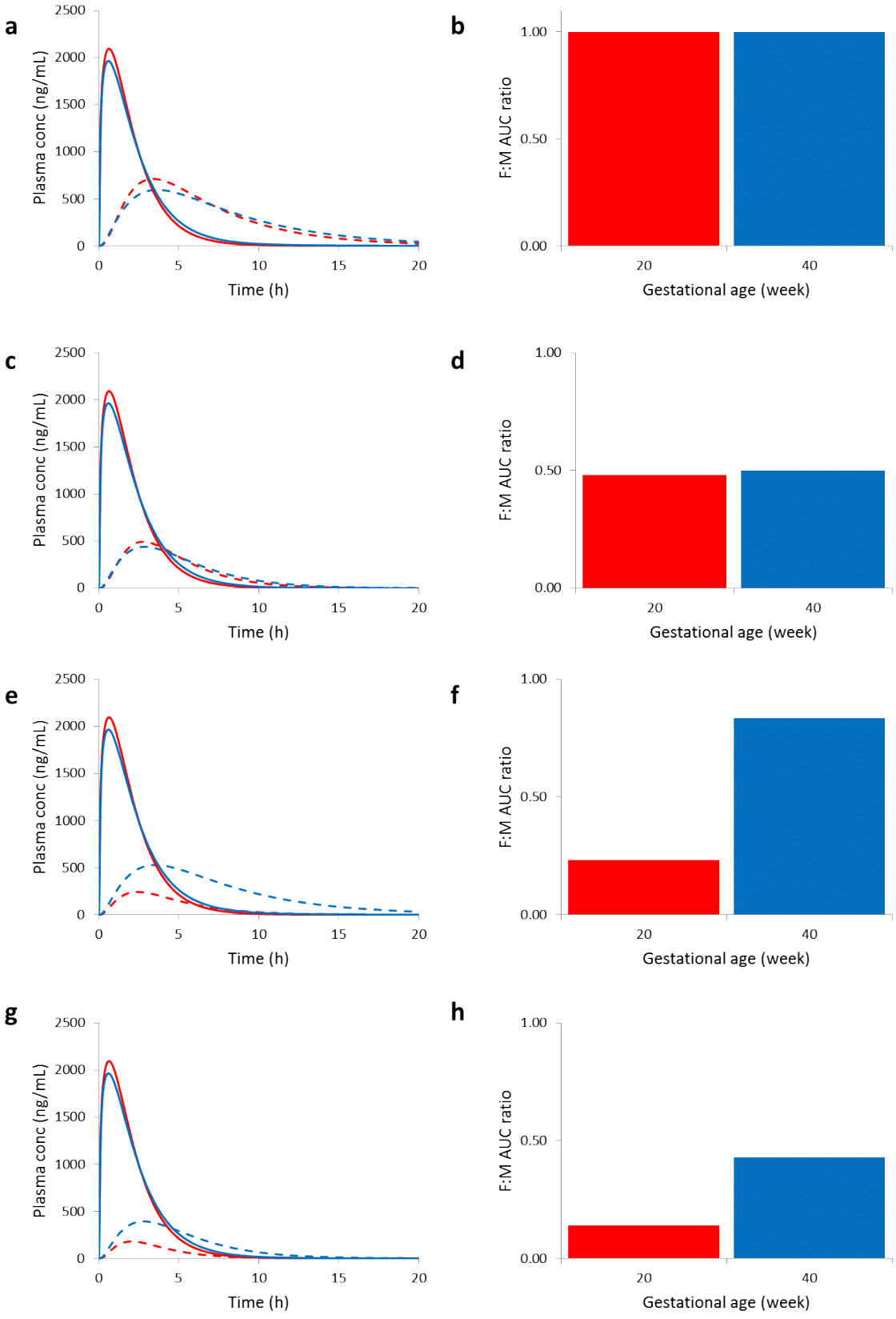
a
Plasma conc (ng/mL)
2500
2000
1500
1000
500
0
0
5
10
15
20
Time (h)
b
F:M AUC ratio
1.00
0.50
0.00
20
40
Gestational age (week)
c
Plasma conc (ng/mL)
Time (h)
d
F:M AUC ratio
Gestational age (week)
e
Plasma conc (ng/mL)
Time (h)
f
F:M AUC ratio
Gestational age (week)
g
Plasma conc (ng/mL)
Time (h)
h
F:M AUC ratio
Gestational age (week)

**Figure 3.5. The effect of gestational age on fetal exposure to drug X varies with fetoplacental clearance mechanisms involved**. Maternal (solid) and fetal (dashed) C-T profiles as well as fetal:maternal (F:M) plasma AUC ratios were simulated after a single 400mg oral dose of drug X at week 20 (red) and week 40 (blue) under different scenarios. In scenario 1, where no irreversible loss of drug X occurred in the fetoplacental unit, the advancement of gestational age did not significantly affect fetal-maternal drug disposition (**a**) or the F:M plasma AUC ratio of unity (**b**). In scenario 2, the addition of fetal metabolism (increased proportionally with the fetal body volume as gestational age increased) significantly reduced fetal plasma drug concentrations (**c** vs. **a**) and resulted in ~50% decrease in F:M AUC plasma ratio at both gestational ages (**d**). In scenario 3, placental P-gp efflux clearance decreased with gestational age (based on reported P-gp expression and changes in placental volume with gestational age). Consequently, fetal exposure to drug X increased with gestational age, reflected by higher fetal plasma drug concentrations (**e**) and increased F:M plasma AUC ratio (**f**). Finally, in scenario 4 where both fetal metabolism and placental efflux were present, further reduction in fetal exposure was observed at both gestational ages (**g, h**). See **Table 3.2** and **Table 3.3** for the clearance values used in these simulations.

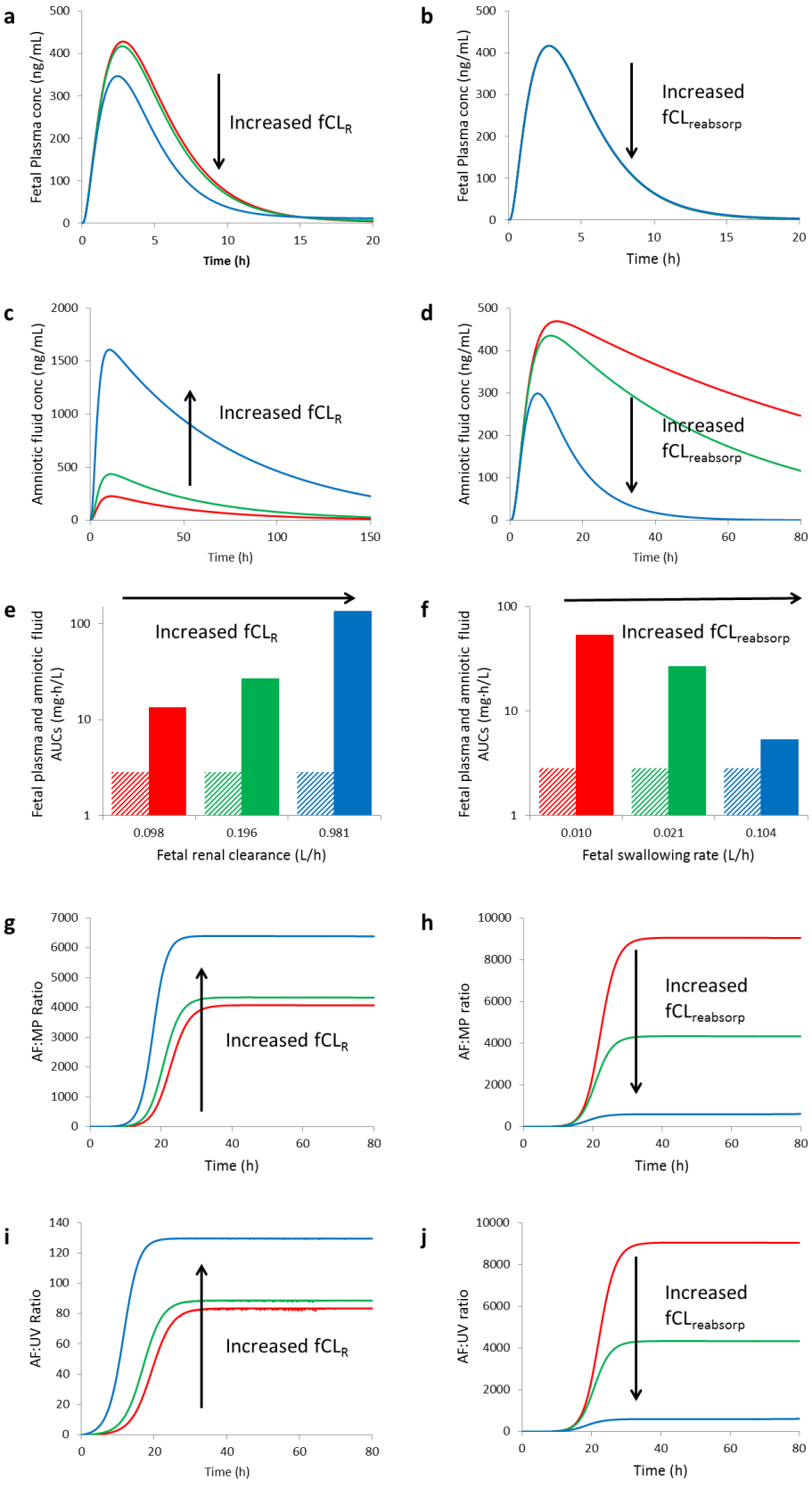
a
Fetal Plasma conc (ng/mL)
Increased fCL_R
Time (h)
b
Fetal Plasma conc (ng/mL)
Increased fCL_reabsorp
Time (h)
c
Amniotic fluid conc (ng/mL)
Increased fCL_R
Time (h)
d
Amniotic fluid conc (ng/mL)
Increased fCL_reabsorp
Time (h)
e
Fetal plasma and amniotic fluid AUCs (mg·h/L)
Increased fCL_R
0.098
0.196
0.981
Fetal renal clearance (L/h)
f
Fetal plasma and amniotic fluid AUCs (mg·h/L)
Increased fCL_reabsorp
0.010
0.021
0.104
Fetal swallowing rate (L/h)
g
AF:MP Ratio
Increased fCL_R
Time (h)
h
AF:MP ratio
Increased fCL_reabsorp
Time (h)
i
AF:UV Ratio
Increased fCL_R
Time (h)
j
AF:UV ratio
Increased fCL_reabsorp
Time (h)

**Figure S3.1. Changes in fetal renal clearance (fCLR) or fetal amniotic fluid swallowing rate (fCLreabsorp) affected drug concentrations in fetal plasma and amniotic fluid differently**. Following a single oral dose of 400 mg drug X at week 40, fCLR (0.196L/h) or fCLreabsorp (0.024 L/h) of drug X was varied by 0.5-,1-,and 5-fold (red, green, and blue, respectively). Fetal plasma drug X concentrations remained independent of changes in either fCLR (a) or in fCLreabsorp (b), except when fCLR was increased by 5-fold (but even in this case the AUC was not changed). In contrast, amniotic fluid drug X concentrations were quite sensitive to changes in these two pathways. Increasing fCLR resulted in higher amniotic fluid drug concentrations (c), whereas increasing fCLreabsorp reduced amniotic fluid drug X exposure (d). Increasing fCLR from 0.098 L/h to 0.981 L/h proportionally increased amniotic fluid drug X AUC (solid bars) while fetal plasma AUC (hatched bars) remained constant (e). Similarly, increasing the magnitude of fCLreabsorp from 0.01 L/h to 0.10 L/h proportionally decreased amniotic fluid AUC (solid bars) without affecting fetal plasma AUC (hatched bars)(f). Similar trends were observed with fetal:maternal (F:M) plasma AUC ratio (circles) and amniotic flud:maternal plasma (AF:MP) AUC ratio (squares) (e and f, respectively). AF:MP and amniotic fluid:umbilical venous plasma (AF:UV) drug X concentration ratios also varied significantly when fCLR (g and i, respectively) or fCLreabsorp (h and j, respectively) was altered. Increasing fCLR resulted in higher AF:MP and AF:UV ratios, while increasing fCLreabsorp reduced both ratios. See Table 3.2 for the clearance values used in these simulations.

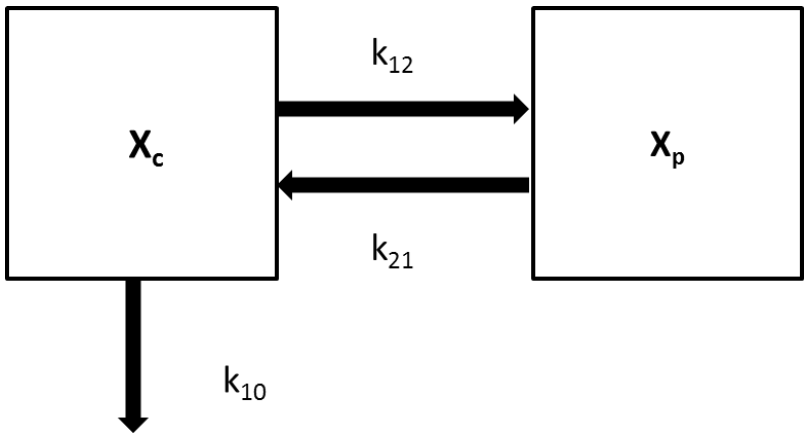


**Figure S3.2. Two compartment maternal-fetal schematic diagram**. In this schematic, $X_c$ and $X_p$ denotes the amount of drug in the central compartment and the peripheral compartments, respectively; $k_{10}$ is the central compartment elimination rate constant, whereas $k_{12}$, and $k_{21}$ are the inter-compartmental distribution rate constants.

**Table 3.1. Key fetal physiological parameters**

| Parameter (units) | Formula[a] | References | Graph[b] |
|---|---|---|---|
| Maternal placental blood flow (L/h) | $1.71 + 0.207GA + 0.0841GA^2 - 0.0015GA^3$ ($R^2 = 0.991$; GA: 0-40 weeks) | Abduljalil, Furness et al. 2012 | 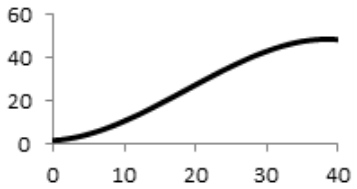  |
| Fetal serum albumin (mg/dL) | $-31.7 + 4.35GA - 0.101GA^2 + 0.0009GA^3$ ($R^2 = 0.987$; GA: 10-40 weeks) | Gitlin and Perricelli 1970; Krauer, Dayer et al. 1984; Moniz, Nicolaides et al. 1985; Weiner, Sipes et al. 1992 | 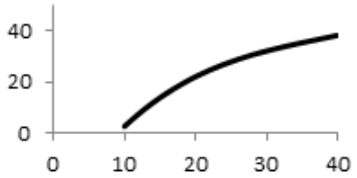  |
| Fetal serum $\alpha_1$-acid glycoprotein (mg/dL) | $0.02e^{0.0616GA}$ ($R^2 = 0.519$; GA: 16-38 weeks) | Krauer, Dayer et al. 1984 | 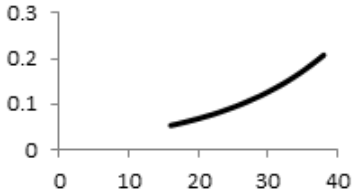  |

| | | | |
|---|---|---|---|
| Fetal brain volume (mL) | $36.0 - 7.53GA + 0.400GA^2$ ($R^2 = 0.998$; GA: 12-41 weeks) | Gruenwald and Minh 1961; Cussen, Scurry et al. 1990; Hansen, Sung et al. 2003; Archie, Collins et al. 2006 | 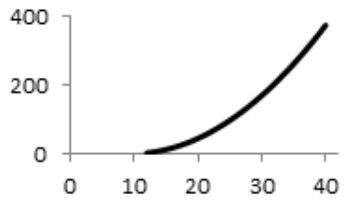 |
| Fetal liver volume (mL) | $16.6 - 2.92GA + 0.143GA^2$ ($R^2 = 0.996$; GA: 12-41 weeks) | Gruenwald and Minh 1961; Cussen, Scurry et al. 1990; Hansen, Sung et al. 2003; Archie, Collins et al. 2006 | 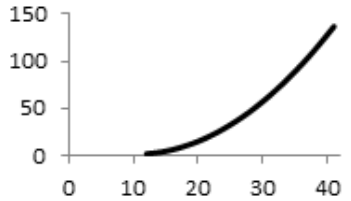 |
| Fetal stomach volume (mL) | $0.127e^{0.101GA}$ ($R^2 = 0.962$; GA: 20-37 weeks)<br>$25.3 - 0.548GA$ ($R^2 = 0.994$; GA: 37-40 | Gruenwald and Minh 1961; Cussen, Scurry et al. 1990; Hansen, Sung et al. 2003 | 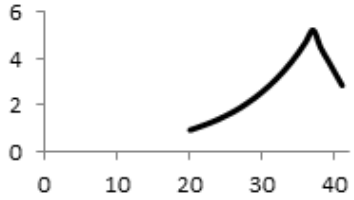 |
| Fetal small intestine volume (mL) | $0.0203e^{0.194GA}$ ($R^2 = 0.998$; GA: 12-25 weeks) * | FitzSimmons, Chinn et al. 1988; Nagata, Koyanagi et al. 1990; Parulekar 1991 | 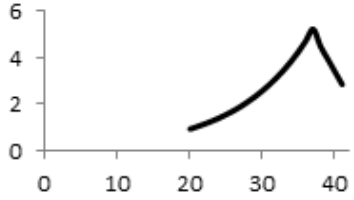 |

| | | | |
|---|---|---|---|
| Fetal large intestine volume (mL) | $0.078e^{0.169GA}$ ($R^2$ = 0.866; GA: 20-37 weeks) | Rubesova, Vance et al. 2009 | 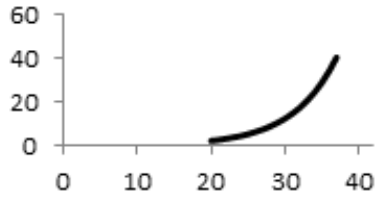 |
| Fetal total gut volume (mL) | $- 54.3 + 8.90GA - 0.479GA^2 + 0.0088GA^3$ ($R^2$ = 0.998)** | Nagata, Koyanagi et al. 1990;<br>Parulekar 1991;<br>Archie, Collins et al. 2006;<br>Rubesova, Vance et al. 2009 | 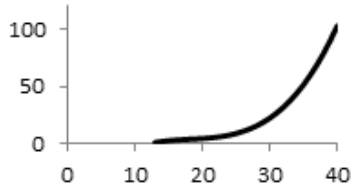 |
| Fetal kidney volume (mL) | $2.37 - 0.619GA + 0.0335GA^2$ ($R^2$ = 0.994; GA: 14-41 weeks) | Cussen, Scurry et al. 1990;<br>Hansen, Sung et al. 2003 | 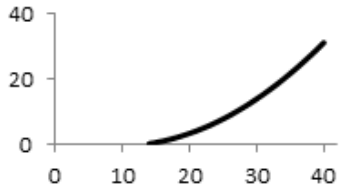 |

| | | | |
|---|---|---|---|
| Fetal umbilical blood flow (L/h) | 0.647 - 0.227GA + 0.0179GA$^2$ ($R^2$ = 0.9984; GA: 18-40) | Sutton, Theard et al. 1990; Tchirikov, Rybakowski et al. 1998; Lees, Albaiges et al. 1999; Kiserud, Rasmussen et al. 2000; Boito, Struijk et al. 2002; Tchirikov, Rybakowski et al. 2002; Acharya, Erkinaro | 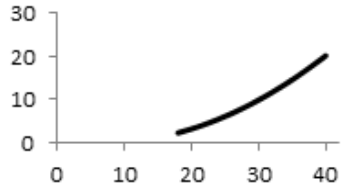 |
| Ductus venosus blood flow (L/h) | 2.05 - 0.297GA + 0.0116GA$^2$ ($R^2$ = 1.00; GA: 20-38 weeks) | Bellotti, Pennati et al. 2004; Kessler, Rasmussen et al. 2008 | 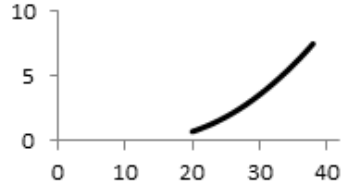 |
| Fetal portal vein blood flow (L/h) | 0.714 + 0.0489GA + 0.0008GA$^2$ ($R^2$= 1.00; GA: 20-38 weeks)** | Bellotti, Pennati et al. 2004; Haugen, Kiserud et al. 2004; Kessler, Rasmussen et al. 2008 | 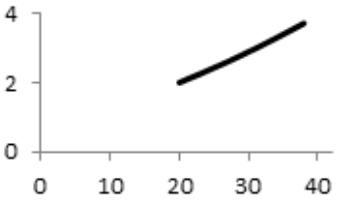 |

| | | | |
|---|---|---|---|
| Fetal brain blood flow (mL/min) | $5.56e^{0.0921GA}$ ($R^2$ = 0.999; GA: 10-20 weeks) † | Rudolph AM 1971; Kenny, Plappert et al. 1986 | 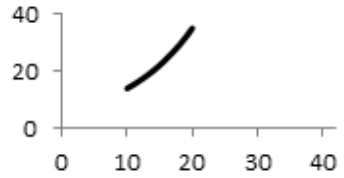  |
| Fetal kidney blood flow (mL/min) | $2.18e^{0.0865GA}$ ($R^2$ = 0.707; GA: 10-41 weeks) † | Rudolph AM 1971; Kenny, Plappert et al. 1986; Veille, Hanson et al. 1993 | 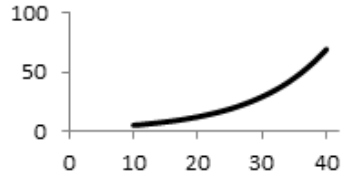  |
| Fetal glomerular filtration clearance (L/h) | $0.00046e^{0.15GA}$ ($R^2$ = 0.69; GA: 23-40 weeks) †† | Arant 1978; Hansen, Oh et al. 1983; Coulthard 1985; van den Anker,de Groot et al. 1995 | 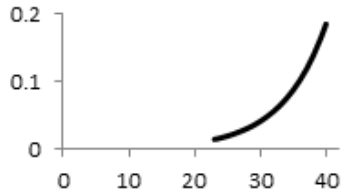  |
| Fetal gut blood flow (mL/min) | $1.67e^{0.124GA}$ ($R^2$= 0.999; GA: 10-20 weeks) † | Kenny, Plappert et al. 1986; Veille, Hanson et al. 1993 | 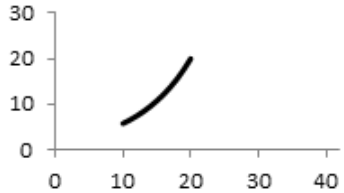  |

| | | | |
|---|---|---|---|
| Fetal peripheral compartment volume (mL) | $290.0 - 62.5GA + 3.22GA^2$ ($R^2 = 0.998$) ††† | Abduljalil, Furness et al. 2012 | 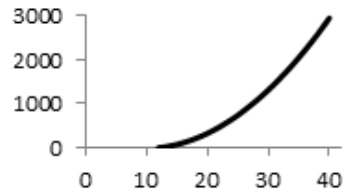 |
| Syncytiotrophoblast volume (mL) | $- 6.83 + 0.650GA + 0.0370GA^2$ ($R^2 = 0.757$; GA: 10-41 weeks) | Mayhew and Barker 2001 | 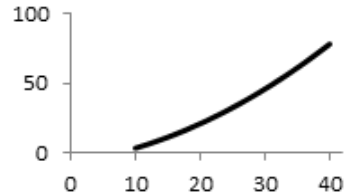 |
| Placental villous surface area ($m^2$) | $4.66 - 0.788GA + 0.0383GA^2 - 0.0004GA^3$ ($R^2 = 0.922$; GA: 12-41 weeks) | Wang 2010 | 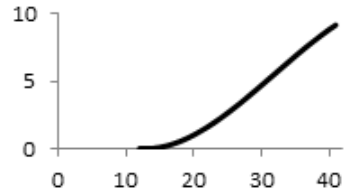 |

a. GA denotes gestational age in weeks.

b. In the graphs above, the x axes are gestational age in weeks, whereas the y axes show the gestational age-dependent trends of the respective parameters in units as indicated in the first cell of each row.

* Calculated using a reported fetal small intestine (SI) diameter formula (Parulekar 1991) and the reported fetal SI length (FitzSimmons, Chinn et al. 1988) assuming cylindrical SI and negligible gut wall thickness.

** Fetal gut consists of fetal stomach, small intestine, and large intestine. Unfortunately, there is no reported data on fetal small intestine volume during the second half of gestation. Because the reported data on these three organs overlapped between week 20 and week 25, the small intestine volume percentage (SI %) of the total gut volume for only this range of gestation was fitted to various models. A linear model (SI% = 0.652GA+11.766), best describing the gestational age dependency of SI% volume within this range, was used to estimate the SI% volume beyond week 25. Then, the total fetal gut volume after week 25 was calculated by dividing the sum of fetal stomach and large intestine volumes by their corresponding volume percentage (i.e. 1 - SI%).

***Calculated as the difference between total liver venous blood flow and umbilical venous blood flow. Formulae provided by the original sources were used when digitization was not possible.

† Calculated as the product of fetal combined cardiac output (CCO) and the percent CCO in respective organs.

†† Because it is not possible to measure fetal glomerular filtration rate (GFR) or renal function in utero, inulin clearance measured in preterm and term newborns were collected as a surrogate for fetal GFR. It is worth pointing out that GFR value continues to increase after birth as a result of the drop in renal vascular resistance and increase in renal blood flow. (Guignard, Torrado et al. 1975) Consequently, only measurements taken within 7 days post birth were included in our literature search.

††† Fetal peripheral compartment was **back-calculated** as fetal weight [based on published fetal volume formula (Abduljalil, Furness et al. 2012) assuming a 1mg/mL density throughout gestation] minus the sum of fetal organ volumes and fetal blood volume [based on

the reported average fetoplacental blood volume of 123mL/kg fetal weight during the second and third trimesters (Pasman et al., 2009)].

**Table 3.2. Clearance values (L/h) used in various scenarios**

| Figure | Dosing regimen | | $CL_{m0}$ | $CL_{PD}$ | $CL_{MP}$ | $CL_{PM}$ | $CL_{p0}$ | $CL_{f0}$ | $fCL_{R}$ | $fCL_{reabsorp}$ |
|---|---|---|---|---|---|---|---|---|---|---|
| Figure 3a,c | week 40, 400mg continuous IV infusion | | 4.5 vs 45 | 1.8 | 0 | 0 | 0 | 0 | 0 | 0 |
| Figure 3b,d | week 40, 400mg continuous IV infusion | | 45 | 1.8 vs 18 | 0 | 0 | 0 | 0 | 0 | 0 |
| Figure 3e,g | week 40, 400mg single oral dose | | 4.5 vs 45 | 1.8 | 0 | 0 | 0 | 0 | 0 | 0 |
| Figure 3f,h | week 40, 400mg single oral dose | | 45 | 1.8 vs 18 | 0 | 0 | 0 | 0 | 0 | 0 |
| Figure 4a | week 40, 400mg single oral dose | | 45 | 1.8 | 0 | 0 | 0,0.18,0.90,1.8 | 0 | 0 | 0 |
| Figure 4b | | | | | 0 | 0 | 0 | 0,0.18,0.9,1.8 | 0 | 0 |
| Figure 4c | | | | | 0 | 0 | 0,0.18,0.9,1.8 | 0,0.18,0.9,1.8 | 0 | 0 |
| Figure 4d | | | | | 0,0.18,0.9,1.8 | 0 | 0 | 0 | 0 | 0 |
| Figure 4e | | | | | 0 | 0,0.18,0.9,1.8 | 0 | 0 | 0 | 0 |
| Figure 5a, b (Scenario 1) | 400mg | week 20 | 44 | 0.21 | 0 | 0 | 0 | 0 | 0 | 0 |
| | | week 40 | 45 | 1.8 | 0 | 0 | 0 | 0 | 0 | 0 |
| Figure 5c, d (Scenario 2) | | week 20 | 44 | 0.21 | 0 | 0 | 0 | 0.11 | 0 | 0 |
| | | week 40 | 45 | 1.8 | 0 | 0 | 0 | 0.90 | 0 | 0 |

| | | | | | | | | | | |
|---|---|---|---|---|---|---|---|---|---|---|
| Figure 5e, f (Scenario 3) | single oral dose | week 20 | 44 | 0.21 | 0 | 0.70 | 0 | 0 | 0 | 0 |
| | | week 40 | 45 | 1.8 | 0 | 0.36 | 0 | 0 | 0 | 0 |
| Figure 5g, h (Scenario 4) | | week 20 | 44 | 0.21 | 0 | 0.70 | 0 | 0.11 | 0 | 0 |
| | | week 40 | 45 | 1.8 | 0 | 0.36 | 0 | 0.90 | 0 | 0 |
| Figure S1 a,c,e,g | week 40, 400mg single oral | | 45 | 1.8 | 0 | 0 | 0 | 0.90 | 0.1,0.20,0.98 | 0.021 |
| FigureS1 b,d,f,h | | | 45 | 1.8 | 0 | 0 | 0 | 0.90 | 0.20 | 0.01,0.02,1.0 |

* $CL_{m0}$, maternal systemic clearance; $CL_{PD}$, transplacental passive diffusion clearance; $CL_{MP}$, placental efflux clearance; $CL_{PM}$, placental uptake clearance; $CL_{p0}$,placental metabolism; $CL_{f0}$, fetal metabolism; week, gestational week.

** At 40 weeks, $CL_{m0}$ was set at 45L/h based on the published didanosine clearance value (see **Table S1**; rounded down to the nearest integer**)**. $CL_{PD}$ was extrapolated from the reported didanosine transplacental passive diffusion clearance in pregnant macaques based on body weight (see **Table S1** for detail).

**Table 3.3. Gestational age-dependent changes in the fetal metabolic ($CL_{f0}$) and placental efflux ($CL_{PM}$) clearances of drug X**

| Clearance | Gestational age week 20 | Gestational age week 40 | week 40: week 20 ratio |
|---|---|---|---|
| $CL_{PD}$* | 0.21 L/h | 1.80 L/h | 8.6 |
| $CL_{f0}$ | 0.11 L/h (53% of | 0.90 L/h | 8.2 |
| $CL_{PM}$**(P-gp mediated) | 0.70 L/h†(330% of $CL_{PD}$) | 0.36 L/h (20% of $CL_{PD}$) | 0.51 |

* Denotes transplacental passive diffusion clearance.

** Denotes efflux clearance mediated by P-gp located on the apical side of placenta; assumed to be 20% of $CL_{PD}$ at week 40. .

† Back extrapolated based on the 5-fold decrease in placental P-gp expression(Mathias et al., 2005) and the reported 2.6-fold increase in the placenta volume (Abduljalil et al., 2012).

**Table S3.1. Summary of drug-specific parameters used in simulation (at week 40)**

| Parameter | Drug X |
|---|---|
| Molecular Weight | 236.23[a] |
| logP | 0.05[b] |
| B/P Ratio | 1.17[c] |
| $V_{ss}$ (L/kg) | 0.71[d] |
| $f_{u,plasma}$ | 0.99[e] |
| $F_a$ | 1.0[f] |
| $k_a$ ($h^{-1}$) | 1.5[g] |
| $F_g$ | 0.78[f] |
| $CL_r$ (L/h) | 18.1[d] |
| $CL_{iv}$ (L/h) | 45.6[d] |
| $CL_{PD}$ (L/h) | 1.80[h] |
| $f_m$ and $f_e$ | $f_m$ =61%, $f_e$ =39% [d] |
| $CL_{f0}$ (L/h) | 0.9[h] |

The above values were based on the reported didanosine (ddI) PK parameters in the literature.

a. Extracted from didanosine product monograph (http://monographs.iarc.fr/ENG/Monographs/vol76/mono76-9.pdf).

b. Literature value (Tuntland et al., 1999).

c. Calculated from the reported blood: plasma didanosine AUC ratio (Barry et al., 1993).

d. Predicted by Simcyp® (V14) based on literature value (Knupp et al., 1991). $V_{ss}$ increased slightly from 0.68 L/kg at week 20 to 0.71 L/kg to week 40.

e. Reported plasma binding of didanosine is <5%. Minimal binding of 1% was assumed for ease of data interpretation.

f. Reported average didanosine absolute bioavailability is 23.5% (Range: 14%-33% ). Animal studies indicate that didanosine is rapidly and completely absorbed. Therefore, $F_a$ was assumed to be 1. The reported intravenous non-renal clearance (~30L/h) (Knupp et al., 1991) does not fully explain the first pass effect. $F_g$ of 0.78 was used to recover oral PK.

g. Literature value (Velasque et al., 2007).

h. Fetal drug X clearance at term was calculated as the product of fetal didanosine clearance in macaque fetus [dam weight normalized(Tuntland et al., 1999)] and the average term body weight of 85 kg in human pregnant women (Abduljalil et al., 2012) . The reported steady-state fetal:dam didanosine concentration ratio is ~0.5 (Tuntland et al., 1999). Therefore, passive diffusion clearance was 1.8 L/h according to Eq. 4, assuming the same ratio holds true for drug X in human maternal-fetal pairs.

**Table S3.2. Maternal and fetal plasma AUC values in various scenarios**

| Figure | Dosing regimen | Factor | Value (L/h) | $AUC_f$ (mg·h/L) | $AUC_m$ (mg·h/L) | $AUC_f$ :$AUC_m$ Ratio | Note |
|---|---|---|---|---|---|---|---|
| Figure 3e,g | week 40, 400mg single oral dose | $CL_{m0}$ | 45 | 5.7 | 5.7 | 1.0 | $AUC_{0-50h}$ |
| | | | 4.5 | 52.3 | 52.3 | 1.0 | |
| Figure 3f,h | week 40, 400mg single oral dose | $CL_{PD}$ | 18 | 5.7 | 5.7 | 1.0 | $AUC_{0-40h}$ |
| | | | 1.8 | 5.7 | 5.7 | 1.0 | |
| Figure 4a | week 40, 400mg single oral dose | $CL_{p0}$ | 0 | 5.7 | 5.7 | 1.0 | $AUC_{0-40h}$ |
| | | | 0.18 | 5.1 | 5.7 | 0.9 | |
| | | | 0.9 | 3.7 | 5.7 | 0.7 | |
| | | | 1.8 | 2.8 | 5.7 | 0.5 | |
| Figure 4b | week 40, 400mg single oral dose | $CL_{f0}$ | 0 | 5.7 | 5.7 | 1.0 | $AUC_{0-40h}$ |
| | | | 0.18 | 4.7 | 5.7 | 0.8 | |
| | | | 0.9 | 2.8 | 5.7 | 0.5 | |
| | | | 1.8 | 1.9 | 5.7 | 0.3 | |
| Figure 4c | week 40, 400mg single oral dose | $CL_{f0}$ plus $CL_{p0}$ | 0 | 5.7 | 5.7 | 1.0 | $AUC_{0-40h}$ |
| | | | 0.18 | 4.4 | 5.7 | 0.8 | |
| | | | 0.9 | 2.1 | 5.7 | 0.4 | |
| | | | 1.8 | 1.1 | 5.7 | 0.2 | |
| Figure 4d | week 40, 400mg single oral dose | $CL_{MP}$ | 0 | 5.7 | 5.7 | 1.0 | $AUC_{0-40h}$ |
| | | | 0.18 | 6.3 | 5.7 | 1.1 | |
| | | | 0.9 | 8.6 | 5.7 | 1.5 | |
| | | | 1.8 | 11.4 | 5.7 | 2.0 | |
| Figure 4e | week 40, 400mg single oral dose | $CL_{PM}$ | 0 | 5.7 | 5.7 | 1.0 | $AUC_{0-40h}$ |
| | | | 0.18 | 5.1 | 5.7 | 0.9 | |
| | | | 0.9 | 3.7 | 5.7 | 0.7 | |
| | | | 1.8 | 2.8 | 5.7 | 0.5 | |
| Figure 5a, b (Scenario 1) | 400mg single oral dose | week | 20 | 5.6 | 5.6 | 1.0 | $AUC_{0-40h}$ |
| | | | 40 | 5.7 | 5.7 | 1.0 | |
| Figure 5c, d (Scenario 2) | | | 20 | 2.7 | 5.6 | 0.5 | |
| | | | 40 | 2.8 | 5.7 | 0.5 | |

| | | | | | | | |
|---|---|---|---|---|---|---|---|
| Figure 5e, f (Scenario 3) | | | 20 | 1.3 | 5.6 | 0.2 | |
| | | | 40 | 4.8 | 5.7 | 0.8 | |
| Figure 5g, h (Scenario 4) | | | 20 | 0.8 | 5.6 | 0.1 | |
| | | | 40 | 2.4 | 5.7 | 0.4 | |

# Chapter 4 Verification of a Maternal-Fetal Physiologically Based Pharmacokinetic Model for Passive Placental Permeability Drugs

The work presented in this chapter has been accepted
by
Drug Metabolism and Disposition

## 4.1 Abstract

Fetal exposure to drugs cannot be readily estimated from single time point cord blood sampling at the time of delivery. Therefore, we developed a physiologically-based pharmacokinetic (PBPK) model to estimate fetal drug exposure throughout pregnancy. Here we report verification of this novel maternal-fetal physiologically-based pharmacokinetic (m-f-PBPK) model for drugs that passively diffuse across the placenta and are not metabolized/transported there. Our recently built m-f-PBPK model was populated with gestational age-dependent changes in maternal drug disposition and maternal-fetal physiology. Using midazolam as an *in vivo* calibrator, the transplacental passive diffusion clearance of theophylline and zidovudine was first estimated. Then, for verification, the predicted maternal plasma (MP) and umbilical venous (UV) plasma drug concentrations by our m-f-PBPK were compared against those observed at term. Overall, our m-f-PBPK model well predicted the maternal and fetal exposure to the two verification drugs, theophylline and zidovudine, at term, across a range of dosing regimens, with nearly all observed MP and UV plasma drug concentrations falling within the 90% prediction interval [i.e.$5^{th}$ -$95^{th}$ percentile range of a virtual pregnant population (n=100)]. Prediction precision and bias of theophylline MP and UV were 14.5% and 12.4%, and 9.4% and 7.5%, respectively. Further, for zidovudine, after the exclusion of one unexpectedly low MP concentration, prediction precision and bias for MP and UV were 50.3 % and 30.2, and 28.3% and 15.0%, respectively. This m-f-PBPK should be useful to predict fetal exposure to drugs, throughout pregnancy, for drugs that passively diffuse across the placenta.

## 4.2 Introduction

Medication use during pregnancy is remarkably common. The average number of over-the-counter and prescription drugs used by women during pregnancy increased from 2.5 in 1976-78 to 4.2 in 2006-08 in the United States alone (Mitchell et al., 2011). The same study also revealed that, over the same period, use of such drugs during the first trimester increased from 1.6 to 2.6. The above statistics are not surprising as pregnant women need to be treated for many medical conditions, either pre-exiting (e.g. epilepsy, asthma, HIV-infection) or pregnancy-induced (e.g. gestational hypertension, diabetes, preeclampsia). In addition, the fetus is sometimes the therapeutic target, for example, to prevent vertical transmission of HIV (e.g. zidovudine, lamivudine), to treat fetal supraventricular tachycardia (e.g. digoxin) or to prevent fetal respiratory distress syndrome (e.g. dexamethasone) (Evans et al., 1993).

Regardless of whether or not the fetus is the intended target of pharmacotherapy during pregnancy, the fetus is *de facto* exposed to all drugs taken by the mother. Clearly, quantitative assessment of fetal exposure to drugs, especially during early gestation when the fetus is more prone to teratogenic effects (Chung, 2004), is important from both efficacy and toxicity standpoint. However, fetal drug exposure cannot be ethically studied before the time of delivery, when a single time cord blood sample [usually umbilical venous (UV) plasma] can be safely obtained. As we have shown before (manuscript submitted), this UV plasma concentration, except at steady-state after maternal drug infusion, does not provide information on fetal drug exposure, a determinant of drug efficacy and/or toxicity. Furthermore, these term or near-term data cannot be readily extrapolated to early gestation. Therefore, there is a pressing need to

develop other *in silico* methods to predict fetal drug exposure, such as **p**hysiologically-**b**ased **p**harmaco**k**inetic (PBPK) modeling and simulation approaches.

Recently, we expanded our previously verified maternal PBPK (m-PBPK) model to include the fetus (m-f-PBPK model) (manuscript submitted). The placenta, amniotic fluid, and fetal organs important for drug disposition as well as the gestational age-dependent fetal physiological changes (when available) were included in this m-f-PBPK model. Once developed, all models need to be verified. However, in this case, the only data available for verification are the UV and maternal plasma (MP) drug concentrations, often obtained simultaneously, at the time of birth. Therefore, as a first step, the primary objective of this study was to verify our novel m-f-PBPK model for drugs that cross the placenta predominantly by passive diffusion and for which UV and MP concentrations at the time of delivery are available in the literature (i.e. theophylline, and zidovudine).

## 4.3 Materials and Methods

### 4.3.1 The General Maternal-Fetal PBPK Model Structure and Key Assumptions

The general m-f-PBPK structure (**Figure 4.5 b**) and the key assumptions made in constructing the model have been described in detail (manuscript submitted). In brief, a fetal PBPK model was developed to replace the lumped, non-eliminating placental-fetal unit in our verified m-PBPK model (Ke et al., 2012; Ke et al., 2013a; Ke et al., 2013b). The resulting m-f-PBPK contained organs that are relevant to fetal disposition of pharmaceutical agents, including those involved in drug disposition (e.g. fetal liver, fetal kidneys) and in drug efficacy/toxicity (e.g. fetal brain). The model also contained compartments representing the placenta and the amniotic fluid. The ordinary differential equations defining mass balance in the maternal PBPK have been described previously

(Gaohua et al., 2012; Ke et al., 2012), whereas those describing the fetal PBPK are provided in **supplementary information.** Briefly, all tissues except the placenta were regarded as well-stirred tissues; that is, the unbound tissue drug concentration is in instant equilibrium with the unbound drug concentration in the emergent venous blood. The placenta was modeled as a permeability-limited tissue and therefore it was subdivided into maternal placental blood, placenta tissue, and fetal placental blood compartments. Only the unbound, unionized fraction of drug can passively diffuse across the placenta. The bidirectional unbound maternal-placental and fetal-placental transplacental passive diffusion clearances ($CL_{PD,u}$) across the placenta were assumed to be equal (Tuntland et al., 1999). Our model has the capability of including placental transport and fetoplacental metabolism of drugs when quantitative data on transporters and metabolic enzymes become available. Since this fetal PBPK does not contain an umbilical vein compartment *per se*, the predicted fetal plasma drug concentration in the central venous blood compartment was assumed to represent that in umbilical vein.

Known gestational age-dependent changes in maternal and fetal physiology (e.g. blood flows, organ volumes, etc.) from recent literature meta-analyses were incorporated into the m-f-PBPK (Abduljalil et al., 2012) (manuscript submitted). The change in drug unbound fraction in plasma ($f_{u,p}$) was assumed to result from altered serum albumin concentration during pregnancy and was accounted for as described previously (Ke et al., 2012). Maternal hepatic 3A and 1A2 activity was assumed to increase by 99% [as measured by 1'-hydroxymidazolam formation clearance (Hebert et al., 2008)] and decrease by 65% [as indicated by salivary caffeine clearance (Tracy et al., 2005)] during the third trimester (T3), respectively]. Current clinical data suggest that maternal

UGT2B7 activity is unchanged during pregnancy (Anderson, 2005; Tasnif et al., 2016). Therefore, we assumed that maternal hepatic or extrahepatic UGT2B7 activity does not alter during pregnancy. Maternal renal glomerular filtration rate was assumed to increase by 33% at term [gestational week (GW) 40] (Abduljalil et al., 2012). For zidovudine, its renal net secretion clearance in the mother was assumed to be unaltered during pregnancy.

### 4.3.2 General Workflow of PBPK Model Development and Model Verification Criterion

Drug-specific parameters of midazolam and theophylline in non-pregnant subjects (**Table 4.1**) were obtained from our previous publications to populate their respective m-f-PBPK models (Ke et al., 2012; Ke et al., 2013a), whereas those of zidovudine were first refined based on the Simcyp Simulator® Version 14 (Simcyp Ltd., A Certara Company, Sheffield, UK) compound library using our previously published approach (Ke et al., 2013b). Briefly, refinements of zidovudine drug-specific parameters were made if the predicted zidovudine population mean plasma C-T curve in non-pregnant population using our MATLAB® 13-compartment PBPK model (**Figure 4.5a**) significantly deviated from that observed. The refined zidovudine PK parameters were subsequently used to populate the zidovudine m-f-PBPK model. In addition, the available interindividual variability in physiological parameters and in drug-specific absorption, distribution, metabolism and elimination (ADME) processes in healthy volunteers (for zidovudine) or in the pregnant women (for midazolam, theophylline, and zidovudine at GW 0) was predicted within the Simcyp Simulator®. In brief, a compound profile was first constructed for each of these drugs within the Simcyp Simulator® using their respective

drug-specific parameters. Interindiviudal variabilities associated with these parameters were those specified by the Simcyp Simulator®. Then, the above predicted ADME characteristics for each virtual individual was used for the simulations conducted by the MATLAB® 13-compartment PBPK model (for zidovudine only) or by the m-f-PBPK model (for midazolam, theophylline, and zidovudine). For the pregnant population, the reported gestational age-dependent changes in maternal and fetal physiology (Abduljalil et al., 2012)(manuscript submitted) and the changes in maternal hepatic enzyme activity based on phenotyping studies conducted in pregnant women were taken into account as described above.

For each of the above test compounds, MP and UV drug C-T profiles were simulated in a virtual population consisting of 100 pregnant women at GW 40. The model was deemed to have met our verification criterion if the observed individual UV and MP drug concentrations (except midazolam MP concentrations, where the mean values from 8 subjects were used) at the time of delivery (extracted or digitized from literature using MATLAB® Grabit m.file ; available free online at http://www.mathworks.com/matlabcentral) fell within the 90% prediction interval ($5^{th}$ - $95^{th}$ percentile range of the virtual population) calculated based on the interindividual variability in the maternal PK. Additionally, model prediction precision and prediction bias were evaluated by calculating the mean absolute prediction error ($\overline{APE}$; calculated as $\frac{\sum_{i=1}^{n} \frac{|Pred_i - Obs_i|}{Obs_i}}{n}$) and the mean prediction error ( $\overline{PE}$; calculated as $\frac{\sum_{i=1}^{n} \frac{Pred_i - Obs_i}{Obs_i}}{n}$ ), where Pred and Obs denote the predicted and observed values, respectively (Sheiner and Beal, 1985).

### 4.3.3 Estimation of in vivo Transplacental Passive Diffusion Clearance of Drugs

Because data on the *in vivo* transplacental passive diffusion clearance ($CL_{PD}$) of drugs are not available in the literature, we chose midazolam as an *in vivo* calibrator to estimate $CL_{PD}$ of theophylline and zidovudine (the same approach can be used for any drug). First, we optimized the *in vivo* $CL_{PD,u}$ of midazolam (see below). Then, the $CL_{PD,u}$ of drug X (theophylline or zidovudine) was estimated by scaling $CL_{PD,u}$ of midazolam using **Eq. 1**.

$$CL_{PD,u,X} = \frac{\overline{P_{app,X}}}{\overline{P_{app,midazolam}}} \times CL_{PD,u,midazolam} \text{ (L/h) (\textbf{Eq. 1})}$$

where $CL_{PD,u,midazolam}$ is the optimized *in vivo* $CL_{PD,u}$ (L/h) of midazolam (see below), and $\overline{P_{app,X}}$ and $\overline{P_{app,MDZ}}$ are the average $P_{app}$ values ($nm \cdot s^{-1}$) of drug X and midazolam, respectively. Reported $P_{app}$ values of model drugs were collected from multiple sources in the literature (**Table 4.2**). For physiological relevance and to avoid the confounding factor of binding, we only included studies conducted in established epithelial cell lines that form tight junctions between cells in monolayer cultures (i.e. MDCK and Caco-2) in the absence of serum/binding proteins. The average $P_{app}$ values of midazolam, theophylline, and zidovudine used were the mean values from 5, 5, and 7 independent reports, respectively.

### 4.4.4 Midazolam m-f-PBPK Model

First, the predicted midazolam plasma C-T profile, following a single 15mg oral dose in thirteen pregnant women (GW=40) proceeding elective cesarean section surgery, was compared against the observed data (Kanto et al., 1983). Midazolam drug-specific parameters, previously validated, are outlined in **Table 4.1** (Ke et al., 2012). CYP3A metabolism occurs in maternal gut, liver, and fetal liver. The observed 99% increase in

CYP3A activity was confined to maternal liver as we have previously shown that only maternal hepatic CYP3A activity appears to be induced during pregnancy (Zhang et al., 2008; Ke et al., 2012). To match the observed midazolam maternal absorption profile, a lag time of 0.1 h was introduced and a first-order absorption rate constant $k_a$ of 4.0 $h^{-1}$ was chosen through sensitivity analysis (data not shown). Because fetal liver predominantly expresses CYP3A7 (Shuster et al., 2014b), fetal hepatic intrinsic clearance of midazolam ($CL_{f,hep,int}$) was estimated using **Eq.2**.

$$CL_{f,hep,int} = \frac{V_{max,3A7} \times A_{CYP3A7} \times MPPGL \times W_{f,liver}}{K_{m,CYP3A7}} \quad \textbf{(Eq. 2)}$$

Where $V_{max,3A7}$ and $K_{m,CYP3A7}$ are the maximal velocity and Michaelis-Menten constant determined in recombinant CYP3A7, $A_{CYP3A7}$ is CYP3A7 abundance per mg microsomal protein, MPPGL is the fetal hepatic microsomal protein concentration per gram fetal liver, and $W_{f,liver}$ is fetal liver weight at term. Reported *in vitro* $V_{max}$ /$K_m$ value of midazolam hydroxylation in recombinant CYP3A7 is 2.1 mL/h /nmol P450 (Williams et al., 2002) and it is estimated that fetal liver microsomes contain 0.3 nmol P450 proteins per mg protein (Barter et al., 2007). Fetal MMPGL is 26 mg/g liver {Barter, 2008 #4976} and the average fetal liver at term weighs ~130 g (Abduljalil et al., 2012). Therefore, fetal hepatic $CL_{f,hep,int,}$ mediated by CYP3A7 was estimated as 2.13 L/h. The $CL_{PD,u}$ value of midazolam was optimized through sensitivity analysis. Briefly, the magnitude of midazolam $CL_{PD,u}$ was varied to reduce the residual sum of squares between the predicated and observed fetal C-T profile [RSS; calculated as $\sum_{i=1}^{n}(y_{pred} - y_{obs})^2$ ,where $y_{pred}$ and $y_{obs}$ refer to the predicted and observed fetal plasma midazolam concentrations, respectively]. The observed fetal C-T profile was created by **pooling** the

reported midazolam UV plasma concentrations from seven newborns in the same study (Kanto et al., 1983).

### 4.4.5 Theophylline m-f-PBPK Model

Maternal theophylline drug-specific parameters were those previously published (**Table 4.1**) (Ke et al., 2013a). Because the major placental CYP1A isoform, CYP1A1, has negligible contribution to theophylline metabolism (Ha et al., 1995) and no report on CYP1A2 expression in the term placenta or fetal liver is available, the placenta and fetal liver were considered as non-metabolizing organs for theophylline. Using the estimated $CL_{PD,u,theophylline}$ (**Eq. 1**), maternal and fetal theophylline C-T profiles following multiple oral doses of theophylline were simulated and compared with the observed data using the verification criterion described above. The observed theophylline data were from a study where 10 asthmatic women with normal pregnancies were administered 160 mg theophylline (in the form of aminophylline) every 6 hours for 30 hours prior to delivery (Ron et al., 1984). The observed maternal and fetal C-T profiles were created by **pooling** single time point MP and UV plasma theophylline concentrations from 10 **maternal-fetal pairs**.

### 4.4.6 Zidovudine m-f-PBPK Model

In non-pregnant adults following an intravenous dose, only ~17% of zidovudine is excreted unchanged in the urine, whereas 67% of the intravenous dose is recovered in the urine as 5'-O-gluduronide via UGT2B7 mediated glucuronidation (Cload, 1989; Stagg et al., 1992). Other identified metabolites include its active triphosphate metabolite formed via sequential intracellular phosphorylation {Veal, 1994 #4763}, 3'-amino-3'-deoxythymidine, and 3'-amino-3'-deoxythymidine glucuronide (Stagg et al., 1992).

Average zidovudine intravenous plasma clearance is 91 L/h normalized to 70 kg body weight (Collins and Unadkat, 1989). Thus, plasma zidovudine glucuronidation clearance is estimated as 61 L/h. These data, in conjunction with the observed zidovudine absolute bioavailability (F) of ~ 63% (Klecker et al., 1987), suggests considerable extra-hepatic zidovudine metabolism. However, although UGT2B7 is expressed in the gut, liver, and kidneys (Ohno and Nakajin, 2009), investigations on the extrahepatic metabolism of zidovudine revealed that zidovudine is not glucuronidated by gut microsomes and that renal glucuronidation is minimal (Cretton et al., 1991; Howe et al., 1992; Knights et al., 2016). Moreover, published *in vitro*-to-*in vivo* (IVIVE) approach based on human liver microsomal data substantially underpredicted zidovudine glucuronidation clearance by a factor of 30.5 (Kilford et al., 2009). Based on these analyses, we speculate that there are unidentified extrahepatic, non-renal pathways responsible for zidovudine metabolism (glucuronidation and non-glucuronidation) *in vivo*. Therefore, to recapitulate zidovudine intravenous clearance, zidovudine hepatic unbound intrinsic clearance ($CL_{hep,int,u}$) was calculated using the well-stirred liver model

$$CL_{hep,int,u} = \frac{CL_{hep,b}}{\frac{fu_p}{B/P} \times \left(1 - \frac{CL_{hep,b}}{Q_H}\right)} \textbf{ (Eq. 3)}$$

Where $fu_p$ is the fraction unbound in the plasma, $CL_{hep,b}$ is hepatic blood clearance [ $\frac{CL_{iv}}{B/P} \cdot \left(1 - \frac{F}{F_a F_g}\right) = 24.94\ L/h$] , B/P is the blood to plasma concentration ratio, and $Q_H$ is the hepatic blood flow (90 L/h). A systemic plasma metabolic clearance of 52.8 L/h ($CL_{iv} - CL_{hep} - CL_r$) was assigned to the unidentified extrahepatic zidovudine metabolic pathways. Using the above detailed PK parameters (**Table 4.1**), the predicted zidovudine plasma C-T curves using the 13-compartment PBPK model were compared

with those observed following one hour intravenous infusion of 2.5 mg/kg (**Figure 4.3a**) or two different single oral doses (200 and 300 mg) in non-pregnant asymptomatic HIV-infected male patients with normal hepatic and renal functions (**Figure 4.3b** and **Figure 4.3c**, respectively) (Cload, 1989; Gallicano et al., 1993; Anderson et al., 2000).

Term human placenta perfusion studies have demonstrated that placental glucuronidation of zidovudine is nonexistent (Liebes et al., 1990; Schenker et al., 1990; Bawdon et al., 1992) or negligible (Collier et al., 2002). The information on fetal glucuronidation of zidovudine is currently unavailable but is likely to be negligible given the size of the fetal liver (~130 g at GW 40 vs. 1.5kg in adults). Therefore, no irreversible loss of zidovudine was assumed to be present in the fetoplacental unit. Using the estimated zidovudine $CL_{PD,u}$, the predicted MP and UV C-T profiles of zidovudine using the m-f-PBPK model were compared against the observed zidovudine plasma concentrations obtained at labor (O'Sullivan et al., 1993) following a single 200mg oral dose (**Figure 4.4a**; n=8) or multiple 200mg oral dose preceding an 1-h intravenous infusion (140mg/h) (**Figure 4.4b**, **c**; n=7). In the latter study, the MP and UV plasma concentrations (observed data) were **simultaneously** obtained from 7 maternal-fetal pairs at the time of birth.

## 4.4 Results

### 4.4.1 Estimated in vivo transplacental passive diffusion clearance of midazolam

Incorporation of a lag time and optimization of $k_a$ resulted in excellent agreement between the predicted and the observed maternal C-T profiles (**Figure 4.1a**). Subsequent sensitivity analysis on midazolam $CL_{PD,u}$ demonstrated that though fetal exposure to midazolam was relatively insensitive to changes in $CL_{PD,u}$ (**Figure 4.6**), a value of 500 L/h [term $f_{u,p}$= 0.045; $CL_{PD}$ of 22.7 L/h) best described the fetal exposure to midazolam

(minimum RSS) (**Table 4.3**). The resulting UV plasma concentrations, except for one data point, were in close agreement with the observed UV plasma concentrations, falling within the 90% prediction interval (**Figure 4.1b**). Additionally, using midazolam as the calibrator, the resultant $CL_{PD,u}$ for theophylline and zidovudine were 342.4 L/h and 216.8 L/h, respectively (**Table 4.2**).

### 4.4.2 Theophylline

Using the estimated theophylline $CL_{PD,u}$ of 342.4 L/h (term $f_{u,p}$ = 0.66 ; $CL_{PD}$ = 226.4L/h), the predicted MP (**Figure 4.2a**) and UV (**Figure 4.2b**) drug concentrations were in good agreement with the observed data. All predictions (except a single MP concentration) met our verification criterion (i.e. observed plasma concentration fall within the 90% prediction interval). Model prediction precision and bias for MP and UV concentrations were 14.5% and 12.4 % and 9.4% and 7.8%, respectively.

### 4.4.3 Zidovudine

First, the predicted zidovudine mean plasma C-T profile in non-pregnant population (n=100) was compared against the observed zidovudine mean plasma C-T profiles following various dosing regimens (**Figure 4.3**). Predicted population mean data matched the observed data with precision of <40% and bias ranging from -30% to 9%. After model verification in non-pregnant population, zidovudine drug-specific parameters were incorporated into our zidovudine m-f-PBPK model. Using the estimated $CL_{PD,u}$ of 216.8 L/h (term $f_{u,p}$=0.8; $CL_{PD}$ = 172.6 L/h, **Table 4.2**), the predicted MP zidovudine plasma before the onset of labor passed our prediction criterion (**Figure 4a**), whereas the majority of maternal-fetal zidovudine plasma concentrations obtained during delivery fell within the 90% prediction interval. In the latter scenario, one out of seven MP (**Figure**

**4b**) and two out of seven UV (**Figure 4c**) plasma concentrations fell outside this 90% prediction interval. Prediction precision and bias for MP and UV plasma drug concentrations were 135.2% and 118.4% and 121.4% and 110.3%, respectively. However, these larger precision and bias data were largely due to the unexpected low MP concentration of 0.17 μg/mL at 43.3h (0.88 h post the initiation of 1-h intravenous infusion to the mother) and consequently low UV concentration. When this point was excluded, the resultant prediction precision and bias for MP and UV drug concentrations reduced considerably to 50.3% and 30.2%, and 28.3 % and 15.0%, respectively.

### 4.5 Discussion

In the current work, we have verified a novel m-f-PBPK model using drugs that passively permeate the placenta and are not known or expected to be metabolized there. Our fetal PBPK model was constructed to be consistent with the distinctive fetal vascular physiology and to allow future incorporation of transport and metabolism within the placenta. The model contains a three compartment placenta consisting of maternal placental blood, placental tissue, and fetal placental blood. The model also accounts for the unique fetal hepatic blood supply as the fetal liver is primarily perfused by umbilical venous blood flow (**Figure 4.5b**). However, a significant portion of the latter (~30-70%) is shunted to the fetal systemic circulation via the ductus venosus. Although this is not the first report of a fetal PBPK model (Yoon et al., 2011; Loccisano et al., 2013; De Sousa Mendes et al., 2016), to our best knowledge it is the first full m-f-PBPK model that: (1) features fetal physiological aspects that are relevant to pharmaceutical drugs, (2) systematically incorporates the gestational age-dependent changes in maternal drug disposition and maternal-fetal physiology, (3) accounts for the interindividual variability

in maternal plasma C-T profile, and (4) well predicts the systemic exposure of test pharmaceutical drugs in maternal-fetal pairs at term.

Crucial for predicting the fetal exposure of passive diffusion drugs is the magnitude of *in vivo* passive diffusion clearance across the placenta. In our model, the mass transfer of a passive diffusion drug from the mother to her fetus is described by equal bidirectional maternal-placental and placental-fetal $CL_{PD,u}$ (Tuntland et al., 1999). In essence, the rate of drug transfer across the placenta is rate-determined by $CL_{PD,u}$ (after accounting for binding) or placental blood flow, whichever is lower. In theory, $CL_{PD,u}$ equals the intrinsic permeability- surface area product. At a given gestational age, the magnitude of this $CL_{PD,u}$ should be directly proportional to its intrinsic permeability (i.e. permeability after adjusting for plasma protein binding) across the syncytiotrophoblast that separates the maternal and fetal circulation. Of note, the differing longitudinal changes in plasma drug binding protein concentrations across the placenta can have a significant impact on the transplacental passage of drugs (Hill and Abramson, 1988; McNamara and Alcorn, 2002) and have been accounted for in our m-f-PBPK model. Despite its importance, IVIVE of passive diffusion clearance across the placenta remains a challenge. Immortalized cell lines of human placenta origin, such as BeWo and Jar, cannot form tight junctions and therefore are poorly suited to estimate placental drug diffusion (Kitano et al., 2004). Although *ex vivo* dually perfused human placentae may represent the most physiologically relevant system, only theophylline and zidovudine have been studied {Dancis, 1993 #5077;Liebes, 1990 #5081;Schenker, 1990 #5072;Omarini, 1992 #4940}. Furthermore, none of these studies provide sufficient data for whole organ scale-up of $CL_{PD.}$ Therefore, we hypothesized that for a passive diffusion drug, the *in vivo* $CL_{PD,u}$ of

the drug can be predicted by calibrating its *in vitro* permeability against the positive control, midazolam. The magnitude of the *in vivo* $CL_{PD,u}$ of a new drug entity can then be calculated assuming that it will be proportional to its passive diffusion permeability relative to that of midazolam in epithelial cell lines that form tight junctions (**Eq.2**). Our *in vivo* calibrator midazolam [BCS class I (Benet, 2010)] crosses the placenta predominantly via passive diffusion. Due to its high passive membrane permeability, the contribution of P-gp towards midazolam tissue distribution is negligible (Tolle-Sander et al., 2003; Doran et al., 2005). Among the three test compounds, only midazolam maternal population average plasma concentrations (n= 8) have been reported at term. Therefore, midazolam was chosen as our *in vivo* calibrator to estimate the *in vivo* placental diffusion clearance of both theophylline and zidovudine (see next paragraph). Consistent with our previous findings, a 99% induction in hepatic CYP3A alone was sufficient to explain the clinically observed changes in maternal midazolam disposition during T3 (Ke et al., 2012). As expected, midazolam readily crosses the placenta. The optimized $CL_{PD}$ resulted in all observed UV midazolam plasma concentrations falling within the 90% prediction interval, suggesting ~50% extraction ratio by the placenta and a blood-flow limited extraction by the fetal placental flow ($CL_{PD}$ of 22.7 L/h vs. term placental and umbilical venous blood flows of ~50L/h and ~20L/h, respectively)(Abduljalil et al., 2012). The first verification drug, theophylline, is also a BCS class I drug (Benet, 2010). So far, only OAT2 has been indicated in theophylline tissue uptake but this transporter is absent in human placenta (Kobayashi et al., 2005; Mao et al., 2014). Theophylline is mainly cleared by CYP1A2 with minor contributions from CYP 3A and CYP2E1 as well as a small renal component (Ke et al., 2013a). The

incorporation of a 65% reduction in maternal hepatic CYP1A2 activity (Tracy et al., 2005) along with the 99% increase in CYP3A activity satisfactorily explained the observed maternal plasma concentrations (**Figure 4.2a**). Using the predicted $CL_{PD,u}$ of 342.4 L/h , fetal exposure was well described (**Figure 4.2b**). Of note, as a result of moderate protein binding ($f_{u,p}$= 0.66 at term) and relatively high $CL_{PD,u}$ (342.4L/h), the predicted transplacental passage of theophylline was blood-flow limited.

The second verification drug, zidovudine, is a nucleoside reverse transcriptase inhibitor and structure analogue of thymidine. Although it has been shown to be transported *in vitro* by several transporters expressed in human placenta (e.g. P-gp, BCRP, MRP5, ENT2, and OAT4), several *ex vivo* placenta perfusion studies indicate that zidovudine crosses the placental via passive diffusion {Dancis, 1993 #5077;Liebes, 1990 #5081;Schenker, 1990 #5072}. Zidovudine is mainly cleared by UGT2B7 *in vivo* with a renal clearance exceeding renal filtration. The activity of UGT2B7 is generally regarded not to be affected by pregnancy (Anderson, 2005) and is supported by our simulation. Several studies have shown that zidovudine is a substrate for human OATs (i.e.OAT1-4), all of which are expressed in the kidney (Takeda et al., 2002). Interestingly, although pregnancy may increase renal OAT1 activity [measured by the 55% increase in amoxicillin net renal secretion during T3, which may be attributed to enhanced renal OAT1 activity and/or reduced reabsorption(Andrew et al., 2007)], our simulations demonstrated that maternal physiological changes along with the increased renal filtration clearance sufficiently described the maternal disposition of zidovudine (**Figure 4.4a** and **b**). zidovudine demonstrates good permeability and was also estimated to have blood flow limited distribution into the fetal compartment.

Overall, the m-f-PBPK model described well-predicted the maternal and fetal exposure to the two verification drugs (zidovudine and theophylline) at term across a range of dosing regimens, with nearly all simulated plasma drug concentrations falling within the 90% prediction interval in both the mother and her fetus. Because these drugs passively diffuse across the placenta and are not significantly metabolized in the fetal liver or the placenta, the overall unbound fetal plasma AUC is predicted to be equal to the unbound maternal plasma AUC. Due to the sparse fetal plasma drug concentration data available, the fetal AUC of the verification drugs could not be estimated. Therefore our goal was to dynamically predict the fetal plasma drug concentrations available in the literature (i.e. predict the time-variant fetal plasma C-T curve). Such dynamic prediction is a true test of any m-f-PBPK model, including when the drugs are extensively transported or metabolized in the placenta. In the future, our aim is to incorporate these processes in our model when quantification data on expression of placental transporters and enzymes are available.

The application of PBPK models for predicting drug disposition in the coupled maternal-fetal pairs is still in its infancy. Therefore, as is the case with other PBPK models, our model has several limitations. First, while interindividual variability in maternal drug disposition, where available, was incorporated in our model, due to lack of data on variability of feto-placental parameters, such variability could not be incorporated in the model. This may underestimate the true variability in fetal exposure. Second, midazolam was not a sensitive calibrator and both theophylline and zidovudine demonstrated blood flow limited passive placental diffusion clearance. Ideally, the passive diffusion clearance of test compounds should span a much wider range, including

hydrophilic drugs that passively diffuse across the placenta with $CL_{PD}$ much lower than the placental blood flow. Unfortunately, coupled maternal-fetal PK data for such drugs are not available. Third, until placental transporters and metabolic enzyme expression are available our model can be applied to only drugs that passively diffuse across the placenta and are not metabolized/transported there. To address this limitation, proteomics based quantification of placental transporters and enzymes is currently underway in our laboratory. Fourth, although our model can predict fetal exposure to passive diffusion drugs across fetal developmental stages (GW 14-term), many fetal physiological parameters are not available for the first half of pregnancy, and the fetal skin is not keratinized at < 20 weeks of gestation (Polin et al., 2004), potentially enabling the bidirectional diffusion of drugs through the fetal skin to the amniotic fluid. While the latter limitation can be overcome by including such a possibility in a future version of our model, the former issue reflects an inherent limitation of studies in this special population. That is, the difficulty of measuring physiological parameters of the fetus at earlier gestational age. As a result, we have less confidence in predicting fetal drug exposure at < 20 weeks of gestation.

The clinical implications of the current study relate to addressing an urgent need for an understudied and vulnerable population: quantitative assessment of fetal exposure to drugs in the maternal-fetal dyad. Drug use during pregnancy is a reality. When the perceived benefits outweigh risks, pharmacotherapy of pregnant women is initiated, in most cases, without prior knowledge on the maternal-fetal disposition of the drug. However, obtaining any fetal drug exposure data at term is fraught with logistical and ethical issues. As a result, there is a paucity of fetal exposure data in this population. As

pointed out earlier, existing fetal drug exposure data are limited to term pregnancy. Furthermore, such data for early gestational age fetuses are virtually impossible to obtain, rendering fetuses orphan population with respect to drug exposure and drug efficacy/toxicity. Instead, the proposed PBPK model can provide information on fetal drug exposure based on sound physiological data and modeling. While data to verify our model for gestational ages other than term are not available, the term verification data presented above lends considerable confidence that our m-f-PBPK model can be used to *a priori* predict fetal exposure to drugs (that passively diffuse across the placenta) during pregnancy. When earlier gestational age data become available, our model can be verified for these gestational ages.

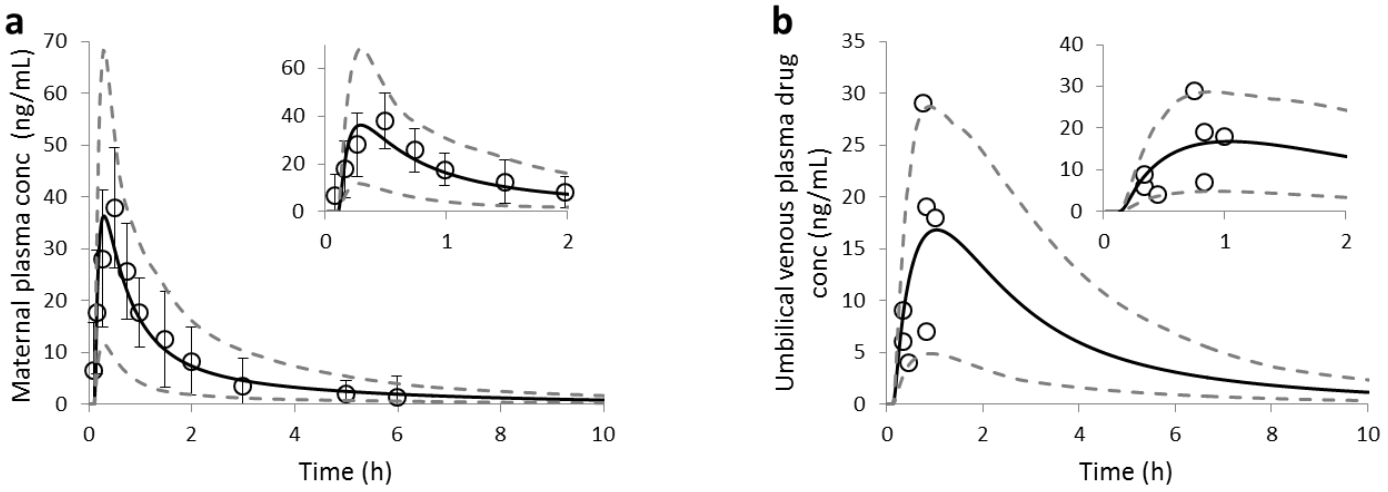


**Figure 4.1. Predicted term midazolam maternal-fetal plasma drug concentration profiles**: population mean (black solid lines) and observed (open circles) maternal plasma (MP) (a) and umbilical venous (UV) plasma (b) midazolam concentration-time (C-T) profiles following a single 15 mg oral dose at term (gestational week 40) (Kanto et al., 1983). In (a), the predicted MP C-T profile is overlaid with the observed maternal plasma data (mean ± SD; n=8). In b, each observed UV data point was derived from a single maternal-fetal pair from another subset of subjects from the same study (n=7). The observed mean midazolam MP concentrations at various time points fell within the 90% prediction interval (5th-95th percentile boundaries; lower and upper grey dashed lines, respectively) for a virtual population consisting of 100 maternal-fetal pairs (a). Consequently, all the observed individual UV plasma concentrations were within the 90% prediction interval (b). Insets are the same data plotted to highlight early time points.

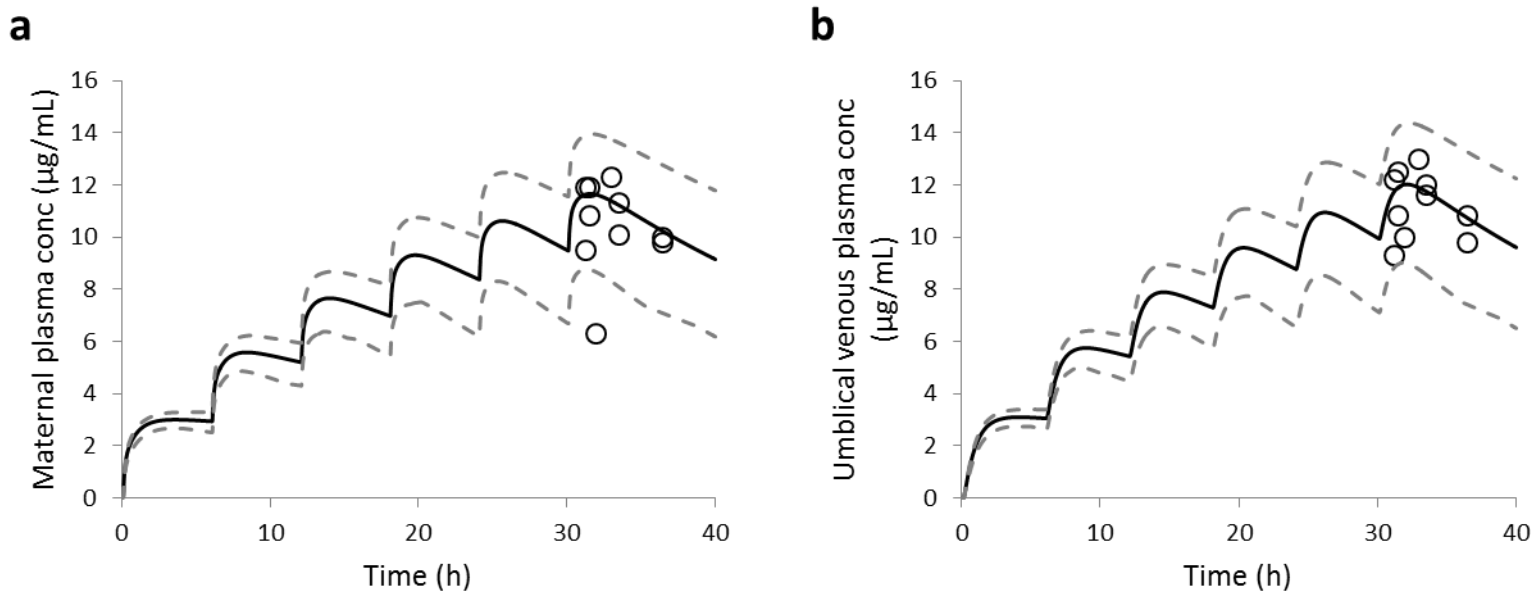


**Figure 4.2. Predicted term theophylline maternal-fetal plasma drug concentration profiles**: population mean (black solid lines) and observed (open circles) maternal plasma (MP) (**a**) and umbilical venous (UV) plasma (**b**) theophylline concentration-time (C-T) profiles following 5 doses of 160mg oral theophylline every 6 hour at term (gestational week 40) (Ron et al, 1984). Each pair of observed data (MP and UV) were derived from a single maternal-fetal pair (n=10). All observed MP drug concentrations, except one data point, and subsequently all observed UV data points, fell within the 90% prediction interval ($5^{th}$-$95^{th}$ percentile boundaries ; lower and upper grey dashed lines, respectively), for a virtual population consisting of 100 maternal-fetal pairs.

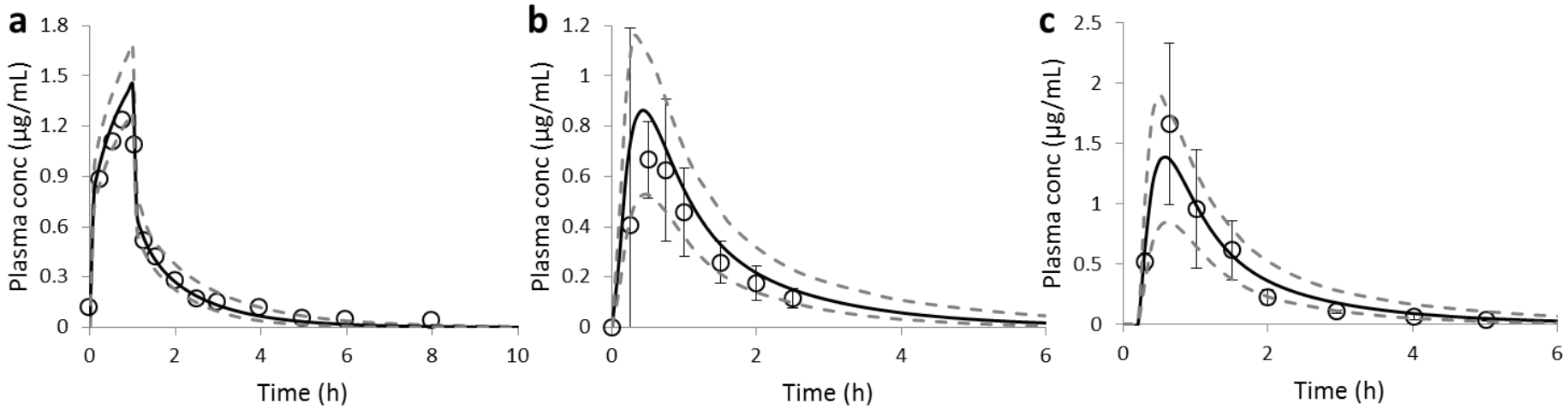


**Figure 4.3. Predicted zidovudine plasma drug concentration-time profiles in nonpregnant population**: population mean (black sloid lines) and observed (open circles) plasma zidovudine concentration-time (C-T) profiles following a 1-h 2.5mg/kg intravenous infusion dose (**a**; Clod et al., 1989, n=8) or a single 200mg oral dose (**b**; Gallicano et al., 1993, n=10) or a single 300mg oral dose (**c**; Anderson et al., 2000, n=4) in non-pregnant population. All observed plasma drug concentrations (mean ± SD), except one terminal phase plasma concentration (**a**), in HIV-infected asymptomatic male volunteers fell within the 90% prediction interval ($5^{th}$-$95^{th}$ percentile boundaries; lower and upper grey dashed lines, respectively) from a virtual population consisting of 100 male subjects.

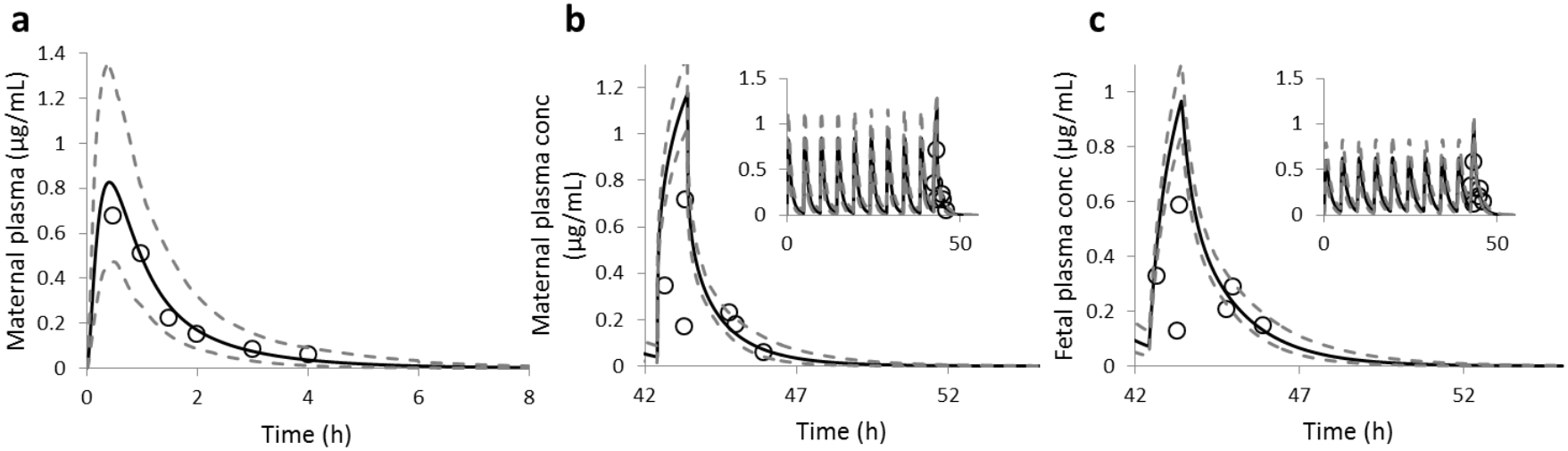


**Figure 4.4. Predicted term zidovudine maternal-fetal plasma drug concentration-time profiles**: population mean (black solid lines) and observed (open circles) maternal plasma (MP) (**a** and **b**) and umbilical venous (UV) plasma (**c**) zidovudine concentration-time (C-T) profiles in HIV-infected, asymptomatic women with uncomplicated pregnancies (O'Sullivan et al., 1993). 200 mg oral dose of zidovudine (5 times per day) was commenced prior to onset of labor (**a**; gestational week 40, n=8) . Then, during labor, 4 hours after last dose, 140mg zidovudine was intravenously infused over 1-h period to the same volunteers (**b** and **c**; n=7 ). In **a**, all the observed mean maternal plasma zidovudine concentrations fell within the 90% prediction interval ($5^{th}$ and $95^{th}$ percentile range; lower and upper grey dashed lines, respectively) for a virtual population consisting of 100 maternal-fetal pairs. In **b** and **c**, each data point (open circles) represents an observed single time point zidovudine concentration from paired MP (**b**) or UV plasma (**c**) samples. Six out of seven observed MP concentrations, and five out of seven UV plasma concentrations, fell within the 90% prediction interval. Insets are the same data replotted with a different time scale to illustrate the dosing regimen.

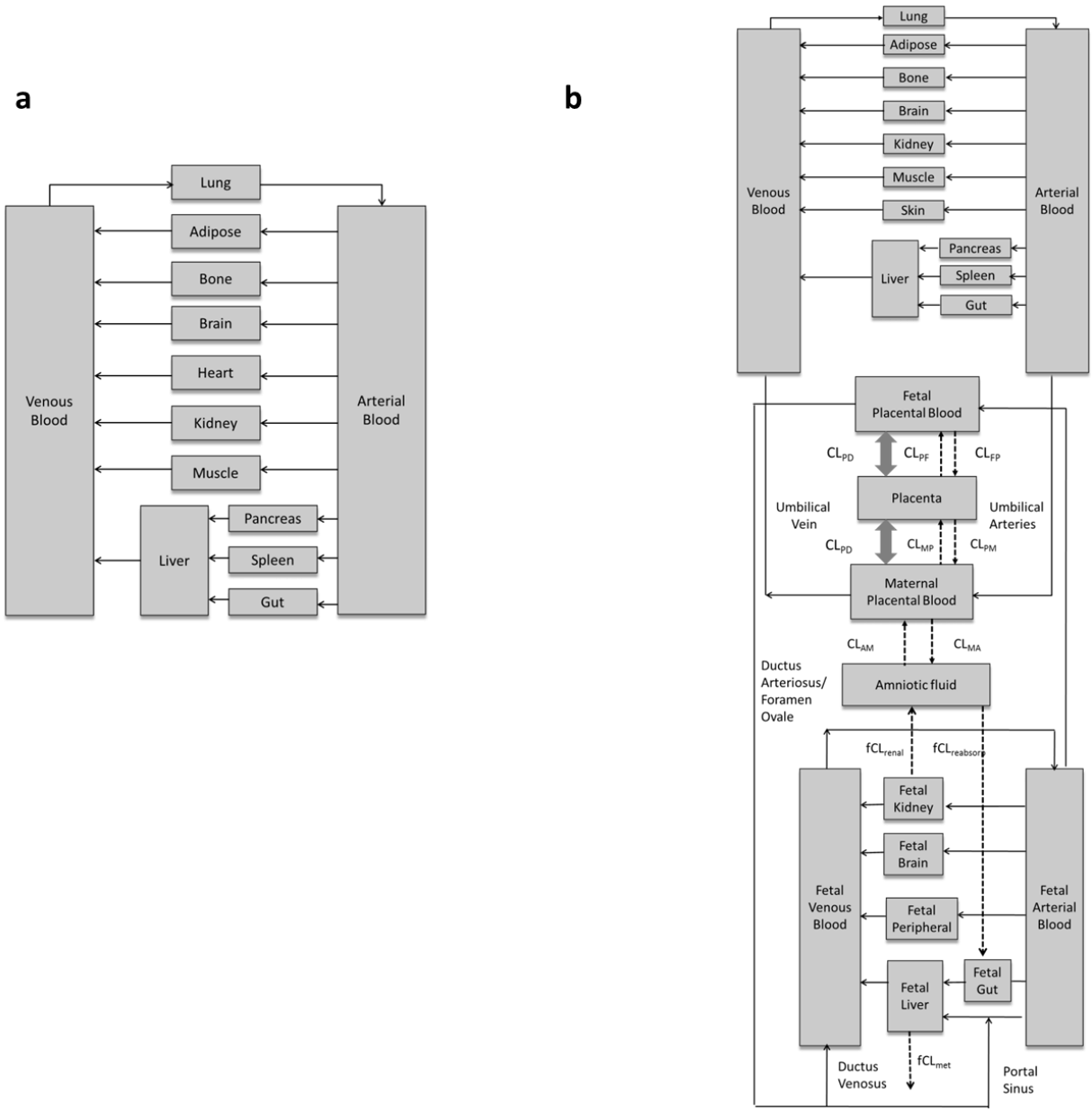


**Figure 4.5. Schematic diagrams depicting the structure of the non-pregnant PBPK and the maternal-fetal PBPK models**:**a** shows the structure of the MATLAB PBPK model for the non-pregnant population. **b** is the schematic diagram of the maternal-fetal full PBPK model. Solid arrows indicate tissue blood flows and dashed arrows indicate clearances. CL: clearance; Prefixes: f-fetal; Subscripts: PD- passive diffusion, M- maternal, P- placenta, F- fetus, A- amniotic fluid, met- metabolism, renal-renal excretion, reabsorp- amniotic fluid swallowing. $CL_{FP/PF}$ and $CL_{MP/PM}$ represent the unidirectional placental transporter-mediated clearances between the fetus and the placenta and between the mother and the placenta.

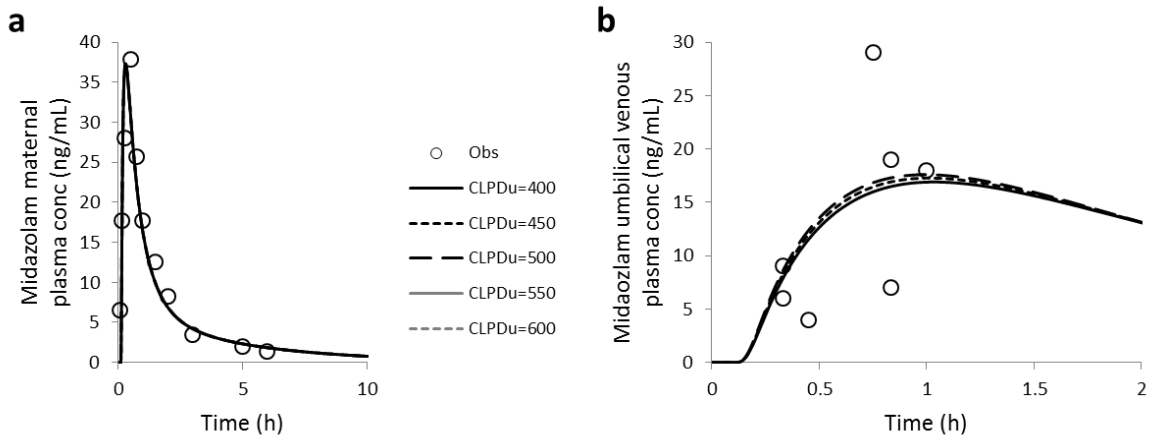


**Figure 4.6. Impact of varying the unbound transplacental passive diffusion clearance (CLPD,u)of midazolam** on its maternal plasma (a) and umbilical venous plasma (b) pharmacokinetics following a single oral dose 15mg. Variations in $CL_{PD,u}$ resulted in virtually no changes in predicted midazolam plasma drug concentrations of maternal plasma and negligible changes of umbilcial venous plasma.

**Table 4.1. Summary of midazolam, theophylline, and zidovudine drug-dependent parameters**

| Parameter | Midazolam value | Methods/ reference | Theophylline value | Methods/ reference | Zidovudine value | Methods/ reference |
|---|---|---|---|---|---|---|
| Molecular Weight | 325.8 | Library[a] | 180.2 | Library[a] | 267.2 | Library[a] |
| Log $P_{o:w}$ | 3.13 | Optimized[b] | -0.02 | Library[a] | 0.05 | Library[a] |
| pKa | 10.95,6.2 | Library[a] | 8.8,0.99 | Library[a] | 9.70 | Library[a] |
| B/P Ratio | 0.66 | Library[a] | 0.82 | Library[a] | 0.91 | Library[a] |
| $f_{u,p}$* | 0.032 | Library[a] | 0.58 | Library[a] | 0.80 | Library[a] |
| $F_a$ | 0.88 | Library[a] | 0.97 | Library[a] | 0.83 | Predicted by ADAM model |
| $k_a$ ($h^{-1}$) | 4.0 | Optimized[c] | 1.0 | Reported [e] | 4.05 | Reported[f] |
| $F_g$ | 0.58 | Library[a] | 1.0 | Reported[d] | 1 | Assumed[g] |
| $V_{ss}$ (L/Kg) | 1.1 | Reported[d] | 0.39 | Reported[d] | 1.10 | Optimized[h] |
| $CL_{iv}$( L/h) | 23.0 | Library[a] | 3.0 | Reported[d] | 91.0 | Reported[i] |
| $CL_r$(L/h) | 0.085 | Library[a] | 0.45 | Reported[d] | 15.5 | Library |
| $CL_{hep,int,u}$(L/h) | 1672.3 | Library[a] | 4.60 | Reported[d] | 30.9 | Calculated[k] |
| $f_m$ and $f_e$ | $f_{m,3A}$ =92%, $f_e \approx 0\%$ | Reported[d] | $f_{m,1A2}$ =68%, $f_{m,3A}$ =7%, $f_{m,2E1}$ =10%, $f_e$ =15% | Reported[d] | $f_{m,UGT2B7}$=67%, $f_e$ =17% | Reported[l] |

*: Note $f_{u,p}$ refers to the reported unbound fraction of drug in plasma in non-pregnant population.

**: Midazolam is a weak base (Andersin, 1991), whereas zidovudine is a weak acid (Gallicano, 2000). In contrast, theophylline is neutral (Hardman, 1962).

[a]: Refers to the SimCYP Simulator® compound library (version 14).

[b]: Previously optimized and validated to match the predicted $V_{ss}$ to the reported $V_{ss}$ value of 1.10 L/kg in the literature (Ke et al., 2012).

[c]: Optimized based on sensitivity analysis to match reported absorption in pregnant subjects(Kanto et al., 1983) .

[d]: Validated literature value used in our pregnancy PBPK model (Ke et al., 2012; Ke et al., 2013a).

[e]: Phoenix® estimate from reported oral absorption data in healthy volunteers (Aslaksen et al., 1981).

[f]: Phoenix® estimate from reported oral absorption data in non-pregnant subjects (Klecker et al., 1987).

[g]: No report on zidovudine $F_g$ is available. zidovudine $F_g$ was assumed 1 since human intestinal microsomes showed negligible UGT2B7 activity measured by two UGT2B7 probes (diclofenac and gemfibrozil) (Furukawa et al., 2014).

[h]: The reported average zidovudine $V_{ss}$ is 1.4 $\pm$0.4 L/kg.(Collins and Unadkat, 1989) This $V_{ss}$ was optimized through manual sensitivity analysis in the range of 0.8-1.6 L/kg to match the predicted peak plasma concentration ($C_{max}$) to the reported $C_{max}$ following intravenous infusion in non-pregnant population (Klecker et al., 1987; Cload, 1989).

[i]: Calculated based on the reported average intravenous clearance of 1.3 L/h/kg assuming 70kg body weight.

[j]: Reported zidovudine fraction excreted in the urine ($f_e$) ranges from 14% to 20%. The SimCYP Simulator® compound library value of 15.5L/h ($f_e$ =17%) was used.

[k]: Back calculation from well-stirred liver model using hepatic blood flow of 90 L/h assuming hepatic clearance of 20.7 L/h.

[l]: Estimated from urinary data (Cload, 1989; Stagg et al., 1992).

**Table 4.2. $P_{app}$ values from *in vitro* studies and the estimated $CL_{PD,u}$ 's**

| Drug | $P_{app}$ value ($nm \cdot s^{-1}$) | | | | $CL_{PD,u}$ (L/h) | Resources |
|---|---|---|---|---|---|---|
| | Mean | S.D | Median | Range | | |
| Midazolam | 489.9 | 158.7 | 490.0 | 320 - 699 | 500.0 | (Yamashita et al., 2000; Mahar Doan et al., 2002; Taub et al., 2002; Tolle-Sander et al., 2003; Gertz et al., 2010) |
| Theophylline | 335.5 | 162.2 | 260.0 | 231-620 | 342.4 | (Yamashita et al., 2000; Masungi et al., 2004; Collett et al., 2008; Teksin et al., 2010; Di et al., 2011) |
| Zidovudine | 212.4 | 217.2 | 69.3 | 31.8-543.3 | 216.8 | (Yazdanian et al., 1998; Irvine et al., 1999; de Souza et al., 2009) |

a. The predicted theophylline maternal fu,p is 0.66 at term.; b. The predicted zidovudine maternal fu,p is ~0.80 at term;

c. The estimated CLPD,u values were based on mean Papp from *in vitro* reports.

**Table 4.3. Sensitivity** analysis on midazolam transplacental passive diffusion clearance ($CL_{PD}$)

| time | Observed UV plasma conc. | $CL_{PD}$ (L/h)* | | | | | | | | | |
|---|---|---|---|---|---|---|---|---|---|---|---|
| | | 18.2 | | 20.4 | | 22.7 | | 25.0 | | 27.2 | |
| | | Pred | PE | Pred | PE | Pred | PE | Pred | PE | Pred | PE |
| h | ng/mL | ng/mL | % | ng/mL | % | ng/mL | % | ng/mL | % | ng/mL | % |
| 0.33 | 6 | 6.93 | 15.42 | 7.41 | 23.43 | 7.83 | 30.49 | 8.20 | 36.75 | 8.54 | 42.33 |
| 0.33 | 9 | 6.93 | -23.06 | 7.41 | -17.71 | 7.83 | -13.00 | 8.20 | -8.83 | 8.54 | -5.11 |
| 0.45 | 4 | 10.40 | 159.97 | 10.99 | 174.83 | 11.51 | 187.75 | 11.96 | 199.09 | 12.36 | 209.11 |
| 0.75 | 29 | 14.82 | -48.90 | 15.44 | -46.75 | 15.98 | -44.91 | 16.44 | -43.33 | 16.83 | -41.95 |
| 0.83 | 7 | 15.35 | 119.25 | 15.95 | 127.86 | 16.46 | 135.16 | 16.90 | 141.42 | 17.28 | 146.83 |
| 0.83 | 19 | 15.35 | -19.23 | 15.95 | -16.05 | 16.46 | -13.36 | 16.90 | -11.06 | 17.28 | -9.06 |
| 1 | 18 | 15.91 | -11.60 | 16.45 | -8.63 | 16.89 | -6.14 | 17.27 | -4.04 | 17.60 | -2.24 |
| Prediction precision | | 56.78 | | 59.32 | | 61.55 | | 63.50 | | 65.23 | |
| Prediction bias | | 27.41 | | 33.86 | | 39.43 | | 44.29 | | 48.56 | |
| Sum of squares | | 334.63 | | 329.03 | | 327.92 | | 329.72 | | 333.39 | |

* term midazolam unbound fraction increases from 0.3 to 0.454 as a result of hemodilution caused by pregnancy.

# Chapter 5 General conclusions and future directions

## 5.1 Overall conclusions

Pregnancy is associated with profound physiological changes in the mother. These changes affect maternal drug disposition reflected by altered pharmacokinetics of many drugs. Indeed, due to these changes, therapeutic drug monitoring and dosing regimen adjustments has been carried out for several classes of drugs (e.g. anti-epileptics, HIV protease inhibitors).{Unadkat, 2007 #2874;FDA, 2004 #5260}

Despite the accumulating knowledge in the fields, we still know far too little about how pregnancy affect the disposition of commonly used approved medications, even lesser about fetal exposures to these drugs. Currently, most clinical data on pregnancy PK are derived from opportunistic studies. Unfortunately, these studies often fail to draw definitive conclusions on the magnitude of change in the activity of DMEs or drug transporters due to the lack of enough statistical power, insensitivity of probes, or confounding factors. Moreover, the vast majority of data are limited to late stages of pregnancy, rather than the early stages when the fetus is more vulnerable to teratogens. For instance, by how much pregnancy induces CYP3A activity during T1 and T2 remained unclear. These knowledge gaps reflect a wider problem in the special population. PK data in the pregnant mother and her fetus are extremely difficult to obtain, especially during T1 and T2, as the maternal safety cannot be guaranteed and the fetal risk cannot be sufficiently ruled out. However, for the very same concerns about maternal-fetal drug exposures, such data are urgently needed. Thus, alternative *in vitro* and *in silico* approaches that shed light on the maternal-fetal disposition of drugs throughout pregnancy are much needed.

In light of this pressing need, we initiated a series of investigations involving *in vitro* systems and PBPK modeling and simulation (M&S). First, to predict the magnitude of change in CYP3A induction during T1 and T2 (**Chapter 2**), incubation studies using pregnancy-related hormones at clinically observed concentrations during T1 and T2 were performed. The results of these studies showed that, consistent with our previous finding,(Papageorgiou et al., 2013) among all the hormones tested, the observed increase in CYP3A activity was a result of the elevated plasma cortisol concentration compared to non-pregnant state. Furthermore, based on the observed 99% induction in CYP3A *in vivo* and the comparable fold-induction in CYP3A activity across different gestational ages *in vitro*, we predicted that the hepatic CYP3A activity, *in vivo*, during T1 and T2 is ~100%. To our knowledge, this is the first time that *in vivo* CYP3A activity during early gestation has been predicted. Of note, although definitive PK data on CYP3A activity during early gestation are currently unavailable, our finding is in agreement with the results from a couple of studies on CYP3A substrates in early gestation. In these studies, the effect of pregnancy on CYP3A activity is gestational age independent. For example, nifedipine serum concentration in pregnant women did not vary significantly with the advancement of gestation.(Marin et al., 2007) The findings from the presented work in **Chapter 2** can be utilized to help make informed decisions on dosing regimens of CYP3A drugs for pregnant women. Particularly, the above predicted change in its activity during early gestation, along with the known magnitude of changes in the activity of other CYP isoforms (see **Table 1-1** for detail), enables us to predict the maternal disposition of CYP-cleared drugs throughout pregnancy using our published mechanistic maternal pregnancy PBPK model (m-PBPK). Moreover, these results will help spur future mechanistic investigations on the molecular mechanism(s) by which hepatic CYP3A is up-regulated during pregnancy. In fact, such studies are in progress in our lab.

Although the fetus is *de facto* exposed to drugs that are given to the mother, the time-varying fetal exposure to various drugs (i.e. fetal plasma drug concentration time profiles) simply cannot be assessed in utero. To overcome this issue, in **Chapter 3**, we sought to 1) provide a physiologically faithful, mechanistic platform that accounts for the known gestational age related changes in maternal-fetal physiology and in maternal drug disposition and 2) to understand how certain drug-specific properties will impact fetal plasma drug exposure (i.e. fetal plasma AUC) in the context of fetopalcental metabolism and placental drug transport. In addition, since the single time point umbilical vein: maternal plasma (UV:MP) drug concentration ratios are often mistaken for the fetal drug exposure relative to that in the mother, we performed a series of simulations to clarify this misconception. A hypothetical drug X with PK properties resembling the nucleoside HIV antiretroviral drug didanosine (ddI) was used for our simulation exercise. To facilitate the conceptual understanding of the transplacental passage of drugs, we also utilized a three compartment maternal-placental-fetal model to demonstrate that the fetal: maternal plasma AUC ratio is affected not only by the various irreversible clearance pathways within the fetalplacental unit but also passive diffusion across the placenta. Then, we simulated various scenarios whereby the magnitude of fetal metabolism, placental metabolism, and placental transport was varied individually (except otherwise mentioned). In addition, we also looked into the effect of gestational age and mode of fetoplacental clearance(s) on fetal exposure of drug X. The results of steady-state infusion simulations using our m-f-PBPK matched the predicted ratios using the three compartment model, thus indirectly verifying the correct implementation of this m-f-PBPK model. UV:MP ratio data were shown to be not only highly variable with time post last maternal dose but also do not represent fetal: maternal plasmas AUC ratio unless at steady-state following infusion. The latter, however, depends on the relative magnitude of irreversible

fetoplacental clearance(s) to the transplacental passive diffusion clearance. Clearly, under the same dosing regimen and assuming that maternal drug disposition is minimally affected by the advancement of gestation, fetal development alone can result in changes in the relative magnitude of fetoplacental metabolism and/or placental transport to the transplacental passive diffusion clearance (thus fetal: maternal plasma AUC ratio). To our knowledge, the presented m-f-PBPK model is the most physiologically relevant population PBPK model for predicting the disputation of pharmaceutical drugs during late stage pregnancy. Once the maternal PK is verified, this m-f-PBPK model can be utilized to predict the fetal exposure from gestational week 20 all the way to term. Furthermore, given the mechanistic, integrative nature of PBPK models, a pharmacodynamics module can be readily incorporated into this m-f-PBPK, thus enabling prediction for drug efficacy or potential teratogenic effects. As demonstrated in **Chapter 3**, mechanistic simulations can be easily performed in the context of the rapidly varying maternal-fetal physiology to delineate the key drug-specific properties that will influence fetal drug disposition and to correctly interpret the available fetal exposure data in the literature.

In **Chapter 4**, we further verified the performance of this m-f-PBPK model for drugs that predominantly cross the placental through passive diffusion. The conventional methods for assessing fetal exposure, such as ex vivo placenta perfusion studies and maternal-fetal PK data obtained from mammals (e.g. rodent, non-human primates, sheep, etc.) are only capable of giving "yes or no" answers, rather than the rate and extent of fetal drug exposure data needed for drug efficacy/toxicology predictions. Unlike these methods above, our m-f-PBPK model provides a quantitative alternative to dynamically predict the drug concentration-time profiles across gestational ages. Using previously validate drug-specific parameters, midazolam maternal PK was satisfactorily predicted. Then, an optimized unbound passive diffusion clearance value

for midazolam was obtained through sensitivity analysis. Using the proposed algorithm, fetal disposition of two test compounds, theophylline and zidovudine, was reasonable well predicted. The empiric approach developed here can predict the magnitude of passive diffusion clearance of a drug *in vivo* from its permeability data *in vitro*, in established epithelial cell lines. Since all small-molecule drugs need to cross the placenta to gain access to fetal circulation with varying magnitude of passive diffusion clearance, our proposed m-f-PBPK model and the empirical approach to estimate the transplacental passive diffusion clearance enables the prediction for fetal exposure to passively diffused drugs. Furthermore, with the incorporated time-varying fetal and placental physiology in this m-f-PBPK, once the predicted fetal exposure to passive diffusion drugs is verified at term, fetal exposure at early gestation can be predicted and utilized to guide making informed decisions on the dosing regimen of drugs targeting the pregnant mother, the fetus, or both.

Taken together, the above studies present a viable, mechanism-based alternative to predicting the maternal-fetal of drugs throughout pregnancy. Through integrating *in vitro* findings and physiologically-based *in silico* modeling and prediction, maternal-fetal exposure to drugs can be **dynamically** predicted at a given gestational age (after embryonic stage). The predictions are in accordance with published clinical data. Additionally, we have also demonstrated how PBPK modeling and simulation provides a visual means to identify the key elements that affect fetal drug exposure in a rapidly evolving biological system (i.e. the fetus).

### 5.2 Future directions

All predictions need to be verified, as should ours. Due to the vulnerable nature of the pregnant population, it is unlikely the PK of all drugs that have been consumed by this population will be

evaluated in pregnant women in all three trimesters. Thus, for a given drug, the only way to fully verify our prediction of maternal-fetal exposure to drugs is to compare the predicted drug disposition at term against clinical observations. Such verification will rely on the availability of term PK data, both from the mother and from her fetus. Once the prediction is verified at term, the predicted drug disposition during early gestation can be used to help make informed decisions on dose adjustments, to conduct risk benefit assessments at term. .

Another remaining challenge is to predict drug disposition in the coupled maternal-fetal pairs during early gestation (i.e. before gestational week 20). Numerous efforts have been made in trying to elucidate the developmental biology of fetus, the rapidly changing fetal physiology, and the ontogeny of fetal DME and placental drug transporters. Such information can be used to refine model structure and to populate the resulting m-f-PBPK model for early gestation with system-specific parameters. In contrast, there are no or little data on maternal PK during early gestation for the purpose of model verification. Fetal exposure cannot be feasibly or ethically assessed until at the time of birth. Therefore, mechanistic modeling and simulation, such as PBPK model that incorporate the multidimensional changes in maternal ADMET and fetal development are desirable. As pointed out in **Chapter 3**, the differing fetal physiology (e.g. highly permeably skin) requires further structural modification of the current m-f-PBPK model. The work presented in **Chapter 3** and **Chapter 4** highlighted the advantages of such physiology-based integrative approach: 1) the ability to extrapolate the observed drug disposition from the general population, the non-pregnant healthy volunteers, to this special population, the pregnant women and their fetuses, and 2) to extrapolate across different stages of life (i.e. from term to early gestation). However, because of its integrative, mechanistic nature, unlike those parsimonious/simplistic empirical models, rich data sets on the longitudinal trends of the system-

specific parameters (i.e. maternal and fetal physiology) and on the drug-specific parameters (parameters characterizing the ADMET processes of a drug) are needed to populate these models prior to predictions.

At present time, there are many gaps in knowledge regarding these data needed to populate a maternal-fetal PBPK model. As pointed out in previous chapters, more clinical investigation using probe drugs are needed to delineate the longitudinal changes in the activity CYP enzyme, UGT enzyme, drug transporters, and other non-CYP enzymes that are involved in drug disposition (e.g. aldehyde dehydrogenase, GST, etc. ). Owing to the limitations of published studies (e.g. small sample size, non-specific probe, diet, concomitant medication, genetic polymorphism, etc.), the magnitude of change in the activity of many enzymes remains unclear or unknown. For instance, contradicting data exist regarding the gestational-dependent activity of UGT2B7.(Watts et al., 1991; O'Sullivan et al., 1993; Anderson, 2005) To resolve these controversies, clinical studies employing sensitive and specific probes are needed. In addition, placental transporter/DME ontogeny data in the literature allowing us to perform the whole-organ clearance scale up are absent.

The placental drug transporters have been shown to play a role in modifying fetal exposure to their substrates in experimental animals. For instance, placental BCRP has been shown to limit the fetal exposure to glyburide.{Zhou, 2008 #5221} Importantly, the expression of some of these transporters is known to vary significant with gestational age. (Mathias et al., 2005) Simulations in **Chapter 4** have suggested that fetal exposure to placental transporter substrates may vary significantly with the changes in these placental drug transporters. Therefore, an important further step is to verify the performance of this m-f-PBPK model for drugs with significant placental transport component at term. As described above, incorporation of

placental drug transport required the generation of placental drug transporter expression data, both at term and at early gestation, and the improvement of expression based *in vitro*-to-*in vivo* extrapolation (IVIVE) of transporter mediated clearance. Studies on placental drug transporter quantification and on improving the current IVIVE of transporter-mediated clearance are in progress in our lab.

References


Abduljalil K, Furness P, Johnson TN, Rostami-Hodjegan A, and Soltani H (2012) Anatomical, physiological and metabolic changes with gestational age during normal pregnancy: a database for parameters required in physiologically based pharmacokinetic modelling. *Clin Pharmacokinet* **51:**365-396.

Andersin R (1991) Solubility and acid-base behaviour of midazolam in media of different pH, studied by ultraviolet spectrophotometry with multicomponent software. *J Pharm Biomed Anal* **9:**451-455.

Anderson GD (2005) Pregnancy-induced changes in pharmacokinetics: a mechanistic-based approach. *Clin Pharmacokinet* **44:**989-1008.

Anderson GD and Carr DB (2009) Effect of pregnancy on the pharmacokinetics of antihypertensive drugs. *Clin Pharmacokinet* **48:**159-168.

Anderson PL, Noormohamed SE, Henry K, Brundage RC, Balfour HH, and Fletcher CV (2000) Semen and serum pharmacokinetics of zidovudine and zidovudine-glucuronide in men with HIV-1 infection. *Pharmacotherapy* **20:**917-922.

Andrew MA, Easterling TR, Carr DB, Shen D, Buchanan ML, Rutherford T, Bennett R, Vicini P, and Hebert MF (2007) Amoxicillin pharmacokinetics in pregnant women: modeling and simulations of dosage strategies. *Clin Pharmacol Ther* **81:**547-556.

Aslaksen A, Bakke OM, and Vigander T (1981) Comparative pharmacokinetics of theophylline and aminophylline in man. *Br J Clin Pharmacol* **11:**269-273.

Barros LF, Yudilevich DL, Jarvis SM, Beaumont N, Young JD, and Baldwin SA (1995) Immunolocalisation of nucleoside transporters in human placental trophoblast and endothelial cells: evidence for multiple transporter isoforms. *Pflügers Archiv* **429:**394-399.

Barry M, Back D, Ormesher S, Beeching N, and Nye F (1993) Metabolism of didanosine (ddI) by erythrocytes: pharmacokinetic implications. *Br J Clin Pharmacol* **36:**87-88.

Barter ZE, Bayliss MK, Beaune PH, Boobis AR, Carlile DJ, Edwards RJ, Houston JB, Lake BG, Lipscomb JC, Pelkonen OR, Tucker GT, and Rostami-Hodjegan A (2007) Scaling factors for the extrapolation of in vivo metabolic drug clearance from in vitro data: reaching a consensus on values of human microsomal protein and hepatocellularity per gram of liver. *Curr Drug Metab* **8:**33-45.

Bastian JR, Chen H, Zhang H, Rothenberger S, Tarter R, English D, Venkataramanan R, and Caritis SN (2016) Dose-adjusted plasma concentrations of sublingual buprenorphine are lower during than after pregnancy. *Am J Obstet Gynecol*.

Baumann G, Davila N, Shaw MA, Ray J, Liebhaber SA, and Cooke NE (1991) Binding of human growth hormone (GH)-variant (placental GH) to GH-binding proteins in human plasma. *J Clin Endocrinol Metab* **73:**1175-1179.

Bawdon RE, Sobhi S, and Dax J (1992) The transfer of anti-human immunodeficiency virus nucleoside compounds by the term human placenta. *Am J Obstet Gynecol* **167:**1570-1574.

Benet LZ (2010) Predicting Drug Disposition via Application of a Biopharmaceutics Drug Disposition Classification System. *Basic Clin Pharmacol Toxicol* **106:**162-167.

Bernick SJ and Kane S (2012) Drug transfer to the fetus and to the breastfeeding infant: what do we know? *Current drug delivery* **9:**350-355.

Bottalico B, Larsson I, Brodszki J, Hernandez-Andrade E, Casslen B, Marsal K, and Hansson SR (2004) Norepinephrine transporter (NET), serotonin transporter (SERT), vesicular monoamine transporter (VMAT2) and organic cation transporters (OCT1, 2 and EMT) in human placenta from pre-eclamptic and normotensive pregnancies. *Placenta* **25:**518-529.

Burchell B, Coughtrie M, Jackson M, Harding D, Fournel-Gigleux S, Leakey J, and Hume R (1989) Development of human liver UDP-glucuronosyltransferases. *Dev Pharmacol Ther* **13:**70-77.

Caufriez A, Frankenne F, Hennen G, and Copinschi G (1993) Regulation of maternal IGF-I by placental GH in normal and abnormal human pregnancies. *Am J Physiol* **265:**E572-577.

Chappuy H, Tréluyer J-M, Jullien V, Dimet J, Rey E, Fouché M, Firtion G, Pons G, and Mandelbrot L (2004a) Maternal-fetal transfer and amniotic fluid accumulation of nucleoside analogue reverse transcriptase inhibitors in human immunodeficiency virus-infected pregnant women. *Antimicrob Agents Chemother* **48:**4332-4336.

Chappuy H, Tréluyer J-M, Rey E, Dimet J, Fouché M, Firtion G, Pons G, and Mandelbrot L (2004b) Maternal-fetal transfer and amniotic fluid accumulation of protease inhibitors in pregnant women who are infected with human immunodeficiency virus. *Am J Obstet Gynecol* **191:**558-562.

Chappuy H, Treluyer JM, Rey E, Dimet J, Fouche M, Firtion G, Pons G, and Mandelbrot L (2004c) Maternal-fetal transfer and amniotic fluid accumulation of protease inhibitors in pregnant women who are infected with human immunodeficiency virus. *Am J Obstet Gynecol* **191:**558-562.

Choi SY, Koh KH, and Jeong H (2013) Isoform-specific regulation of cytochromes P450 expression by estradiol and progesterone. *Drug Metab Dispos* **41:**263-269.

Chung W (2004) Teratogens and their effects, in: , http://www.columbia.edu/itc/hs/medical/humandev/2004/Chpt23-Teratogens.pdf.

Ciarimboli G, Lancaster CS, Schlatter E, Franke RM, Sprowl JA, Pavenstadt H, Massmann V, Guckel D, Mathijssen RH, Yang W, Pui CH, Relling MV, Herrmann E, and Sparreboom A (2012) Proximal tubular secretion of creatinine by organic cation transporter OCT2 in cancer patients. *Clin Cancer Res* **18:**1101-1108.

Cload PA (1989) A review of the pharmacokinetics of zidovudine in man. *J Infect* **18 Suppl 1:**15-21.

Collett A, Stephens RH, Harwood MD, Humphrey M, Dallman L, Bennett J, Davis J, Carlson GL, and Warhurst G (2008) Investigation of regional mechanisms responsible for poor oral absorption in humans of a modified release preparation of the alpha-adrenoreceptor antagonist, 4-amino-6,7-dimethoxy-2-(5-methanesulfonamido-1,2,3,4 tetrahydroisoquinol-2-yl)-5-(2-pyridyl)quinazoline (UK-338,003): the rational use of ex vivo intestine to predict in vivo absorption. *Drug Metab Dispos* **36:**87-94.

Collier AC, Ganley NA, Tingle MD, Blumenstein M, Marvin KW, Paxton JW, Mitchell MD, and Keelan JA (2002) UDP-glucuronosyltransferase activity, expression and cellular localization in human placenta at term. *Biochem Pharmacol* **63:**409-419.

Collier AC, Keelan JA, Van Zijl PE, Paxton JW, Mitchell MD, and Tingle MD (2004) Human placental glucuronidation and transport of 3'azido-3'-deoxythymidine and uridine diphosphate glucuronic acid. *Drug Metab Dispos* **32:**813-820.

Collins JM and Unadkat JD (1989) Clinical pharmacokinetics of zidovudine. An overview of current data. *Clin Pharmacokinet* **17:**1-9.

Coonen J, Marcus M, Joosten E, van Kleef M, Neef C, van Aken H, and Gogarten W (2010) Transplacental transfer of remifentanil in the pregnant ewe. *Br J Pharmacol* **161:**1472-1476.

Court MH, Zhang X, Ding X, Yee KK, Hesse LM, and Finel M (2012) Quantitative distribution of mRNAs encoding the 19 human UDP-glucuronosyltransferase enzymes in 26 adult and 3 fetal tissues. *Xenobiotica* **42:**266-277.

Cressey TR, Best BM, Achalapong J, Stek A, Wang J, Chotivanich N, Yuthavisuthi P, Suriyachai P, Prommas S, Shapiro DE, Watts DH, Smith E, Capparelli E, Kreitchmann R, Mirochnick M, and team IP (2013) Reduced indinavir exposure during pregnancy. *Br J Clin Pharmacol* **76:**475-483.

Cressey TR, Stek A, Capparelli E, Bowonwatanuwong C, Prommas S, Sirivatanapa P, Yuthavisuthi P, Neungton C, Huo Y, Smith E, Best BM, and Mirochnick M (2012) Efavirenz Pharmacokinetics during the Third Trimester of Pregnancy and Postpartum. *J Acquir Immune Defic Syndr* **59:**245-252.

Cretton EM, Xie MY, Bevan RJ, Goudgaon NM, Schinazi RF, and Sommadossi JP (1991) Catabolism of 3'-azido-3'-deoxythymidine in hepatocytes and liver microsomes, with evidence of formation of 3'-amino-3'-deoxythymidine, a highly toxic catabolite for human bone marrow cells. *Mol Pharmacol* **39:**258-266.

De Sousa Mendes M, Hirt D, Vinot C, Valade E, Lui G, Pressiat C, Bouazza N, Foissac F, Blanche S, Le MP, Peytavin G, Treluyer JM, Urien S, and Benaboud S (2016) Prediction of human fetal pharmacokinetics using ex vivo human placenta perfusion studies and physiologically based models. *Br J Clin Pharmacol* **81:**646-657.

de Souza J, Benet LZ, Huang Y, and Storpirtis S (2009) Comparison of bidirectional lamivudine and zidovudine transport using MDCK, MDCK-MDR1, and Caco-2 cell monolayers. *J Pharm Sci* **98:**4413-4419.

Deshmukh SV, Nanovskaya TN, and Ahmed MS (2003) Aromatase Is the Major Enzyme Metabolizing Buprenorphine in Human Placenta. *Journal of Pharmacology and Experimental Therapeutics* **306:**1099-1105.

DeSisto CL, Kim SY, and Sharma AJ (2014) Prevalence estimates of gestational diabetes mellitus in the United States, Pregnancy Risk Assessment Monitoring System (PRAMS), 2007-2010. *Prev Chronic Dis* **11:**E104.

Di L, Whitney-Pickett C, Umland JP, Zhang H, Zhang X, Gebhard DF, Lai Y, Federico JJ, Davidson RE, Smith R, Reyner EL, Lee C, Feng B, Rotter C, Varma MV, Kempshall S, Fenner K, El-Kattan AF, Liston TE, and Troutman MD (2011) Development of a new permeability assay using low-efflux MDCKII cells. *J Pharm Sci* **100:**4974-4985.

Doody KJ and Carr BR (1989) Aromatase in human fetal tissues. *Am J Obstet Gynecol* **161:**1694-1697.

Doran A, Obach RS, Smith BJ, Hosea NA, Becker S, Callegari E, Chen C, Chen X, Choo E, Cianfrogna J, Cox LM, Gibbs JP, Gibbs MA, Hatch H, Hop CE, Kasman IN, Laperle J, Liu J, Liu X, Logman M, Maclin D, Nedza FM, Nelson F, Olson E, Rahematpura S, Raunig D, Rogers S, Schmidt K, Spracklin DK, Szewc M, Troutman M, Tseng E, Tu M, Van Deusen JW, Venkatakrishnan K, Walens G, Wang EQ, Wong D, Yasgar AS, and Zhang C (2005) The impact of P-glycoprotein on the disposition of drugs targeted for indications of the central nervous system: evaluation using the MDR1A/1B knockout mouse model. *Drug Metab Dispos* **33:**165-174.

Egan TD (1995) Remifentanil pharmacokinetics and pharmacodynamics. A preliminary appraisal. *Clin Pharmacokinet* **29:**80-94.
Ekstrom L, Johansson M, and Rane A (2013) Tissue distribution and relative gene expression of UDP-glucuronosyltransferases (2B7, 2B15, 2B17) in the human fetus. *Drug Metab Dispos* **41:**291-295.
Else LJ, Taylor S, Back DJ, and Khoo SH (2011) Pharmacokinetics of antiretroviral drugs in anatomical sanctuary sites: the fetal compartment (placenta and amniotic fluid). *Antivir Ther* **16:**1139-1147.
Enokizono J, Kusuhara H, and Sugiyama Y (2007) Effect of breast cancer resistance protein (Bcrp/Abcg2) on the disposition of phytoestrogens. *Mol Pharmacol* **72:**967-975.
Errasti-Murugarren E, D ́az P, Godoy V, Riquelme G, and Pastor-Anglada M (2011) Expression and Distribution of Nucleoside Transporter Proteins in the Human Syncytiotrophoblast. *Molecular Pharmacology* **80:**809-817.
Evans MI, Pryde PG, Reichler A, Bardicef M, and Johnson MP (1993) Fetal drug therapy. *Western Journal of Medicine* **159:**325-332.
Eyal S, Easterling TR, Carr D, Umans JG, Miodovnik M, Hankins GDV, Clark SM, Risler L, Wang J, Kelly EJ, Shen DD, and Hebert MF (2010) Pharmacokinetics of Metformin during Pregnancy. *Drug Metab Dispos* **38:**833-840.
Fanni D, Fanos V, Ambu R, Lai F, Gerosa C, Pampaloni P, Van Eyken P, Senes G, Castagnola M, and Faa G (2014) Overlapping between CYP3A4 and CYP3A7 expression in the fetal human liver during development. *J Matern Fetal Neonatal Med***:**1-5.
Fokina VM, West H, Oncken C, Clark SM, Ahmed MS, Hankins GD, and Nanovskaya TN (2016) Bupropion therapy during pregnancy: the drug and its major metabolites in umbilical cord plasma and amniotic fluid. *Am J Obstet Gynecol*.
Fotopoulou C, Kretz R, Bauer S, Schefold JC, Schmitz B, Dudenhausen JW, and Henrich W (2009) Prospectively assessed changes in lamotrigine-concentration in women with epilepsy during pregnancy, lactation and the neonatal period. *Epilepsy Res* **85:**60-64.
Fuglsang J and Ovesen P (2006) Aspects of placental growth hormone physiology. *Growth Horm IGF Res* **16:**67-85.
Furukawa T, Naritomi Y, Tetsuka K, Nakamori F, Moriguchi H, Yamano K, Terashita S, Tabata K, and Teramura T (2014) Species differences in intestinal glucuronidation activities between humans, rats, dogs and monkeys. *Xenobiotica* **44:**205-216.
Gallicano K (2000) Antiretroviral-Drug Concentrations in Semen. *Antimicrob Agents Chemother* **44:**1117-1118.
Gallicano K, Sahai J, Ormsby E, Cameron DW, Pakuts A, and McGilveray I (1993) Pharmacokinetics of zidovudine after the initial single dose and during chronic-dose therapy in HIV-infected patients. *Br J Clin Pharmacol* **36:**128-131.
Gaohua L, Abduljalil K, Jamei M, Johnson TN, and Rostami-Hodjegan A (2012) A pregnancy physiologically based pharmacokinetic (p-PBPK) model for disposition of drugs metabolized by CYP1A2, CYP2D6 and CYP3A4. *Br J Clin Pharmacol* **74:**873-885.
Gertz M, Harrison A, Houston JB, and Galetin A (2010) Prediction of human intestinal first-pass metabolism of 25 CYP3A substrates from in vitro clearance and permeability data. *Drug Metab Dispos* **38:**1147-1158.
Gibaldi M and Perrier D (1982) *Pharmacokinetics*. M. Dekker, New York.
Gilbert WM and Brace RA (1993) Amniotic fluid volume and normal flows to and from the amniotic cavity. *Semin Perinatol* **17:**150-157.

Gorski JC, Wang Z, Haehner-Daniels BD, Wrighton SA, and Hall SD (2000) The effect of hormone replacement therapy on CYP3A activity. *Clin Pharmacol Ther* **68:**412-417.
Griffiths M, Beaumont N, Yao SY, Sundaram M, Boumah CE, Davies A, Kwong FY, Coe I, Cass CE, Young JD, and Baldwin SA (1997a) Cloning of a human nucleoside transporter implicated in the cellular uptake of adenosine and chemotherapeutic drugs. *Nat Med* **3:**89-93.
Griffiths M, Yao SY, Abidi F, Phillips SE, Cass CE, Young JD, and Baldwin SA (1997b) Molecular cloning and characterization of a nitrobenzylthioinosine-insensitive (ei) equilibrative nucleoside transporter from human placenta. *Biochem J* **328 ( Pt 3):**739-743.
Ha HR, Chen J, Freiburghaus AU, and Follath F (1995) Metabolism of theophylline by cDNA-expressed human cytochromes P-450. *Br J Clin Pharmacol* **39:**321-326.
Hakkola J, Pasanen M, Hukkanen J, Pelkonen O, Maenpaa J, Edwards RJ, Boobis AR, and Raunio H (1996a) Expression of xenobiotic-metabolizing cytochrome P450 forms in human full-term placenta. *Biochem Pharmacol* **51:**403-411.
Hakkola J, Pelkonen O, Pasanen M, and Raunio H (1998) Xenobiotic-metabolizing cytochrome P450 enzymes in the human feto-placental unit: role in intrauterine toxicity. *Crit Rev Toxicol* **28:**35-72.
Hakkola J, Raunio H, Purkunen R, Pelkonen O, Saarikoski S, Cresteil T, and Pasanen M (1996b) Detection of cytochrome P450 gene expression in human placenta in first trimester of pregnancy. *Biochem Pharmacol* **52:**379-383.
Hakkola J, Raunio H, Purkunen R, Saarikoski S, V ähäkangas K, Pelkonen O, Edwards RJ, Boobis AR, and Pasanen M (2001) Cytochrome P450 3A expression in the human fetal liver: evidence that CYP3A5 is expressed in only a limited number of fetal livers. *Biol Neonate* **80:**193-201.
Handschin C and Meyer UA (2003) Induction of drug metabolism: the role of nuclear receptors. *Pharmacol Rev* **55:**649-673.
Hardman HF (1962) Molecular form of theophylline responsible for positive inotropic activity. *Circ Res* **10:**598-607.
He J, Yu Y, Prasad B, Chen X, and Unadkat JD (2014) Mechanism of an unusual, but clinically significant, digoxin-bupropion drug interaction. *Biopharm Drug Dispos* **35:**253-263.
Hebert MF, Easterling TR, Kirby B, Carr DB, Buchanan ML, Rutherford T, Thummel KE, Fishbein DP, and Unadkat JD (2008) Effects of pregnancy on CYP3A and P-glycoprotein activities as measured by disposition of midazolam and digoxin: a University of Washington specialized center of research study. *Clin Pharmacol Ther* **84:**248-253.
Hill MA (2016) Embryology: Timeline human development.
Hill MD and Abramson FP (1988) The significance of plasma protein binding on the fetal/maternal distribution of drugs at steady-state. *Clin Pharmacokinet* **14:**156-170.
Howe JL, Back DJ, and Colbert J (1992) Extrahepatic metabolism of zidovudine. *Br J Clin Pharmacol* **33:**190-192.
Hutson JR, Garcia-Bournissen F, Davis A, and Koren G (2011) The human placental perfusion model: a systematic review and development of a model to predict in vivo transfer of therapeutic drugs. *Clin Pharmacol Ther* **90:**67-76.
Irvine JD, Takahashi L, Lockhart K, Cheong J, Tolan JW, Selick HE, and Grove JR (1999) MDCK (Madin-Darby canine kidney) cells: A tool for membrane permeability screening. *J Pharm Sci* **88:**28-33.

Isoherranen N and Thummel KE (2013) Drug metabolism and transport during pregnancy: how does drug disposition change during pregnancy and what are the mechanisms that cause such changes? *Drug Metab Dispos* **41:**256-262.

Jaffe CA, Turgeon DK, Lown K, Demott-Friberg R, and Watkins PB (2002) Growth hormone secretion pattern is an independent regulator of growth hormone actions in humans. *Am J Physiol Endocrinol Metab* **283:**E1008-1015.

Jamei M, Dickinson GL, and Rostami-Hodjegan A (2009) A framework for assessing inter-individual variability in pharmacokinetics using virtual human populations and integrating general knowledge of physical chemistry, biology, anatomy, physiology and genetics: A tale of 'bottom-up' vs 'top-down' recognition of covariates. *Drug Metab Pharmacokinet* **24:**53-75.

Jeong H (2010) Altered drug metabolism during pregnancy: hormonal regulation of drug-metabolizing enzymes. *Expert Opin Drug Metab Toxicol* **6:**689-699.

Johansson M, Strahm E, Rane A, and Ekström L (2014) CYP2C8 and CYP2C9 mRNA expression profile in the human fetus. *Frontiers in Genetics* **5**.

Jones SM, Boobis AR, Moore GE, and Stanier PM (1992) Expression of CYP2E1 during human fetal development: methylation of the CYP2E1 gene in human fetal and adult liver samples. *Biochem Pharmacol* **43:**1876-1879.

Jonker JW, Buitelaar M, Wagenaar E, van der Valk MA, Scheffer GL, Scheper RJ, Plösch T, Kuipers F, Elferink R, Rosing H, Beijnen JH, and Schinkel AH (2002) The breast cancer resistance protein protects against a major chlorophyll-derived dietary phototoxin and protoporphyria. *Proc Natl Acad Sci U S A* **99:**15649-15654.

Kalleinen N, Polo-Kantola P, Irjala K, Porkka-Heiskanen T, Vahlberg T, Virkki A, and Polo O (2008) 24-hour serum levels of growth hormone, prolactin, and cortisol in pre- and postmenopausal women: the effect of combined estrogen and progestin treatment. *J Clin Endocrinol Metab* **93:**1655-1661.

Kanebratt KP and Andersson TB (2008) HepaRG cells as an in vitro model for evaluation of cytochrome P450 induction in humans. *Drug Metab Dispos* **36:**137-145.

Kanto J, Sjovall S, Erkkola R, Himberg JJ, and Kangas L (1983) Placental transfer and maternal midazolam kinetics. *Clin Pharmacol Ther* **33:**786-791.

Ke AB, Nallani SC, Zhao P, Rostami-Hodjegan A, Isoherranen N, and Unadkat JD (2013a) A physiologically based pharmacokinetic model to predict disposition of CYP2D6 and CYP1A2 metabolized drugs in pregnant women. *Drug Metab Dispos* **41:**801-813.

Ke AB, Nallani SC, Zhao P, Rostami-Hodjegan A, and Unadkat JD (2012) A PBPK Model to Predict Disposition of CYP3A-Metabolized Drugs in Pregnant Women: Verification and Discerning the Site of CYP3A Induction. *CPT Pharmacometrics Syst Pharmacol* **1:**e3.

Ke AB, Nallani SC, Zhao P, Rostami-Hodjegan A, and Unadkat JD (2013b) Expansion of a PBPK Model to Predict Disposition in Pregnant Women of Drugs Cleared via Multiple CYP Enzymes, Including CYP2B6, CYP2C9 and CYP2C19. *Br J Clin Pharmacol*.

Kharasch ED, Mautz D, Senn T, Lentz G, and Cox K (1999) Menstrual cycle variability in midazolam pharmacokinetics. *J Clin Pharmacol* **39:**275-280.

Kilford PJ, Stringer R, Sohal B, Houston JB, and Galetin A (2009) Prediction of drug clearance by glucuronidation from in vitro data: use of combined cytochrome P450 and UDP-glucuronosyltransferase cofactors in alamethicin-activated human liver microsomes. *Drug Metab Dispos* **37:**82-89.

Kitano T, Iizasa H, Hwang I-W, Hirose Y, Morita T, Maeda T, and Nakashima E (2004) Conditionally immortalized syncytiotrophoblast cell lines as new tools for study of the blood-placenta barrier. *Biol Pharm Bull* **27:**753-759.

Klecker RW, Jr., Collins JM, Yarchoan R, Thomas R, Jenkins JF, Broder S, and Myers CE (1987) Plasma and cerebrospinal fluid pharmacokinetics of 3'-azido-3'-deoxythymidine: a novel pyrimidine analog with potential application for the treatment of patients with AIDS and related diseases. *Clin Pharmacol Ther* **41:**407-412.

Knights KM, Spencer SM, Fallon JK, Chau N, Smith PC, and Miners JO (2016) Scaling factors for the in vitro-in vivo extrapolation (IV-IVE) of renal drug and xenobiotic glucuronidation clearance. *Br J Clin Pharmacol*.

Knupp CA, Shyu WC, Dolin R, Valentine FT, McLaren C, Martin RR, Pittman KA, and Barbhaiya RH (1991) Pharmacokinetics of didanosine in patients with acquired immunodeficiency syndrome or acquired immunodeficiency syndrome-related complex. *Clin Pharmacol Ther* **49:**523-535.

Kobayashi Y, Sakai R, Ohshiro N, Ohbayashi M, Kohyama N, and Yamamoto T (2005) Possible involvement of organic anion transporter 2 on the interaction of theophylline with erythromycin in the human liver. *Drug Metab Dispos* **33:**619-622.

Koukouritaki SB, Manro JR, Marsh SA, Stevens JC, Rettie AE, McCarver DG, and Hines RN (2004) Developmental Expression of Human Hepatic CYP2C9 and CYP2C19. *Journal of Pharmacology and Experimental Therapeutics* **308:**965-974.

Kulo A, Peeters MY, Allegaert K, Smits A, de Hoon J, Verbesselt R, Lewi L, van de Velde M, and Knibbe CAJ (2013) Pharmacokinetics of paracetamol and its metabolites in women at delivery and post-partum. *Br J Clin Pharmacol* **75:**850-860.

Kushnir MM, Rockwood AL, Bergquist J, Varshavsky M, Roberts WL, Yue B, Bunker AM, and Meikle AW (2008) High-sensitivity tandem mass spectrometry assay for serum estrone and estradiol. *Am J Clin Pathol* **129:**530-539.

Lacroix MC, Guibourdenche J, Frendo JL, Muller F, and Evain-Brion D (2002) Human placental growth hormone--a review. *Placenta* **23 Suppl A:**S87-94.

Lander CM, Smith MT, Chalk JB, de Wytt C, Symoniw P, Livingstone I, and Eadie MJ (1984) Bioavailability and pharmacokinetics of phenytoin during pregnancy. *Eur J Clin Pharmacol* **27:**105-110.

Leakey JE, Hume R, and Burchell B (1987) Development of multiple activities of UDP-glucuronyltransferase in human liver. *Biochem J* **243:**859-861.

Lee N, Hebert MF, Prasad B, Easterling TR, Kelly EJ, Unadkat JD, and Wang J (2013) Effect of Gestational Age on mRNA and Protein Expression of Polyspecific Organic Cation Transporters during Pregnancy. *Drug Metab Dispos* **41:**2225-2232.

Leeder JS, Gaedigk R, Marcucci KA, Gaedigk A, Vyhlidal CA, Schindel BP, and Pearce RE (2005) Variability of CYP3A7 Expression in Human Fetal Liver. *Journal of Pharmacology and Experimental Therapeutics* **314:**626-635.

Lehmann JM, McKee DD, Watson MA, Willson TM, Moore JT, and Kliewer SA (1998) The human orphan nuclear receptor PXR is activated by compounds that regulate CYP3A4 gene expression and cause drug interactions. *J Clin Invest* **102:**1016-1023.

Liddle C, Goodwin BJ, George J, Tapner M, and Farrell GC (1998) Separate and interactive regulation of cytochrome P450 3A4 by triiodothyronine, dexamethasone, and growth hormone in cultured hepatocytes. *J Clin Endocrinol Metab* **83:**2411-2416.

Liebes L, Mendoza S, Wilson D, and Dancis J (1990) Transfer of zidovudine (AZT) by human placenta. *J Infect Dis* **161:**203-207.

Lindholm J and Schultz-Moller N (1973) Plasma and urinary cortisol in pregnancy and during estrogen-gestagen treatment. *Scand J Clin Lab Invest* **31:**119-122.

Loccisano AE, Longnecker MP, Campbell JL, Andersen ME, and Clewell HJ (2013) Development of PBPK models for PFOA and PFOS for human pregnancy and lactation life stages. *J Toxicol Environ Health A* **76:**25-57.

Lu C and Li AP (2001) Species comparison in P450 induction: effects of dexamethasone, omeprazole, and rifampin on P450 isoforms 1A and 3A in primary cultured hepatocytes from man, Sprague-Dawley rat, minipig, and beagle dog. *Chem Biol Interact* **134:**271-281.

Ludden TM, Beal SL, and Sheiner LB (1994) Comparison of the Akaike Information Criterion, the Schwarz criterion and the F test as guides to model selection. *J Pharmacokinet Biopharm* **22:**431-445.

Macfie AG, Magides AD, Richmond MN, and Reilly CS (1991) Gastric emptying in pregnancy. *Br J Anaesth* **67:**54-57.

Maezawa K, Matsunaga T, Takezawa T, Kanai M, Ohira S, and Ohmori S (2010) Cytochrome P450 3As gene expression and testosterone 6 beta-hydroxylase activity in human fetal membranes and placenta at full term. *Biol Pharm Bull* **33:**249-254.

Mahar Doan KM, Humphreys JE, Webster LO, Wring SA, Shampine LJ, Serabjit-Singh CJ, Adkison KK, and Polli JW (2002) Passive permeability and P-glycoprotein-mediated efflux differentiate central nervous system (CNS) and non-CNS marketed drugs. *J Pharmacol Exp Ther* **303:**1029-1037.

Mao Q (2008) BCRP/ABCG2 in the Placenta: Expression, Function and Regulation. *Pharm Res* **25:**1244-1255.

Mao Q, Ganapathy V, and Unadkat JD (2014) Drug Transport in the Placenta, in: *Drug Transporters*, pp 341-353, John Wiley & Sons, Inc.

Marin TZ, Meier R, Kraehenmann F, Burkhardt T, and Zimmermann R (2007) Nifedipine serum levels in pregnant women undergoing tocolysis with nifedipine. *J Obstet Gynaecol* **27:**260-263.

Maroulis GB, Manlimos FS, Garza R, and Abraham GE (1976) Serum cortisol and 11-desoxycortisol levels in hirsute premenopausal women. *Obstet Gynecol* **48:**388-391.

Marzolini C and Kim RB (2005) Placental transfer of antiretroviral drugs. *Clin Pharmacol Ther* **78:**118-122.

Mastorakos G and Ilias I (2003) Maternal and fetal hypothalamic-pituitary-adrenal axes during pregnancy and postpartum. *Ann N Y Acad Sci* **997:**136-149.

Masungi C, Borremans C, Willems B, Mensch J, Van Dijck A, Augustijns P, Brewster ME, and Noppe M (2004) Usefulness of a novel Caco-2 cell perfusion system. I. In vitro prediction of the absorption potential of passively diffused compounds. *J Pharm Sci* **93:**2507-2521.

Mathias AA, Hitti J, and Unadkat JD (2005) P-glycoprotein and breast cancer resistance protein expression in human placentae of various gestational ages. *Am J Physiol Regul Integr Comp Physiol* **289:**R963-969.

Matsuzaka H, Maeshima H, Kida S, Kurita H, Shimano T, Nakano Y, Baba H, Suzuki T, and Arai H (2013) Gender differences in serum testosterone and cortisol in patients with major depressive disorder compared with controls. *Int J Psychiatry Med* **46:**203-221.

May K, Minarikova V, Linnemann K, Zygmunt M, Kroemer HK, Fusch C, and Siegmund W (2008) Role of the Multidrug Transporter Proteins ABCB1 and ABCC2 in the Diaplacental Transport of Talinolol in the Term Human Placenta. *Drug Metabolism and Disposition* **36:**740-744.

McCormack SA and Best BM (2014) Protecting the Fetus Against HIV Infection: A Systematic Review of Placental Transfer of Antiretrovirals. *Clin Pharmacokinet* **53:**989-1004.

McGowan JP and Shah SS (2000) Prevention of perinatal HIV transmission during pregnancy. *J Antimicrob Chemother* **46:**657-668.

McGready R, Stepniewska K, Seaton E, Cho T, Cho D, Ginsberg A, Edstein MD, Ashley E, Looareesuwan S, White NJ, and Nosten F (2003) Pregnancy and use of oral contraceptives reduces the biotransformation of proguanil to cycloguanil. *Eur J Clin Pharmacol* **59:**553-557.

McNamara PJ and Alcorn J (2002) Protein binding predictions in infants. *AAPS PharmSci* **4:**E4.

Meyer zu Schwabedissen HE, Jedlitschky G, Gratz M, Haenisch S, Linnemann K, Fusch C, Cascorbi I, and Kroemer HK (2005a) Variable expression of MRP2 (ABCC2) in human placenta: influence of gestational age and cellular differentiation. *Drug Metab Dispos* **33:**896-904.

Meyer zu Schwabedissen HEU, Grube M, Heydrich B, Linnemann K, Fusch C, Kroemer HK, and Jedlitschky G (2005b) Expression, Localization, and Function of MRP5 (ABCC5), a Transporter for Cyclic Nucleotides, in Human Placenta and Cultured Human Trophoblasts : Effects of Gestational Age and Cellular Differentiation. *Am J Pathol* **166:**39-48.

Mihaly GW, Morgan DJ, Marshall AW, Smallwood RA, Cockbain S, MacLellan D, and Hardy KJ (1982) Placental transfer of ranitidine during steady-state infusions of maternal and fetal sheep. *J Pharm Sci* **71:**1008-1010.

Mitchell AA, Gilboa SM, Werler MM, Kelley KE, Louik C, and Hernandez-Diaz S (2011) Medication use during pregnancy, with particular focus on prescription drugs: 1976-2008. *Am J Obstet Gynecol* **205:**51 e51-58.

Mnif W, Pascussi JM, Pillon A, Escande A, Bartegi A, Nicolas JC, Cavailles V, Duchesne MJ, and Balaguer P (2007) Estrogens and antiestrogens activate hPXR. *Toxicol Lett* **170:**19-29.

Morgan DJ, Blackman GL, Paull JD, and Wolf LJ (1981) Pharmacokinetics and plasma binding of thiopental. II: Studies at cesarean section. *Anesthesiology* **54:**474-480.

Muller AE, Dorr PJ, Mouton JW, De Jongh J, Oostvogel PM, Steegers EA, Voskuyl RA, and Danhof M (2008) The influence of labour on the pharmacokinetics of intravenously administered amoxicillin in pregnant women. *Br J Clin Pharmacol* **66:**866-874.

Murray FA, Erskine JP, and Fielding J (1957) Gastric secretion in pregnancy. *The Journal of obstetrics and gynaecology of the British Empire* **64:**373-381.

Myllynen P, Immonen E, Kummu M, and Vahakangas K (2009) Developmental expression of drug metabolizing enzymes and transporter proteins in human placenta and fetal tissues. *Expert Opin Drug Metab Toxicol* **5:**1483-1499.

Myllynen P, Pasanen M, and Vahakangas K (2007) The fate and effects of xenobiotics in human placenta. *Expert Opin Drug Metab Toxicol* **3:**331-346.

Nagashige M, Ushigome F, Koyabu N, Hirata K, Kawabuchi M, Hirakawa T, Satoh S, Tsukimori K, Nakano H, Uchiumi T, Kuwano M, Ohtani H, and Sawada Y (2003) Basal membrane localization of MRP1 in human placental trophoblast. *Placenta* **24:**951-958.

Ngan Kee WD, Khaw KS, Tan PE, Ng FF, and Karmakar MK (2009) Placental transfer and fetal metabolic effects of phenylephrine and ephedrine during spinal anesthesia for cesarean delivery. *Anesthesiology* **111:**506-512.

NICHD F Inter-Agency Agreement Between the Eunice Kennedy Shriver National Institute of Child Health and Human Development (NICHD) and the U.S.Food and Drug Administration (FDA).

O'Hare MF, Leahey W, Murnaghan GA, and McDevitt DG (1983) Pharmacokinetics of sotalol during pregnancy. *Eur J Clin Pharmacol* **24:**521-524.

O'Sullivan MJ, Boyer PJ, Scott GB, Parks WP, Weller S, Blum MR, Balsley J, and Bryson YJ (1993) The pharmacokinetics and safety of zidovudine in the third trimester of pregnancy for women infected with human immunodeficiency virus and their infants: phase I acquired immunodeficiency syndrome clinical trials group study (protocol 082). Zidovudine Collaborative Working Group. *Am J Obstet Gynecol* **168:**1510-1516.

Ohno S and Nakajin S (2009) Determination of mRNA expression of human UDP-glucuronosyltransferases and application for localization in various human tissues by real-time reverse transcriptase-polymerase chain reaction. *Drug Metab Dispos* **37:**32-40.

Pacifici GM, Franchi M, Colizzi C, Giuliani L, and Rane A (1988) Glutathione S-transferase in humans: development and tissue distribution. *Arch Toxicol* **61:**265-269.

Pacifici GM, S äwe J, Kager L, and Rane A (1982) Morphine glucuronidation in human fetal and adult liver. *Eur J Clin Pharmacol* **22:**553-558.

Panigel M, Pascaud M, and Brun JL (1967) [Radioangiographic study of circulation in the villi and intervillous space of isolated human placental cotyledon kept viable by perfusion]. *Journal de physiologie* **59:**277.

Papageorgiou I, Grepper S, and Unadkat JD (2013) Induction of hepatic CYP3A enzymes by pregnancy-related hormones: studies in human hepatocytes and hepatic cell lines. *Drug Metab Dispos* **41:**281-290.

Pascolo L, Fernetti C, Pirulli D, Crovella S, Amoroso A, and Tiribelli C (2003) Effects of maturation on RNA transcription and protein expression of four MRP genes in human placenta and in BeWo cells. *Biochem Biophys Res Commun* **303:**259-265.

Pascussi JM, Drocourt L, Fabre JM, Maurel P, and Vilarem MJ (2000) Dexamethasone induces pregnane X receptor and retinoid X receptor-alpha expression in human hepatocytes: synergistic increase of CYP3A4 induction by pregnane X receptor activators. *Mol Pharmacol* **58:**361-372.

Patel P, Weerasekera N, Hitchins M, Boyd CA, Johnston DG, and Williamson C (2003) Semi quantitative expression analysis of MDR3, FIC1, BSEP, OATP-A, OATP-C,OATP-D, OATP-E and NTCP gene transcripts in 1st and 3rd trimester human placenta. *Placenta* **24:**39-44.

Patilea-Vrana G and Unadkat JD (2016) Transport vs. Metabolism: What Determines the Pharmacokinetics and Pharmacodynamics of Drugs? Insights From the Extended Clearance Model. *Clinical Pharmacology & Therapeutics* **100:**413-418.

Pereira CM, Nosbisch C, Winter HR, Baughman WL, and Unadkat JD (1994) Transplacental pharmacokinetics of dideoxyinosine in pigtailed macaques. *Antimicrob Agents Chemother* **38:**781-786.

Philipson A (1977) Pharmacokinetics of ampicillin during pregnancy. *J Infect Dis* **136:**370-376.

Philipson A, Stiernstedt G, and Ehrnebo M (1987) Comparison of the pharmacokinetics of cephradine and cefazolin in pregnant and non-pregnant women. *Clin Pharmacokinet* **12:**136-144.

Pidoux G, Gerbaud P, Guibourdenche J, Therond P, Ferreira F, Simasotchi C, Evain-Brion D, and Gil S (2015) Formaldehyde Crosses the Human Placenta and Affects Human Trophoblast Differentiation and Hormonal Functions. *PLoS One* **10:**e0133506.

Polin RA, Fox WW, and Abman SH (2004) *Fetal and neonatal physiology*. W.B. Saunders Co., Philadelphia, Pa.

Prevost RR, Akl SA, Whybrew WD, and Sibai BM (1992) Oral nifedipine pharmacokinetics in pregnancy-induced hypertension. *Pharmacotherapy* **12:**174-177.

Ramamoorthy S, Bauman AL, Moore KR, Han H, Yang-Feng T, Chang AS, Ganapathy V, and Blakely RD (1993) Antidepressant- and cocaine-sensitive human serotonin transporter: molecular cloning, expression, and chromosomal localization. *Proc Natl Acad Sci U S A* **90:**2542-2546.

Reimers A, Ostby L, Stuen I, and Sundby E (2011) Expression of UDP-glucuronosyltransferase 1A4 in human placenta at term. *Eur J Drug Metab Pharmacokinet* **35:**79-82.

Richard K, Hume R, Kaptein E, Stanley EL, Visser TJ, and Coughtrie MW (2001) Sulfation of thyroid hormone and dopamine during human development: ontogeny of phenol sulfotransferases and arylsulfatase in liver, lung, and brain. *J Clin Endocrinol Metab* **86:**2734-2742.

Richens A (1979) Clinical pharmacokinetics of phenytoin. *Clin Pharmacokinet* **4:**153-169.

Romero R, Kadar N, Gonzales Govea F, and Hobbins JC (1983) Pharmacokinetics of intravenous theophylline in pregnant patients at term. *Am J Perinatol* **1:**31-35.

Ron M, Hochner-Celnikier D, Menczel J, Palti Z, and Kidroni G (1984) Maternal-fetal transfer of aminophylline. *Acta Obstet Gynecol Scand* **63:**217-218.

Rudolph AM (1985) Animal models for study of fetal drug exposure. *NIDA research monograph* **60:**5-16.

Ryu RJ, Eyal S, Easterling TR, Caritis SN, Venkataraman R, Hankins G, Rytting E, Thummel K, Kelly EJ, Risler L, Phillips B, Honaker MT, Shen DD, and Hebert MF (2016) Pharmacokinetics of metoprolol during pregnancy and lactation. *J Clin Pharmacol* **56:**581-589.

Samtani MN and Jusko WJ (2007) Quantification of dexamethasone and corticosterone in rat biofluids and fetal tissue using highly sensitive analytical methods: assay validation and application to a pharmacokinetic study. *Biomed Chromatogr* **21:**585-597.

Sandhar BK, Elliott RH, Windram I, and Rowbotham DJ (1992) Peripartum changes in gastric emptying. *Anaesthesia* **47:**196-198.

Sata R, Ohtani H, Tsujimoto M, Murakami H, Koyabu N, Nakamura T, Uchiumi T, Kuwano M, Nagata H, Tsukimori K, Nakano H, and Sawada Y (2005) Functional Analysis of Organic Cation Transporter 3 Expressed in Human Placenta. *Journal of Pharmacology and Experimental Therapeutics* **315:**888-895.

Schenker S, Johnson RF, King TS, Schenken RS, and Henderson GI (1990) Azidothymidine (zidovudine) transport by the human placenta. *The American journal of the medical sciences* **299:**16-20.

Schinkel AH (1999) P-Glycoprotein, a gatekeeper in the blood-brain barrier. *Adv Drug Deliv Rev* **36:**179-194.

Schneider H, Panigel M, and Dancis J (1972) Transfer across the perfused human placenta of antipyrine, sodium and leucine. *Am J Obstet Gynecol* **114:**822-828.
Schulze A, Mills K, Weiss TS, and Urban S (2012) Hepatocyte polarization is essential for the productive entry of the hepatitis B virus. *Hepatology* **55:**373-383.
Shao J, Stapleton PL, Lin YS, and Gallagher EP (2007) Cytochrome P450 and Glutathione S-Transferase mRNA Expression in Human Fetal Liver Hematopoietic Stem Cells . *Drug Metabolism and Disposition* **35:**168-175.
Sheiner LB and Beal SL (1985) Pharmacokinetic parameter estimates from several least squares procedures: superiority of extended least squares. *J Pharmacokinet Biopharm* **13:**185-201.
Shirasaka Y, Sager JE, Lutz JD, Davis C, and Isoherranen N (2013) Inhibition of CYP2C19 and CYP3A4 by omeprazole metabolites and their contribution to drug-drug interactions. *Drug Metab Dispos* **41:**1414-1424.
Shu Y, Bello CL, Mangravite LM, Feng B, and Giacomini KM (2001) Functional characteristics and steroid hormone-mediated regulation of an organic cation transporter in Madin-Darby canine kidney cells. *J Pharmacol Exp Ther* **299:**392-398.
Shugarts S and Benet LZ (2009) The Role of Transporters in the Pharmacokinetics of Orally Administered Drugs. *Pharm Res* **26:**2039-2054.
Shuster DL, Risler LJ, Liang CKJ, Rice KM, Shen DD, Hebert MF, Thummel KE, and Mao Q (2014a) Maternal-Fetal Disposition of Glyburide in Pregnant Mice Is Dependent on Gestational Age. *J Pharmacol Exp Ther* **350:**425-434.
Shuster DL, Risler LJ, Prasad B, Calamia JC, Voellinger JL, Kelly EJ, Unadkat JD, Hebert MF, Shen DD, Thummel KE, and Mao Q (2014b) Identification of CYP3A7 for glyburide metabolism in human fetal livers. *Biochem Pharmacol* **92:**690-700.
Silva CM, Kloth MT, Lyons CE, Dunn CR, and Kirk SE (2002) Intracellular signaling by growth hormone variant (GH-V). *Growth Horm IGF Res* **12:**374-380.
Simpson KH, Stakes AF, and Miller M (1988) Pregnancy delays paracetamol absorption and gastric emptying in patients undergoing surgery. *Br J Anaesth* **60:**24-27.
Sitras V, Fenton C, Paulssen R, V årtun Å, and Acharya G (2012) Differences in Gene Expression between First and Third Trimester Human Placenta: A Microarray Study. *PLoS One* **7**.
St-Pierre MV, Serrano MA, Macias RI, Dubs U, Hoechli M, Lauper U, Meier PJ, and Marin JJ (2000) Expression of members of the multidrug resistance protein family in human term placenta. *Am J Physiol Regul Integr Comp Physiol* **279:**R1495-1503.
Stagg MP, Cretton EM, Kidd L, Diasio RB, and Sommadossi JP (1992) Clinical pharmacokinetics of 3'-azido-3'-deoxythymidine (zidovudine) and catabolites with formation of a toxic catabolite, 3'-amino-3'-deoxythymidine. *Clin Pharmacol Ther* **51:**668-676.
Stanley EL, Hume R, Visser TJ, and Coughtrie MW (2001) Differential expression of sulfotransferase enzymes involved in thyroid hormone metabolism during human placental development. *J Clin Endocrinol Metab* **86:**5944-5955.
Stevens JC, Hines RN, Gu C, Koukouritaki SB, Manro JR, Tandler PJ, and Zaya MJ (2003) Developmental Expression of the Major Human Hepatic CYP3A Enzymes. *Journal of Pharmacology and Experimental Therapeutics* **307:**573-582.

Stevens JC, Marsh SA, Zaya MJ, Regina KJ, Divakaran K, Le M, and Hines RN (2008) Developmental changes in human liver CYP2D6 expression. *Drug Metab Dispos* **36:**1587-1593.

Sturgiss SN, Wilkinson R, and Davison JM (1996) Renal reserve during human pregnancy. *Am J Physiol* **271:**F16-20.

Takeda M, Khamdang S, Narikawa S, Kimura H, Kobayashi Y, Yamamoto T, Cha SH, Sekine T, and Endou H (2002) Human organic anion transporters and human organic cation transporters mediate renal antiviral transport. *J Pharmacol Exp Ther* **300:**918-924.

Tasnif Y, Morado J, and Hebert MF (2016) Pregnancy-Related Pharmacokinetic Changes. *Clin Pharmacol Ther*.

Taub ME, Kristensen L, and Frokjaer S (2002) Optimized conditions for MDCK permeability and turbidimetric solubility studies using compounds representative of BCS classes I-IV. *Eur J Pharm Sci* **15:**331-340.

Teksin ZS, Seo PR, and Polli JE (2010) Comparison of drug permeabilities and BCS classification: three lipid-component PAMPA system method versus Caco-2 monolayers. *AAPS J* **12:**238-241.

Thangavel C, Boopathi E, and Shapiro BH (2011) Intrinsic sexually dimorphic expression of the principal human CYP3A4 correlated with suboptimal activation of GH/glucocorticoid-dependent transcriptional pathways in men. *Endocrinology* **152:**4813-4824.

Toda K, Simpson ER, Mendelson CR, Shizuta Y, and Kilgore MW (1994) Expression of the gene encoding aromatase cytochrome P450 (CYP19) in fetal tissues. *Mol Endocrinol* **8:**210-217.

Tolle-Sander S, Rautio J, Wring S, Polli JW, and Polli JE (2003) Midazolam exhibits characteristics of a highly permeable P-glycoprotein substrate. *Pharm Res* **20:**757-764.

Tracy TS, Venkataramanan R, Glover DD, and Caritis SN (2005) Temporal changes in drug metabolism (CYP1A2, CYP2D6 and CYP3A Activity) during pregnancy. *Am J Obstet Gynecol* **192:**633-639.

Tran TA, Leppik IE, Blesi K, Sathanandan ST, and Remmel R (2002) Lamotrigine clearance during pregnancy. *Neurology* **59:**251-255.

Tuntland T, Nosbisch C, Baughman WL, Massarella J, and Unadkat JD (1996) Mechanism and rate of placental transfer of zalcitabine (2',3'-dideoxycytidine) in Macaca nemestrina. *Am J Obstet Gynecol* **174:**856-863.

Tuntland T, Odinecs A, Pereira CM, Nosbisch C, and Unadkat JD (1999) In vitro models to predict the in vivo mechanism, rate, and extent of placental transfer of dideoxynucleoside drugs against human immunodeficiency virus. *Am J Obstet Gynecol* **180:**198-206.

Unadkat JD, Dahlin A, and Vijay S (2004) Placental drug transporters. *Curr Drug Metab* **5:**125-131.

Unadkat JD, Wara DW, Hughes MD, Mathias AA, Holland DT, Paul ME, Connor J, Huang S, Nguyen BY, Watts DH, Mofenson LM, Smith E, Deutsch P, Kaiser KA, and Tuomala RE (2007) Pharmacokinetics and safety of indinavir in human immunodeficiency virus-infected pregnant women. *Antimicrob Agents Chemother* **51:**783-786.

Underwood MA, Gilbert WM, and Sherman MP (2005) Amniotic fluid: not just fetal urine anymore. *Journal of perinatology : official journal of the California Perinatal Association* **25:**341-348.

Urakami Y, Okuda M, Saito H, and Inui K (2000) Hormonal regulation of organic cation transporter OCT2 expression in rat kidney. *FEBS Lett* **473:**173-176.

Vaidya SS, Walsh SW, and Gerk PM (2009) Formation and efflux of ATP-binding cassette transporter substrate 2,4-dinitrophenyl-S-glutathione from cultured human term placental villous tissue fragments. *Mol Pharm* **6:**1689-1702.

van der Sandt IC, Vos CM, Nabulsi L, Blom-Roosemalen MC, Voorwinden HH, de Boer AG, and Breimer DD (2001) Assessment of active transport of HIV protease inhibitors in various cell lines and the in vitro blood--brain barrier. *AIDS* **15:**483-491.

Velasque LS, Estrela RCE, Suarez-Kurtz G, and Struchiner CJ (2007) A new model for the population pharmacokinetics of didanosine in healthy subjects. *Braz J Med Biol Res* **40:**97-104.

Viau M, Lafond J, and Vaillancourt C (2009) Expression of placental serotonin transporter and 5-HT 2A receptor in normal and gestational diabetes mellitus pregnancies. *Reproductive biomedicine online* **19:**207-215.

Vyhlidal CA, Pearce RE, Gaedigk R, Calamia JC, Shuster DL, Thummel KE, and Leeder JS (2015) Variability in Expression of CYP3A5 in Human Fetal Liver. *Drug Metabolism and Disposition* **43:**1286-1293.

Vyhlidal CA, Riffel AK, Haley KJ, Sharma S, Dai H, Tantisira KG, Weiss ST, and Leeder JS (2013) Cotinine in Human Placenta Predicts Induction of Gene Expression in Fetal Tissues. *Drug Metab Dispos* **41:**305-311.

Watkins PB, Murray SA, Winkelman LG, Heuman DM, Wrighton SA, and Guzelian PS (1989) Erythromycin breath test as an assay of glucocorticoid-inducible liver cytochromes P-450. Studies in rats and patients. *J Clin Invest* **83:**688-697.

Watts DH, Brown ZA, Tartaglione T, Burchett SK, Opheim K, Coombs R, and Corey L (1991) Pharmacokinetic disposition of zidovudine during pregnancy. *J Infect Dis* **163:**226-232.

Wilkinson GR (2005) Drug metabolism and variability among patients in drug response. *N Engl J Med* **352:**2211-2221.

Williams JA, Ring BJ, Cantrell VE, Jones DR, Eckstein J, Ruterbories K, Hamman MA, Hall SD, and Wrighton SA (2002) Comparative metabolic capabilities of CYP3A4, CYP3A5, and CYP3A7. *Drug Metab Dispos* **30:**883-891.

Wu Z, Bidlingmaier M, Friess SC, Kirk SE, Buchinger P, Schiessl B, and Strasburger CJ (2003) A new nonisotopic, highly sensitive assay for the measurement of human placental growth hormone: development and clinical implications. *J Clin Endocrinol Metab* **88:**804-811.

Yamashita S, Furubayashi T, Kataoka M, Sakane T, Sezaki H, and Tokuda H (2000) Optimized conditions for prediction of intestinal drug permeability using Caco-2 cells. *Eur J Pharm Sci* **10:**195-204.

Yazdanian M, Glynn SL, Wright JL, and Hawi A (1998) Correlating partitioning and caco-2 cell permeability of structurally diverse small molecular weight compounds. *Pharm Res* **15:**1490-1494.

Yeboah D, Sun M, Kingdom J, Baczyk D, Lye SJ, Matthews SG, and Gibb W (2006) Expression of breast cancer resistance protein (BCRP/ABCG2) in human placenta throughout gestation and at term before and after labor. *Can J Physiol Pharmacol* **84:**1251-1258.

Yerby MS, Friel PN, McCormick K, Koerner M, Van Allen M, Leavitt AM, Sells CJ, and Yerby JA (1990) Pharmacokinetics of anticonvulsants in pregnancy: alterations in plasma protein binding. *Epilepsy Res* **5:**223-228.

Yoon M, Schroeter JD, Nong A, Taylor MD, Dorman DC, Andersen ME, and Clewell HJ, 3rd (2011) Physiologically based pharmacokinetic modeling of fetal and neonatal manganese

exposure in humans: describing manganese homeostasis during development. *Toxicol Sci* **122:**297-316.
Zhang H, Wu X, Wang H, Mikheev AM, Mao Q, and Unadkat JD (2008) Effect of pregnancy on cytochrome P450 3a and P-glycoprotein expression and activity in the mouse: mechanisms, tissue specificity, and time course. *Mol Pharmacol* **74:**714-723.
Zhang Y, Wang H, Unadkat JD, and Mao Q (2007) Breast Cancer Resistance Protein 1 Limits Fetal Distribution of Nitrofurantoin in the Pregnant Mouse. *Drug Metabolism and Disposition* **35:**2154-2158.
Zhang Z, Farooq M, Prasad B, Grepper S, and Unadkat JD (2015) Prediction of gestational age-dependent induction of in vivo hepatic CYP3A activity based on HepaRG cells and human hepatocytes. *Drug Metab Dispos* **43:**836-842.